Characterization of pluripotency genes in axolotl spinal cord regeneration

DISSERTATION

zur Erlangung des akademischen Grades

Doctor rerum naturalium
(Dr. rer. nat.)

vorgelegt

der Fakultät Mathematik und Naturwissenschaften
der Technischen Universität Dresden

von

Annett Dümmler
geboren am 05.01.1979 in Freital, Deutschland

Gutachter:

Prof. Dr. Elly M. Tanaka
Chair, Animal Models of Regeneration, DFG-Center for Regenerative Therapies Dresden, University of Technology Dresden.
Fetscherstrasse 105, 01309 Dresden, Deutschland

Dr. Patrizia Ferretti
Head of Developmental Biology Unit, UCL Institute of Child Health
30 Guilford Street, London WC1N 1EH, Grossbritannien

Eingereicht am: 30. November 2012
Verteidigt am: 25. Juni 2013

Declaration according to §5.5 of the doctorate regulations

I herewith declare that I have produced this thesis without the prohibited assistance of third parties and without making use of aids other than those specified; notions taken over directly or indirectly from other sources have been identified as such.

This thesis has not previously been presented in identical or similar form to any other German or foreign examination board.

The thesis work was conducted from 01.12.2008 to 30.11.2012 under the supervision of Prof. Dr. Elly Tanaka at the DFG-Center for Regenerative Therapies Dresden.

I declare that I have not undertaken any previous unsuccessful doctorate proceedings.

I declare that I recognize the doctorate regulations of the Fakultät für Mathematik und Naturwissenschaften of the Technische Universität Dresden.

30^{th} November 2012

Date Signature

Contents

List of Figures

List of Tables

1 LIST OF PUBLICATIONS

1.1 Manuscripts in preparation

Khattak, S.; Schuez, M.; Richter, T.; Sandoval Guzman, T.; Knapp, D.; Fei, J.; Hradlikova, K.; Duemmler, A.; Kerney, R.; Stanke, N.; Lindemann, D.; Tanaka, E. M.: Transgenic methods for testing gene function and tracking cells during regeneration in the axolotl.

Duemmler, A.; Tazaki, A.; Taniguchi, Y.; Tanaka, E. M.: Regenerating spinal cord cells are pluripotent.

1.2 Manuscript accepted for publication

Tapia, N.*; Reinhardt, R.*; Duemmler, A.*; Arazo-Bravo, M. J.; Greber, B.; Wu, G.; Cojacaru, V.; Rascon, C. A.; Tazaki, A.; Tanaka, E. M.; Schoeler, H. R.: Reprogramming to pluripotency is an ancient trait of vertebrate POU5F1 and POU2 proteins. *Nature Communication.*

* These authors contributed equally to this work.

1.3 Publications

Mchedlishvili, L.; Mazurov, V.; Grassme, K.S.; Goehler, K.; Robl, B.; Tazaki, A.; Roensch, K.; Duemmler, A.; Tanaka, E. M.: Reconstitution of the central and peripheral nervous system during salamander tail regeneration. *Proc. Natl. Acad. Sci. U S A.*, 2012; 109 (34): 2258-2266

Duemmler, A.; Montes-Vizuet, A. R.; Santiago-Cruz, J.; Teran, L. M.: CXCL5 en el tracto respiratorio superior de nios con influenza A. *Rev. Med. Inst. Mex. Seguro. Soc.*, 2010; 48 (4): 393-398.

Duemmler, A.; Lawrence, A.-M.; de Marco, A.: Simplified screening for the detection of soluble fusion constructs expressed in *E. coli* using a modular set of vectors. *Microbial Cell Factories* 2005; 4: 34.

2 SUMMARY

Regeneration is a process that renews damaged or lost cells, tissues, or even of entire body structures, and is a phenomenon which is widespread in the animal kingdom. Urodeles such as newts and salamanders have a remarkable regeneration ability. They can regenerate organs such as gills, lower jaws, retina, appendages like fore- and hind limbs, and also the tail including the spinal cord.

The regeneration process requires the use of resident stem cells or somatic cells, which have to be reprogrammed. In both cases the reprogrammed cells are less differentiated, meaning the cell would have the ability to form any kind of fetal or adult cell which rose from the three different germ layers, the ectoderm, mesoderm and endoderm.

Artificial reprogramming of differentiated mammalian somatic cell had been reported previously. It was shown that four pluripotency factors, OCT4 (also called POU5f1), SOX2, c-MYC and KLF4 are sufficient to generate an induced pluripotent stem (iPS) cell. It has been shown that some of these factors are also involved in regenerating processes. In newt limb and lens tissue, *Sox2, c-Myc* and *Klf4* mRNA levels were upregulated in the beginning of blastema formation when compared to non-amputated tissue. *Oct4* mRNA however, was not detected. During xenopus tail regeneration, *Sox2* and *c-Myc* were expressed, while the xenopus *Pou* homologs *Pou25, Pou60, Pou79, Pou91* were not detected. In regenerating zebrafish fin tissue, *Sox2, Pou2, c-Myc* and *Klf4* mRNA were not upregulated.

The mammalian transcription factor OCT4, a class V POU protein, is responsible in maintaining pluripotency in gastrula stage embryos. It was reported that mouse OCT4 is also expressed in the caudal node of embryos having 16 somites. It is further known that progenitors exist in mouse tailbud, which give rise to neural and mesodermal cell lineage. This suggests that the OCT4 expressing cells in caudal node might be a stem cell reservoir.

Oct4 was detected in axolotl during embryonic development, and prior to my work we found *Oct4* when screening the axolotl blastema cDNA library. In addition, we also identified *Pou2*, another class V POU gene. Phylogenetic analysis showed a clear distinction of both genes in the axolotl. We determined the mRNA pattern of *Pou2* during embryogenesis and compared it to *Oct4* mRNA and protein. Both genes are expressed in the primordial germ cells and the pluripotent animal cap region of the embryo. Apart from this similarity, both genes have a different expression pattern in the embryo.

We are interested in the involvement of OCT4, POU2, as well as the transcription factor SOX2 in regenerating axolotl spinal cord. We asked whether the cellular pluripotent character conferred by POU factors is limited to mammals or if it is an ancient characteristic of lower vertebrates. To answer the question we performed *in vitro* and *in vivo* studies. Hence this thesis is separated into two chapter.

By *in vitro* studies we investigated the pluripotent *PouV* orthologs from different species. Therefore, we performed reprogramming experiments using mouse or human fibroblasts and transduced them with axolotl

Oct4 or *Pou2*, in combination with human or axolotl *Sox2, c-Myc* and/or *Klf4*. The generated iPS cells with the different sets of factors had similar endogenous pluripotency gene expression profiles to embryonic stem cells. Further, iPS cells expressed the pluripotency markers like OCT4, NANOG, SSEA4, TRA1-60 and TRA1-81. Another evaluation of the iPS cells was the formation of embryoid bodies. Immunouorescence staining showed that tissue from all three germ layers was formed after induction. We observed a positive staining for the endoderm marker α-FEROPROTEIN, the mesoderm marker α-SMOOTH MUSCLE ACTIN and the ectoderm marker βIII TUBULIN in the generated cells. This indicated that the iPS cells generated using axolotl *Oct4* and *Sox2* in combination with mammalian *Klf4* and with or without *c-Myc*, as well as iPS cell generated with axolotl *Pou2* and mammalian *Sox2* and *Klf4* and with or without *c-Myc* have a pluripotent potential. In addition, the axolotl factors are able to form heterodimers with the mammalian proteins. Furthermore, we compared the reprogramming ability with POU factors from mouse, human, zebrash, medaka and xenopus. We showed that xenopus *Pou91*, as the only non-mammalian example, is nearly as efficient as mouse and human *Oct4* cDNAs in inducing GFP expressing cells. Also axolotl *Pou2*, axolotl *Oct4* and medaka *Pou2* showed reprogramming character however at a much lower efficiency. In contrast, zebrash *Pou2* is not able to establish iPS cells. This indicates that a reprogramming ability to a pluripotent cell state is an ancient trait of *Pou2* and *Oct4* homologs.

By *in vivo* studies we investigated the role of *Oct4, Pou2* and *Sox2* gene expression in regenerating spinal cord tissue. Performed *in situ* hybridizations and antibody staining studies in the regenerating spinal cord showed that *Oct4, Pou2* and *Sox2* were expressed during spinal cord regeneration.

Knockdown experiments in regenerating spinal cord using morpholino showed that *Pou2*-morpholino does not have an effect. In contrast, SOX2 was required for spinal cord regeneration but to a lesser extent, than OCT4, which decreased the regenerated length signicantly compared to control. Even though, with Sox2-morpholino we did not observe the phenotype as a significantly shorter regenerated spinal cord, about 45% of SOX2 knocked down cells were not cycling and proliferating anymore. This indicates that axolotl SOX2 has an effect in regeneration.

Therefore we wanted to know whether spinal cord cells would also have a pluripotent character *in vivo* and form other tissue types. Regenerating cells of the spinal cord are only able to form the same cell type and thus they keep their cell memory. However, when we performed transplantations of OCT4/SOX2 expressing spinal cord cells into somite stage embryos, we could show the formation of muscle cells. This shows that the spinal cord cells have the potential to change their fate in an embryonic context, where the normal environment of spinal cord has changed. However, our data do not indicate whether muscle is formed directly from the spinal cord or whether spinal cord cells fuse to developmental myoblasts, a cell type of embryonic progenitors, which give rise to muscle cells. To clearly state whether regenerating OCT4/SOX2 expressing spinal cord cells are pluripotent we have to perform OCT4 knock down in spinal cord and transplant these less proliferating cells

into embryos, observing their cell fate.

3 ACKNOWLEDGEMENTS

I would like to thank my supervisor Elly Tanaka for introducing me to the field of regeneration and for giving me the opportunity to work on such an interesting project. I am very grateful for all the helpful discussions, excellent supervision and the support during my entire PhD period. In addition, I thank her for the possibilities to attend different conferences and workshops during my studies.

Many, many thanks to the Tanaka lab. Especially I want to thank Akira Tazaki for all the support and critical discussions, and Heino Andreas, Beate Gruhl, Sabine Mögel and Mark Armstead for the excellent animal care take.

Many thanks to the antibody facility and the protein expression facility in MPI-CBG. In particular I thank David Drechsel for offering me a personal bench and desk in his lab - a luxury compared to the overfull Tanaka lab in MPI-CBG. Many thanks to Barbara Borgonovo, Régis Lemaitre and Mike Tipsword for the great atmosphere in the lab.

I am grateful for the helpful discussions and critical comments from Konstantinos Anastassiadis and Karla Neugebauer from my "Thesis Advisory Committee".

I would like to thank Patrizia Ferretti and Elly Tanaka for taking the responsibility to review my PhD thesis.

A special thanks to Yuka Taniguchi who introduced me to all the little experimental details of transplantation in order to label cell types.

I also thank the DNA sequencing facility in MPI-CBG for fast sequencing often at short notice.

I am very grateful to Christian Schläger and Ines Wagner for introducing me to LaTex to write up my thesis.

4 ABBREVIATIONS

BF	.....	Brightfield
BrdU	.....	5-bromo-2-deoxyuridine
BSA	.....	Bovine serum albumin
CNS	.....	Central nervous system
CV	.....	Column volumes
DF	.....	Darkfield
DNA	.....	Deoxyribonucleic acid
dpa	.....	Days post amputation
EGFP	.....	Enhanced green fluorescence protein
ES cells	.....	Embryonic stem cells
EST	.....	Expressed sequence tag
FACS	.....	Fluorescence-activated cell sorting
FGF	.....	Fibroblast growth factor
FITC	.....	Fluorescein isothiocyanate
GFP	.....	Green fluorescent protein
GST	.....	Glutathione S-transferase
hES cells	.....	Human embryonic stem cells
hFib	.....	Human fibroblasts
HS-AMEM	.....	High serum - Amphibian MEM - A1 cell culture medium
iPS cells	.....	Induced pluripotent stem cells
IPTG	.....	Isopropyl-β-D-thiogalactopyranosid
KLF4	.....	Krueppel-like factor 4 transcription factor
MBP	.....	Maltose binding protein
MEF	.....	Mouse embryonic fibroblasts
mES cells	.....	Mouse embryonic stem cells
MHC	.....	Myosin heavy chains
N-M	.....	Progenitor cells for neural and mesodermal (N-M) lineages in the tailbud
c-MYC	.....	Transcription factor
NA	.....	Numerical aperture
NANOG	.....	Homeodomain containing transcription factor
OCT4	.....	Octamer binding transcription factor 4
PBS	.....	Phosphate-Buffered Saline
PCR	.....	Polymerase chain reaction
PEC	.....	Pigment epithelial cells
qRT-PCR	.....	Quantitative real time polymerase chain reaction
RNA	.....	Ribonucleic acid
RT	.....	Room temperature
SOX2	.....	SRY (sex determining region Y)-box 2 transcription factor
SSEA	.....	Stage specific embryonic antigen

5 INTRODUCTION

In this thesis I am going to talk about class V POU factors. There is an alternative nomenclature for *Pou* orthologs across the literature. In this study the xenopus factors are named as POU25, POU60 and POU91. The factor in medaka, the zebrafish and the chicken is named as POU2. Human, mouse and lizard factors are termed as OCT4, and the two different factors in axolotl as OCT4 and POU2.

5.1 Regeneration is a natural phenomenon in a variety of species

Regeneration is defined as a process of renewal of damaged or lost cells, of tissue or even of entire body parts. It is a phenomenon that is widespread but not uniformly represented in the animal kingdom. Regenerative strategies involve rearranging of pre-exsisting tissue, utilization of adult stem cells, as well as dedifferentiation and transdifferentiation of cells (see chapter 5.2). All these strategies can act in different tissues of the same animal (Alvarado and Tsonis, 2006).

The birth on experimental biology in regeneration dates back to the 17th century when Abraham Trembley performed the first experiments on *Hydra*, a prominent species regenerating lost body structures (Lenhoff and Lenhoff, 1986).

While whole body regeneration can take place from a small amount of cells in *Hydra* or planaria, the regeneration in mammals is restricted. Mammals are able to regenerate adult liver, depending on the dimension of the damage (Yoshizato:2007p231, Hata:2007p230), intestinal-tract epithelium, skin and muscle cells and even digit tips of infants, if the amputation is distal of the first phalange and the wound not covered with epithelium (Stevenson, 1992; Han *et al.*, 2008; Yoshizato, 2007; Hata *et al.*, 2007). Other injured tissue can be replaced by connective tissue including scar formation and thus has differences and loss in function and structure compared to the original.

Urodeles such as newts and salamanders keep their remarkable regeneration capacity also as adult. Anurans like toads and frogs on the other hand lose their capacity in metamorphosis (for review see Tanaka and Ferretti (2009)). The highest vertebrates and thus, evolutionary the closest relative to human that have regenerative abilities are newts and salamanders. They can regenerate organs along the primary body axis like the tail including the spinal cord, gills, lower jaws, retina and even partially the heart but also appendages like fore- and hind limbs (Tsonis (2000), reviewed in Brockes and Kumar (2002)).

In the past decades the development of novel molecular biological tools enabled research on regenerative aspects and became more interesting. To establish therapeutic treatments to restore human tissue or entire organs at some point in the future it became important to understand the basic concept of the regeneration mechanism. Thus, various animals are necessary model organisms to study regeneration.

5.2 The source of stem cells

Regeneration requires the rearrangement of cells from pre-existing tissue, either by utilizing resident stem cells, or through cell dedifferentiation, redifferentiation, or transdifferentiation processes. This chapter describes the source of the stem cells.

5.2.1 Resident stem cells

Resident stem cells can be divided into two groups **(i)** pluripotent cells and **(ii)** reactivated tissue progenitor cells.

(i) *Hydra* has interstitial stem cells, located in the extracellular matrix which separates two single germ layers - the endoderm and the ectoderm (Galliot, 1997). All three cell types are able to self-renew, thus this animal is considered negligibly senescent (Martinez, 1998). In addition, interstitial stem cells can also produce neurons, nematocytes, secretory cells and gametes.

Another animal containing residential pluripotent stem cells is planaria. The pluripotent proliferative pre-existing cell population in adult planarians is called neoblasts. Neoblasts, are an essential cell source for regenerative processes in planaria, since they give rise to regenerating blastema cells - the key for the regenerative event. Irradiation of neoblasts and thus killing of these proliferative cells however, leads to death of the organism (Lange, 1968; Curtis and Hickman, 1926). When single clonogenic neoblasts were transplanted into lethally irradiated host, the neoblasts were able to generate all adult cells, such as the head containing neurons (ectoderm), muscle cells (mesoderm), and intestine (endoderm) (Wagner *et al.*, 2011). However, since the clonogenic neoblast implanted into irradiated host was from an asexual strain, it can not be concluded whether single neoblasts can also regenerate gonads. The clonogenic neoblasts could restore the regeneration of the lethal host, indicating that at least a subset of neoblasts are pluripotent stem cells. It had been reported that neoblasts contain genes necessary for pluripotency in embryonic stem (ES) cells, including regulators and targets of OCT4 (Onal *et al.*, 2012).

(ii) The second group of resident stem cells are tissue progenitor cells which are usually quiescent but can become reactivated after e.g. an injury. One example is the mononuclear satellite cells in mature muscle tissue. The cells are quiescent. However, after an injury they become activated and re-enter the cell cycle. Satellite cells form new myofibers in a process similar to muscle development in the embryo.

5.2.2 Reprogrammed somatic cells

The process of reprogramming somatic cells during regeneration can be categorized into two groups: **(i)** dedifferentiation followed by redifferentiation, or **(ii)** dedifferentiation followed by transdifferentiation. The transdifferentiation process can be either restricted or non-restricted. However, in literature the terms are not used in a consistent manner.

Dedifferentiation is a process where a differentiated cell returns to a stage earlier in development.

(i) Redifferentiation defines a process by which a once dedifferentiated cell returns to the original cell type. This is a lineage restricted process.

Kragl *et al.* (2009) had shown that during axolotl limb regeneration muscle cells regenerate only muscle, and not cartilage or epidermis. However, in their study it is unresolved whether the regenerated muscle cells derived from dedifferentiation of muscle cells followed by redifferentiation, or whether the muscle formation takes places due to satellite cells (see chapter 5.2.1 (ii)).

Recently it had been shown that mature osteoblasts from zebrafish dedifferentiate in regenerating bone fin tissue (Knopf *et al.*, 2011). After amputation, mature osteoblasts dedifferentiate, and due to fibroblast growth factor (FGF) signaling cells, proliferate before they migrate further distal to form part of the blastema. During regenerative outgrowth of the fin blastema cells derived from osteoblast redifferentiate only into osteoblasts but no other cell type, which means that their cell fate is restricted and dedifferentiation is not associated with obtaining a multipotent cell state (Knopf *et al.*, 2011).

(ii) Transdifferentiation describes a process in which the somatic dedifferentiated cell converts into another somatic cell type. This transdifferentiation process is either **(a)** restricted or **(b)** non-restricted.

(a) It was reported that amputated fin rays from zebrafish can regenerate *de novo* osteoblasts (Singh *et al.*, 2012). The researchers used a genetic ablation technology to destroy all skeletal osteoblasts in adult zebrafish fin. The organism was able to restore the osteoblast population within two weeks after amputation. This experiment showed that the new bone can form from a source other than dedifferentiated osteoblasts. There is a multiple cell source, including nonosteoblasts with the potential to contribute to bone regeneration (Singh *et al.*, 2012). The scientists suggest that the predominant cell type for nonosteoblasts would be intraray fibroblasts. Intraray fibroblasts express similar markers like osteblasts (e.g. MSXb, MSXc, SOX9a, COL2a1) (Akimenko *et al.*, 1995; Smith *et al.*, 2006), which in mammals is known to induce osteoblast cell fate (Karsenty, 2008).

Experiments in salamanders showed that new bone tissue can regenerate after removal of the skeletal elements followed by amputation through this area (Thornton, 1938). Kragl *et al.* (2009) had shown that dermal cells in axolotl limb are able to form cartilage and tendons during regeneration. The different cell types have a close lineage relationship since all arise from lateral plate mesoderm (Kragl *et al.*, 2009). However, from this study it is unclear whether this process is transdifferentiation from dermal cells or whether there are resident stem cells in the limb.

Another example of transdifferentiation is the process of lens regeneration in newt. Early after injury, differentiated iris cells lose its differentiated phenotype and re-enter the cell cycle (Maki *et al.*, 2009) (see chapter 7.1.2). Afterwards cells transdifferentiate and form the lens tissue. The researchers showed that stem cell pluripotency-inducing factors are expressed during lens regeneration. They hypothesize that the factors regulate a tissue-specific reprogramming (Maki *et al.*, 2009) (see chapter 5.3.1). This restricted

transdifferentiation process is further supported by observations from transplantations of reaggregated dorsal iris pigment epithelial cells (PEC) into blastema of forelimb in newt (Ito *et al.*, 1999) (see chapter 7.1.2). Ito *et al.* (1999) showed that the cells are only able to form lens tissue.

(b) A non-restricted transdifferentiation process takes place in anthomedusa. Here, isolated striated muscle fragments can undergo a pluripotent transdifferentiation and form smooth muscle cells, glandular cells, and even endoderm, nematocytes, digestive secretory gland, interstitial, and nerve cells (Schmid and Alder, 1984). This transdifferentiation to a completely new cell types indicates, that the dedifferentiated cell must have a potent character to be able to form each cell type.

The colonial tunicate *Botrylloides leachi* is able to regenerate functional adults from minute vasculature fragments, by a process called Whole Body Regeneration. Rinkevich *et al.* (2010) found that the Whole Body Regeneration takes place through activation, mobilization and expansion of "dormant" internal vasculature epithelium cells. These cells express PIWI, a *bona fide* stemness marker for self-renewal and maintenance of germ line and somatic stem cells in multicellular organisms (Carmell *et al.*, 2007; Kuramochi-Miyagawa *et al.*, 2004; O'Donnell and Boeke, 2007). Hence, the PIWI expressing cells change morphology, proliferate and differentiate, and can regenerate a new intact organism (Rinkevich *et al.*, 2010).

5.3 Pluripotency network

Pluripotency refers to a cell that has the potential to differentiate into any kind of fetal or adult cell made from the three different germ layers, the ectoderm, mesoderm and endoderm.

It has been shown recently, that a differentiated mammalian cell can be reprogrammed artificially to become an induce pluripotent stem (iPS) cell that can differentiate to various tissue types (Takahashi and Yamanaka, 2006). It was shown by *in vitro* studies that mouse embryonic and adult fibroblast cultures as well as many other differentiated cell types can be induced to form pluripotent stem cells by four transcription factors through overexpression: OCT4 (also called POU5f1) , SOX2, c-MYC and KLF4 (Takahashi and Yamanaka, 2006; Wernig *et al.*, 2007; Aasen *et al.*, 2008; Huangfu *et al.*, 2008b; Kim *et al.*, 2009b; Takahashi *et al.*, 2007; Loh *et al.*, 2009). NANOG is another factor that seems to play an important role in pluripotency and the reprogramming event (Wernig *et al.*, 2007; Okita *et al.*, 2007; Yu *et al.*, 2007; Takahashi and Yamanaka, 2006). These transcription factors are expressed in ES cells (Mitsui *et al.*, 2003; Niwa *et al.*, 2000; Scholer *et al.*, 1990) and in the early embryo (Nichols *et al.*, 1998) and are essential to maintain a pluripotent cell state.

It would be interesting to know whether the *in vitro* reprogramming to iPS cells and the *in vivo* reprogramming event during regeneration share any similarities. The pluripotency factor OCT4 is a reprogramming factor to generate iPS cells. The involvement of *Oct4* during regeneration processes in different organisms had been studied to some extend and will be described in the following chapters.

5.3.1 Expression of pluripotency associated factors in regenerating urodeles

Maki *et al.* (2009) investigated pluripotency-inducing factors during limb and lens regeneration in newt. They collected tissue of six limbs on the day of amputation, and regenerating tissue from each of six animals at 7 (early blastema stage) and 15 days post amputation (dpa) (late blastema stage). They observed significant up-regulation of *Sox2*, *c-Myc* and *Klf4* with the emergence of blastema formation. *c-Myc* expression decreased after day 7. The pluripotency-associated genes *Oct4* and *Nanog* however, were not detected by quantitative polymerase chain reaction (PCR). During lens regeneration, *Sox2* and *Klf4* showed up-regulation in very early regenerating stages (2 dpa), a feature typical to prepare pre-existing tissue for reprogramming and cell cycle re-entry (Maki *et al.*, 2009). This correlates with establishing the lens vesicle. On the other hand *c-Myc* mRNA peaked at day 8 post lentectomy, characteristic for establishing the vesicle. Since *Sox2*, *c-Myc* and *Klf4* mRNA were expressed in different stages during regeneration, and *Oct4* and *Nanog* mRNA were absent, this may explain why regenerating newt cells are not pluripotent (Maki *et al.*, 2009).
Interestingly, *Oct4* and *Nanog* mRNA are expressed in ovarian tissue indicating that newt contains both genes (Maki *et al.*, 2009).
Oct4 in axolotl was identified by Bachvarova *et al.* (2004). They localized *Oct4* mRNA in the posterior mesoderm of late gastrula stage embryos that gives rise to primordial germ cells, as well as in diplotene growing oocytes. However, they did not perform regeneration studies to investigate OCT4 expression (Bachvarova *et al.*, 2004).
Jhamb *et al.* (2011) performed an *in silico* analysis of network based transcription factors in regenerating axolotl limb to understand protein interactions present in blastema formation during limb regenerative processes. The most interconnected transcription factors in this study were c-MYC, specificity factor1 (SP1), the hepatocyte nuclear factor 4-alpha, the estrogen receptor1 and cellular tumor antigen p53. c-MYC was the factor which interacted most. Further, they identified the epigenetic reprogramming factors KLF4, OCT4, and LIN28 which interacted with c-MYC and SP1. However, they did not state whether the reprogramming factors are upregulated during limb regeneration.

5.3.2 Expression of pluripotency associated factors in regenerating xenopus

Christen *et al.* (2010) studied limb and tail regeneration in xenopus at four different time points: **(i)** non-regenerating tissue (0 dpa), **(ii)** blastema formation (1 dpa), **(iii)** blastema expansion (3 dpa) and **(iv)** blastema redifferentiation (5 dpa) performing quantitative real time PCR (Christen:2010p198). They compared the results to those obtained from cells of the animal cap, which were used as pluripotent control cells. A further control was made by using regenerating incomplete limbs during metamorphosis, a time when xenopus loses its regeneration capacity.
Christen *et al.* (2010) showed that in the tail, the mRNAs of the pluripotency associated factors *Zic3, Tert-A,*

Dppa2/4 and *Sall4* were expressed at a lower level in 1 dpa and 3 dpa compared to cells of the animal cap. The two reprogramming factors *Sox2* and *c-Myc*, and *Fut-1*, an early marker in the reprogramming process, however, were expressed similarly or even at higher level in 1 dpa to 5 dpa samples. However, they did not detect any of the xenopus *Pou* homologs *Pou25, Pou60, Pou79, Pou91* in the tail at the time points tested. In limb regeneration, *Zic3* mRNA was not expressed in the time points tested (Christen *et al.*, 2010). *Dppa2/4* did show expression but at a very low level. *Sall4* mRNA expression peaked on 1 dpa, but the level was lower than in pluripotent animal cap cells. *Sox2* mRNA was highly upregulated in non-regenerating tissue (0 dpa) compared to animal cap cells and the level decreased over time. *c-Myc* did not show a significant change in expression levels during limb regeneration, and xenopus *Pou* homologs were not detected in the tested time points (Christen *et al.*, 2010).

Interestingly, in regenerating incomplete limbs from xenopus Christen *et al.* (2010) also detected *Sox2, c-Myc* and *Fut1* mRNA upregulation that peaked at 1 dpa and decreased to the level of non-regenerating limbs by 3 dpa. However, they did not further speculate on that observation. The investigators also observed a higher mRNA level of *c-Myc* in the older limbs than in young limbs.

The shortcoming of this study is that the expression levels mentioned here were compared to cells of the animal cap, a pluripotent cells source. However, since these are cells in a developing embryo, it cannot be compared to expression levels in regenerating cells directly. The results would have had more significance had the expression levels of the regenerate been compared to the levels obtained using mature non-amputated tissue.

5.3.3 Expression of pluripotency associated factors in regenerating zebrafish

Regeneration studies on zebrafish fin investigating the role of pluripotency related genes *Pou2, Klf4, Sox2, c-Myc, Tert, Zic3, Hsp90a* and *Sall4* was also performed by quantitative real time PCR (Christen *et al.*, 2010). The researchers compared the expression of these factors in both regenerating (four different time points) and non-regenerating limbs to blastula stage embryos, a pluripotent cell source and thus expressing all eight pluripotency related factors.

Pou2, Klf4 and *Sall4* mRNA expression in early regenerating fin was significantly lower compared to blastula stage embryos (Christen *et al.*, 2010). All three factors have also been present in non-regenerating fin, but at much lower level than in the blastula. *c-Myc, Tert, Zic3* and *Hsp90a* mRNA showed similar expression levels in non-regenerating fin and blastula stage embryos (Christen *et al.*, 2010). *Sox2* mRNA on the other hand was upregulated in non-regenerating fin in contrast to blastula embryo (Christen *et al.*, 2010). However, none of the tested markers showed an upregulation in the process of fin regeneration.

Again, it is not clear why the investigators chose to compare the expression levels of regenerating fin to blastula stage embryos and not to levels in non-amputated fin tissue.

It was reported that regeneration of retina tissue induces expression of some pluripotency factors (Ramachan-

dran *et al.*, 2010). The proneural transcription factor *Ascl1a* induces the microRNA-binding protein LIN-28 expression in Müller glia cells after injury. Müller glia cells are cells giving rise to neurons in the retina upon injury. LIN-28 suppresses *Let-7* microRNA and hence blocks expression of the regeneration-associated genes *Ascl1a, Lin-28* and *Pou2* (Ramachandran *et al.*, 2010). POU2 protein shows a low expression in uninjured retina. It is assumed that *Let-7* represses this expression to prevent premature Müller glia cells dedifferentiation (Ramachandran *et al.*, 2010).

5.4 Aim of this thesis

It is well known that the mammalian transcription factor *Oct4* (also called *Pou5f1*), a class V POU gene (see also chapter 6.1.2), is responsible in maintaining pluripotency in developing embryos. Further, it is a key factor in reprogramming differentiated cells. An *Oct4* ortholog was also identified in *Ambystoma mexicanum* - the axolotl, a salamander with remarkable abilities of regeneration. However, it is unclear whether axolotl OCT4 has a similar effect like the mammalian OCT4. In general, it is unknown whether reprogramming of cells during regenerative processes, and reprogramming of somatic cells to generate induced pluripotent stem (iPS) cells, share any similarities.

We are interested in the involvement of pluripotency genes *Oct4* and the newly identified *Pou2*, as well as the gene for the transcription factor *Sox2* in regenerating axolotl spinal cord. Is the pluripotent character of POU factors limited to mammals or is it an ancient characteristic of lower vertebrates? However, this model organism would be a very complex *in vivo* system with which to study pluripotency. Thus, we decided first for the simpler system of using an *in vitro* assay to investigate the pluripotent ability of the POU factors. Therefore this work is separated into two chapters:

(1) Reprogramming to pluripotency is an ancient trait of vertebrate OCT4 and POU2 proteins

So far, only studies about the maintaining of ES cell pluripotency using class V POU proteins from different vertebrate species have been performed (Morrison and Brickman, 2006). However, it is not clear whether class V POU proteins from different species are able to generate iPS cells. To our knowledge this is the first study investigating pluripotent character of different PouV homologs.

We first identified a new gene, *Pou2*, a member of the class V POU family, in axolotl and examined whether the *Pou2* ortholog is different from the already identified putative *Oct4* sequence. Phylogenetic analysis showed a clear distinction of both genes in the axolotl. Afterwards we determined the mRNA pattern of *Pou2* during embryogenesis and compared it to *Oct4* mRNA and protein. Both genes are expressed in the pluripotent animal cap region of the embryo. Apart from this similarity, both genes have a different expression pattern. Next, we wanted to know whether the axolotl POU2 as well as the axolotl OCT4 have a potent character like POU orthologs in other species. Therefore, we performed reprogramming experiments using mouse or human fibroblasts and transduced them with axolotl *Pou2* or *Oct4*, in combination with human or

axolotl *Sox2, c-Myc* and/or *Klf4*. Furthermore, we compared the reprogramming ability with POU factors from mouse, human, zebrafish, medaka and xenopus. The iPS cells generated were further characterized in terms of their endogenous pluripotency gene expression profile.

(2) Regenerating spinal cord cells are pluripotent

We investigated the role of *Pou2, Oct4* as well as *Sox2* gene expression in regenerating spinal cord tissue to determine whether OCT4 and POU2 have similar pluripotent character as it was shown in our *in vitro* studies. We performed *in situ* hybridizations and antibody staining to localize the factors in the regenerating spinal cord. *Sox2* and *Oct4* were expressed during spinal cord regeneration and thus we wanted to know whether these cells would also have a pluripotent character *in vivo*, meaning that cells would not be restricted in their linage but rather able to form other tissue types. To investigate this, we performed transplantations of enhanced green fluorescence protein (EGFP) labeled spinal cord into somite stage embryos and showed the formation of muscle cells.

6 Chapter I: Reprogramming to pluripotency is an ancient trait mediated by vertebrate OCT4 and POU2 proteins

6.1 Introduction

6.1.1 Composition and interactions of OCT4 - a class V POU transcription factor

The name POU is an abbreviation from three transcription factors. "*P*" stands for the Pituitary-specific Pit-1, "*O*" for the octamer transcription factors Oct-1 and Oct-2 with an octamer sequence of ATGCAAAT and "*U*" for the neural transcription factor Unc-86. The POU family consists of 14 different members, which all have the conserved POU domain, and a variable N- and C-terminus in common.

The POU domain is composed of two subunits separated by a non-conserved flexible linker region of 15 to 55 amino acids. The N-terminal subunit is named the POU specific domain and the C-terminal subunit is the homeobox domain.

In order to bind to the target genes OCT4 forms a heterodimer with SOX2. SOX2, the short form of SRY (sex determining region Y)-box 2, is a SOX family transcription factor. This family features a highly conserved DNA binding domain called High-mobility group (HMG) box domains which contains approximately 80 amino acids. To bind to target genes, the POU domain of OCT4 has to first interact with the HMG domain of the transcription factor SOX2 to form a heterodimer on the promoter region of the target DNA (Ambrosetti *et al.*, 2000). The target DNA has a specific character of the OCT4/SOX2 binding sites (Badis *et al.*, 2009; Ambrosetti *et al.*, 2000). The binding leads to a stronger interaction of DNA and protein domains, and activates intrinsic activation domains of the proteins. Interactions between proteins and protein-DNA can result in conformational changes causing activation of gene expression (Ambrosetti *et al.*, 2000).

OCT4 and SOX2 dimerization activate many different promoters of pluripotency-associated genes (Remenyi *et al.*, 2003), and thus contribute to the pluripotent state of a cell (Boyer *et al.*, 2005).

Next to OCT4, NANOG is another homeodomain transcription factor which essentially regulates ES cell identity and early development by maintaining pluripotency of cells (Nichols *et al.*, 1998; Mitsui *et al.*, 2003). Genetic mouse studies showed that both intrinsic factors have distinct roles but they may function in related pathways. Hence the regulators maintain the developmental potential of ES cells (Chambers, 2004). It was shown that disruption of NANOG and OCT4 leads to inadequate differentiation of ES cells and ICM to extra-embryonic endoderm and trophectoderm respectively (Mitsui *et al.*, 2003; Nichols *et al.*, 1998; Chambers *et al.*, 2003). On the other hand, overexpression of OCT4 in ES cells results in a similar phenotype to the loss of NANOG function (Chambers *et al.*, 2003; Mitsui *et al.*, 2003; Nichols *et al.*, 1998; Niwa *et al.*, 2000).

Boyer *et al.* (2005) performed chromatin immunoprecipitation combined with DNA microarrays using human H9 ES cells and determined target sites which are occupied by OCT4. They detected protein-DNA interaction similar to analysis in mouse ES cells, including *Oct4, Sox2, Nanog, Lefty2/ebaf, Cdx2, Hand1, Dppa4,*

Gja1/Connexin43, Foxo1A, Cripto/Tdgf1, and *Zic3* (Abeyta *et al.*, 2004; Brandenberger *et al.*, 2004; Niwa, 2001; Sato *et al.*, 2003; Kuroda *et al.*, 2005; Wei *et al.*, 2005; Okumura-Nakanishi *et al.*, 2005). Results from Boyer *et al.* (2005) indicate that OCT4, SOX2, and NANOG co-occupy the promoter regions of a large number of genes. In addition, many of these target genes encode homeodomain transcription factors necessary in development, and further, these regulators contribute to ES cells identity.

6.1.2 Evolution of class V POU transcription factors

About 350 million years ago the first amphibial ancestors of frogs and salamanders evolved. Sauropsids developed from basal amniotes approximately 320 million years ago. Their progeny are turtles, snakes, lizards, crocodilians, and birds. About 90 million years ago synapsida evolved. The first monotreme mammals developed and about 50 million years ago marsupials and placentals evolved. How the transcription factors POU2 and OCT4 have evolved in these organisms has been discussed controversially. POU2 and OCT4 (also called POU5f1), belong to the class V POU family. The different hypotheses for class V POU evolution are discussed here.

(1) Niwa *et al.* (2008) reported first that *Oct4* had only been identified in marsupials and eutherian mammals. Zebrafish *Pou2* and xenopus *Pou91* were previously thought to be *Oct4* orthologs (Burgess *et al.*, 2002; Snir *et al.*, 2006). However, synteny analysis identified different genomic positions suggesting these genes are paralogs (Niwa *et al.*, 2008). These scientists claim that a single proto-orthologous class V POU gene existed in ancestral jawed vertebrates, which is *Pou2* related and gave rise to *Oct4* by a gene duplication event in early mammalian evolution. Co-existence of *Oct4* and *Pou2* in monotremes and marsupials, and *Pou2* being present in non-mammalian vertebrates from which *Oct4* is absent support the gene duplication hypothesis in early mammalian development (Niwa *et al.*, 2008). It was considered that OCT4 is a mammal specific transcription factor (Burgess *et al.*, 2002; Niwa *et al.*, 2008).

The initially identified *Oct4* gene in axolotl, a salamander (and thus a lower non-mammalian vertebrate) showed an protein sequence similarity of 88% to mammalian OCT4. It was the most closely related ortholog to mammals identified at that time (Bachvarova *et al.*, 2004).

(2) Frankenberg *et al.* (2010) have also investigated the evolution of class V POU domain transcription factors and refute the previous hypothesis. They affirm that there was a gene duplication event in the ancestral class V POU during early evolution of tetrapods when *Oct4* arose from *Pou2*. This means that *Oct4* is not mammal specific, as previously described. Using BLAST search they did not detected a *Pou2* ortholog in lamprey, lancelet, or tunicate genomes. But they identified at least one *Pou2* ortholog in higher taxa, indicating that class V POU domain transcription factors generated during gnathostome evolution (Frankenberg *et al.*, 2010). Besides *Oct4* and *Pou2* orthologs present in platypus and opposum (Niwa *et al.*, 2008), they also found both orthologs in tammar (Frankenberg *et al.*, 2010). Investigation of the axolotl OCT4 (Bachvarova *et al.*, 2004) and the assembled sequence of lizard OCT4 showed a significant protein similarity to other OCT4 factors.

This conclusion is supported by two more observations. First, there is a conserved transcription starting sequence, MAGH, at the N-terminus which is not present in all other analyzed putative *Pou2* orthologs. On the other hand, there is an absence of a single arginine residue in all *Oct4* orthologs within the POU specific domain (see chapter 6.1.1). These characteristics are highly unlikely to have occurred independently in different lineages. An additional verication of the relationship among class V POU genes was performed by synteny analysis. Since, the lizard genome was not completely known, the synteny is at least conserved with respect to OCT4 (Frankenberg *et al.*, 2010). Hence, the scientists concluded that lizard *Oct4* is an orthologue of mammalian *Oct4*. Further, they claimed that there was a gene duplication in early tetrapod evolution where *Oct4* arose from *Pou2* (Frankenberg *et al.*, 2010). Actinopterygii like zebrafish and medaka, aves (e.g. chicken), and amphibia from the anura order (e.g. frog) have retained *Pou2*. On the other hand urodeles like axolotl and reptilian (e.g. lizard), and eutherian like mouse and human mammals kept the *Oct4* gene (Frankenberg *et al.*, 2010; Bachvarova *et al.*, 2004).

6.1.3 Expression of class V POUs during embryonic development

The mammalian *Oct4* encodes for a key regulator to maintain pluripotent character in ES cells (Boyer *et al.*, 2005; Rodda *et al.*, 2005; Scholer, 1991), the inner cell mass, and the epiblast. After gastrulation OCT4 is downregulated. The cells maintaining OCT4 expression are the posterior epiblast and the primitive streak (Morrison and Brickman, 2006) as well as the primordial germ cells (reviewed in Pesce and Scholer (2001)) to facilitate germ cell lineage (Frankenberg *et al.*, 2010; Boyer *et al.*, 2005; Rodda *et al.*, 2005; Scholer, 1991; Pesce and Scholer, 2001; Kehler *et al.*, 2004).

In mouse, OCT4 is also expressed after gastrulation until the 16-somite stage embryo (Downs, 2008). At headfold stage, OCT4 is present in surface ectoderm and neural ectoderm of caudal node, which is the anterior end of the primitive streak formed in early gastrulation (Downs, 2008) (see also chapter 7.1.3).

In zebrafish *Pou2* is also involved in early embryo development. mRNA was observed from the one-cell stage to the gastrula stage embryos (Takeda *et al.*, 1994). *Pou2* mRNA was found in blastomeres until the midblastula stage. During gastrulation the expression was restricted to the epiblast (Takeda *et al.*, 1994).

Xenopus laevis contains three POU factors, OCT25, OCT60 and OCT91 (Cao *et al.*, 2006, 2010). In this thesis they are referred as POU25, POU60 and POU91, respectively. POU25, POU60 and POU91 are expressed during oogenesis and early embryogenesis (Hinkley *et al.*, 1992). *Pou25* mRNA was localized at low levels in oocytes and cleavage-stage embryos and reached its maximum during gastrulation (Hinkley *et al.*, 1992). *Pou60* mRNA was located in the animal hemisphere of mature oocyte (Hinkley *et al.*, 1992) and accumulated after fertilization (Whitfield *et al.*, 1995). The highest mRNA level was observed in the animal cap of mid-blastula embryo (Whitfield *et al.*, 1995). *Pou91* mRNA levels increased after midblastula transition and peaked during late gastrulation (Whitfield *et al.*, 1995). The expression of all three genes decreased during late gastrulation and early neurulation.

All these factors have in common that they are expressed during early embryonic development and maintain the pluripotent character of the embryonic cells.

6.1.4 Self-renewal and pluripotent ability of class V POU transcription factors

Morrison *et al.* investigated the conserved roles for OCT4 homologues concerning the maintainance of multipotency during early vertebrate development (Morrison and Brickman, 2006). Since *Oct4* is essential for ES cell self-renewal (Niwa *et al.*, 2000) they tested POU V proteins from xenopus, axolotl and zebrafish for the ability to substitute *Oct4* in mouse ES cells. For these *in vitro* rescue studies they used *Oct4*$^{-/-}$ knockout mouse murine ES, and electroporated the cells with plasmid constructs encoding for one of the POU factors. They measured the extent of *Oct4* rescue conveyed by the production of ES cell-like alkaline phosphatase positive colonies, as well as the generation of clonal cell lines in long-term self-renewal, and by the expression of ES cell specific proteins. The investigators showed that *Pou91* has the ability to rescue the wild type phenotype in *Oct4*$^{-/-}$ knockout cells (Morrison and Brickman, 2006). *Pou60* and *Pou25* from *Xenopus laevis* as well as *Oct4* from axolotl has some capacity to rescue ES cell self-renewal in the absence of endogenous *Oct4* (Morrison and Brickman, 2006). On the other hand, Morrison and Brickman (2006) reported that zebrafish *Pou2* is not able to substitute for *Oct4* in ES cells nor to rescue the Xenopus *PouV* depletion phenotype.

Studies using the chicken *PouV* ortholog demonstrated the maintenance of pluripotency and self-renewal ability of chicken ES cells (Lavial *et al.*, 2007a).

These different behavior of vertebrate *Oct4/Pou2*-like homologs in the rescue ability suggests a variability in self-renewal activity between the *Oct4* and *Pou2* genes (Niwa *et al.*, 2008; Morrison and Brickman, 2006).

6.1.5 Reprogramming of somatic cells to generate induced pluripotent stem cells

Induced pluripotent stem (iPS) cells are a cell type similar to pluripotent stem cell but generated artificially from non-pluripotent somatic cell. The induction is triggered by the expression of maximally four proteins: OCT4, SOX2, KLF4 and c-MYC, first shown by Takahashi and Yamanaka (2006).

The researchers tested 24 gene candidates encoding proteins which play a role in maintaining ES cell state and evaluated them in a G418 resistance *in vitro* assay. They inserted β-galactosidase and neomycin resistance genes (βgeo) into the mouse *Fbx15* gene (Tokuzawa *et al.*, 2003). ES cells were resistant to high concentrations of G418 in culture, whereas somatic cells were sensitive to a normal concentration. Mouse embryonic fibroblasts (MEF) from homozygous (βgeo) knockin *Fbx15* mouse were transduced with retrovirus (Morita *et al.*, 2000) encoding for the 24 candidate factors.

They identified OCT4, SOX2, KLF4 and c-MYC as the factors inducing pluripotency. In contrast, NANOG is not necessary for induction and maintenance of iPS cells.

The iPS cells have similar characteristics to stem cells e.g. the expression of stem cell marker proteins such

as NANOG, OCT4, SSEA4; the embryoid body and teratoma formation (Takahashi and Yamanaka, 2006) and the chromatin methylation pattern of the promoter.
Generating iPS cells from somatic tissue might prove to be of huge importance for treating diseases like spinal cord injury, and because cells generated from their own somatic tissue cells avoid both the ethical difficulties regarding the application of human embryos and the tissue rejection after an transplantation in patients.

6.1.6 The goal of this project

In early tetrapod evolution the ancestral class V *Pou* gene duplicated and gave rise to *Oct4* and *Pou2* (Frankenberg *et al.*, 2010). Both transcription factors are responsible in maintaining pluripotency in early developing embryos. Further, some of the factors have the ability to confer self-renewal to ES cells.
Axolotl has *Oct4* and *Pou2*. However, it is not clear whether the factors have a similar potent conferring ability like the mammalian OCT4. Is the pluripotent character of cells expressing POU factors limited to mammals or is it an ancient character of lower vertebrates? It is unknown whether PouV proteins from different species are able to generate iPS cells. We used an *in vitro* assay to investigate the pluripotent ability of different POU factors.

6.2 Results

This part of the thesis was a joined project with the group of Prof. Dr. Hans Schöler from MPI for Molecular Biomedicine in Münster. They performed all reprogramming studies and the analysis of reprogrammed cell lines.

In the following experiments we applied axolotl and human transcription factors. For clarity we use lower case characters when axolotl factors *AxOct4* (o), *AxPou2* (p) and *AxSox2* (s) were applied. On the other hand capital letters symbolize the human factors *Oct4* (O), *Sox2* (S), *Klf4* (K) and *c-Myc* (M).

6.2.1 Identification of the *Pou2* gene in axolotl

Prior to this work, a *Pou2* ortholog in axolotl had not been identified. We were interested whether axolotl has also *Pou2* as well as *Oct4*, first isolated and identified by Bachvarova *et al.* (2004). If so, we wanted to know whether the *Pou2* ortholog can be distinguished from the existing putative *Oct4* sequence. To examine this we carried out a BLAST search on contiguously assembled expressed sequence tags (ESTs) which we obtained from Sanger, and 454 sequences using the *AxOct4* sequence. We identified a single partial sequence which was similar but different to the known Oct4 sequence. BLAST search with the identified new sequence determined the vertebrate Pou2 family members as the closest orthologs. We performed a screening of our axolotl long-insert cDNA library to define the entire *Pou2* coding sequence which is shown in Figure 1. The *Pou2* coding sequence has a length of 1359 base pairs which corresponds to a POU2 protein sequence of 453 amino acids. BLAST analysis showed that the putative protein sequence has a variable N- and C-terminus, and a POU domain composed of two subunits, the POU specific domain and the homeobox domain.

Figure 1: Coding region of axolotl *Pou2* sequence
Axolotl *Pou2* was isolated from our long-insert cDNA library using primers designed from the identified contig sequence. The insert was sequenced, and the coding sequence (green) and deduced protein sequences (black) are shown here.

6.2.2 Phylogenetic analysis of class V POU proteins shows that axolotl has *Pou2* and *Oct4* ortholog

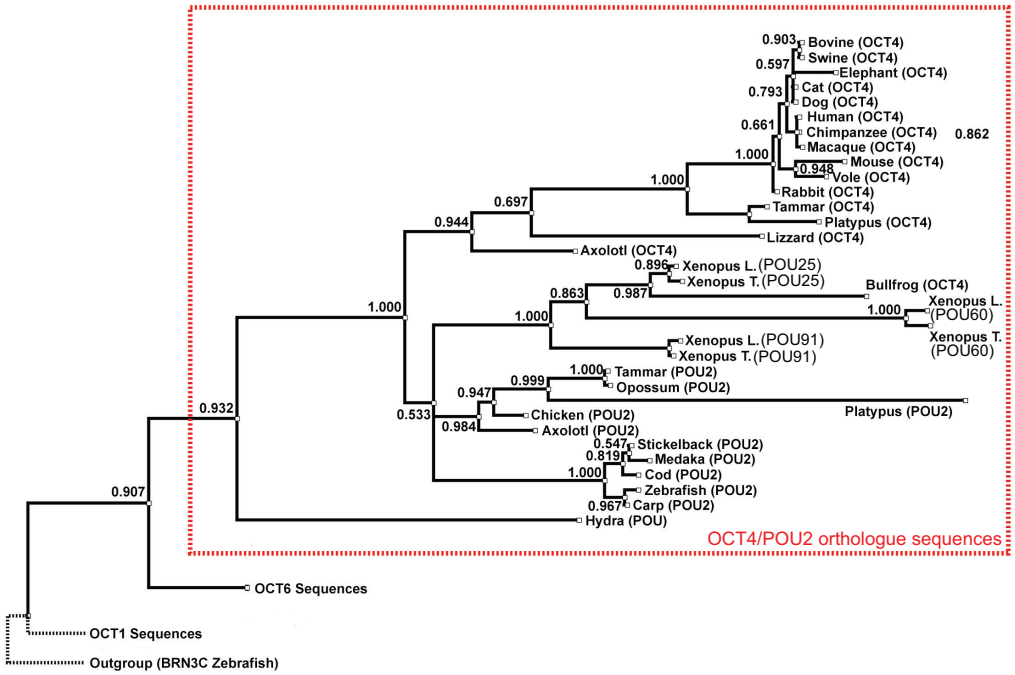

Figure 2: Phylogenetic tree of POU factors from various species
Shows the phylogenetic tree of OCT4 and POU2 homologs from a variety of species. The assembly of the POU sequences suggests that axolotl has the *Pou2* as well as the *Oct4* homolog. Branches are labeled with their relative length and the posterior probabilities are marked at the corresponding nodes. As an outgroup BRN3C from zebrafish was used. OCT1 and OCT6 sequences, and the dotted branches indicate the split of the subtree of the OCT4/POU2 sequences. The length of the dotted branches is not scaled. Xenopus OCT25, OCT60 and OCT91 are referred here as POU25, POU60 and POU91, respectively.

We identified *Pou2* in the axolotl. We want to know whether the axolotl *Pou2* is a true *Pou2* ortholog or an *Oct4* ortholog.

We therefore identified the gene orthology of the putative axolotl POU2 and the OCT4 by performing a multiple sequence alignment from various species. The conclusion using either the entire POU protein sequences or of only the POU DNA-binding domains for analysis, were the same. The phylogenetic tree illustrated in Figure 2 is based on the multiple sequence alignment of the DNA-binding domains in the POU factors.

We observe a splitting of class V POU factors into two major branches, one for OCT4 sequences the other one for POU2. The POU2 branch is divided into three different sub-categories. We monitored a cluster formation of the newly identified axolotl POU2 sequence together with POU2 sequences from chicken, platypus, opossum and tammar. In addition, a distinct sub-branch is formed by assembling the POU2 sequences from stickleback,

medaka, cod, zebrafish and carp. Xenopus POU class V ancestor gene underwent a gene duplication in evolution. Thus, we observed a separate branch for the different xenopus POU orthologs POU25, POU60 and POU91.

On the other hand, the OCT4 sequence from axolotl clusters with sequences from lizard, platypus, tammar and different eutherian mammals like rabbit, mouse, chimpanzee and bovine.

Our results indicate that axolotl *Pou2* and *Oct4* are clearly distinguishable genes. This means that like marsupials and monotremes the axolotl has both *Pou2* as well as *Oct4* ortholog and both belong to the class V POU domain proteins. This shows that *Pou2/Oct4* orthologs can be traced back to a gene duplication at the beginning of early tetrapod lineage.

6.2.3 Synteny analyses of axolotl *Oct4* and *Pou2* support orthology to *Oct4* and *Pou2*, respectively

To confirm the genetic relationship of axolotl *Oct4* and *Pou2*, our collaborators Kevin Kump and Randal Voss analyzed the conserved synteny on these genes. Synteny analysis is used to study the genetic and thus the evolutionary relationship of different species by examining the physical co-localization of genetic loci on the same chromosome within an organism. This method is based on genetic linkage, which describes the location of genes on a chromosome.

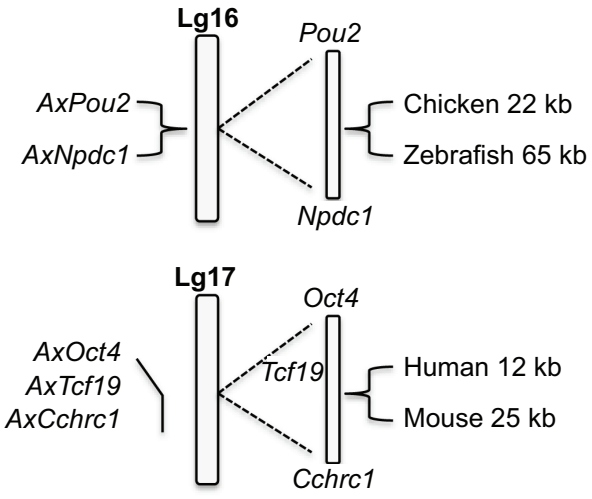

Figure 3: Synteny analysis of axolotl *Oct4* and *Pou2*
Assignment of *AxPou2* and *AxOct4* to Ambystoma linkage group (Lg) 16 and 17, respectively. *AxPou2* sequence mapped to the position of *AxNpdc1* (20 cM) and *AxOct4* (76 cM) mapped to the position of *AxTcf19* and *AxCchrc1*. The linkage relationships of *Pou2-Npdc1* and *Oct4-Tcf19-Cchrc1* show conserved syntenies in chicken-zebrafish and mouse-human, respectively. Thanks to Kevin Kump and Randal Voss who performed this experiment.

They positioned axolotl *Pou2* (*AxPou2*) and axolotl *Oct4* (*AxOct4*) within the Ambystoma genetic linkage map based on AxTg mapping panel (Voss *et al.*, 2011). The analysis is shown in Figure 3.
We could show that *AxPou2* maps to the position of *AxNpdc1* (LG16, 20 cM), *AxOct4* on the other hand to *AxCchcr1* and *AxTcf19* (LG17, 76 cM). A tight physical linkage of *Pou2-Npdc1* was noticed in chicken and zebrafish. For *Oct4-Cchcr1-Tcf19* we noted a tight physical linkage to human and mouse. This result is another support of the orthology of axolotl *Pou2* and *Oct4*.

6.2.4 Localization of axolotl *Oct4* and *Pou2* during embryogenesis

Axolotl *Oct4* was already shown to be highly abundant in gastrula stage embryos by Northern blot analysis (Bachvarova *et al.*, 2004) and they localized *Oct4* mRNA in cells of the ectoderm and presumptive mesoderm. We wanted to compare mRNA and protein of *Oct4* and *Pou2*, and determine whether the factors are expressed in pluripotent cells. Therefore, we performed *in situ* hybridization on blastula and gastrula stage embryos (Figure 4 A).
We observed a weak *Oct4* mRNA expression level in the animal half of blastula stage embryo. The *Oct4* mRNA becomes more abundant in the ectodermal surface of gastrula stage embryo. *Oct4* mRNA is expressed in the animal cap region, an area with pluripotent cells and thus equivalent to the mouse epiblast. *Oct4* was also localized in the blastopore lip of gastrula stage embryos, a region similar to the primitive streak in mouse.
To determine OCT4 protein in gastrula stage embryos we performed OCT4 antibody staining and observed a similar expression pattern of OCT4 protein when compared to *Oct4* mRNA pattern (Figure 4 B). OCT4 was expressed in the animal cap region as well as the blastopore lip.
In addition to the localization of *Oct4* we also performed *Pou2 in situ* hybridization on embryos. We detected *Pou2* similarly to *Oct4* in the ectoderm of blastula and gastrula stage embryos (Figure 5 A and B respectively). *Pou2* is highly abundant in cells of the animal cap region and the blastopore lip in gastrula stage embryos. In contrast to *Oct4*, *Pou2* was still expressed in the ectoderm and mesoderm of late neurula I stage embryos, a phase when the neural folds are close to each other but not yet fused (Figure 5 C). In late neurula IV stage embryos, where neural folds are fused in the spinal region, *Pou2* was localized in the hindbrain (Figure 5 D). This is similar to *Pou2* expression in zebrafish, which is responsible for the formation of mid-hindbrain boundary (Belting *et al.*, 2001; Burgess *et al.*, 2002).

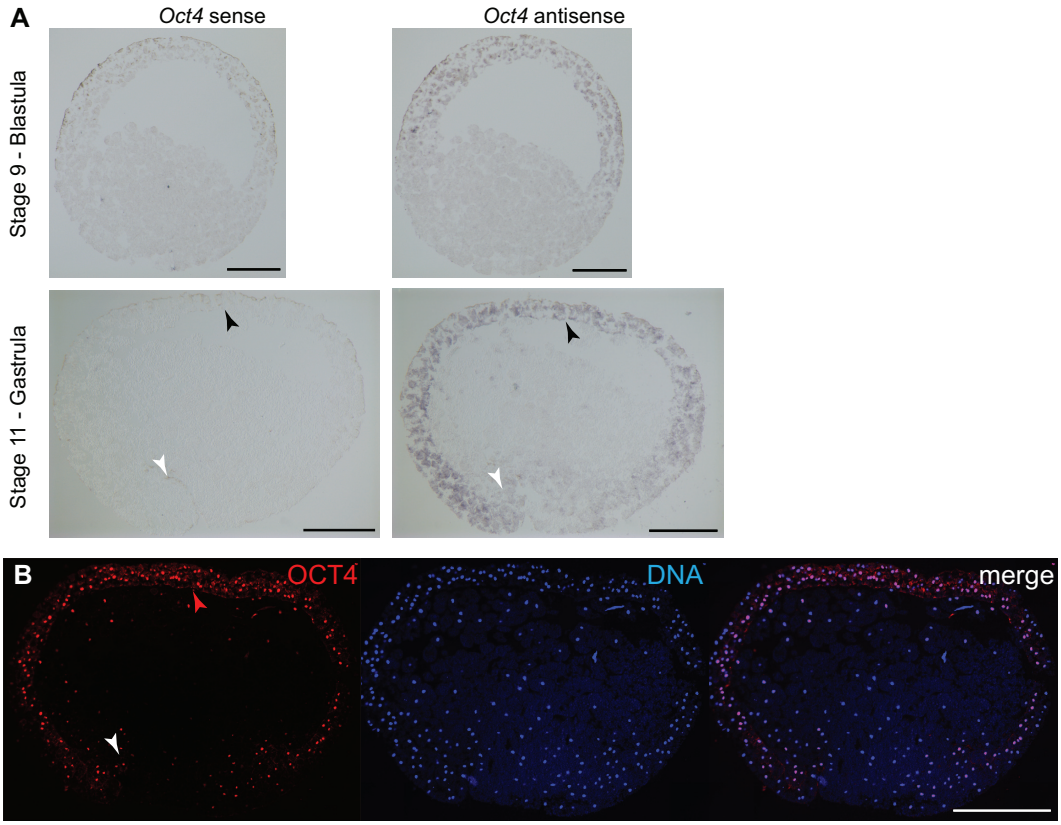

Figure 4: ***Oct4*** **mRNA pattern and OCT4 protein expression pattern in axolotl embryos** **(A)** Axolotl *Oct4* mRNA *in situ* hybridization in blastula and gastrula stage axolotl embryos. For negative controls the sense *Oct4* probe was used, which did not show any background signal. In the right panel the specific signal from the antisense probe is shown. The black arrowheads in gastrula stage embryos mark the axolotl animal cap which is equivalent to the mouse epiblast. White arrowheads indicate the axolotl blastopore lip, a region equivalent to the primitive streak in mouse. Scale bars 500 μm. **(B)** OCT4 in gastrula stage embryo is expressed in ectoderm of the animal cap (red arrowhead) and the axolotl blastopore lip (white arrowhead). Scale bar 500 μm.

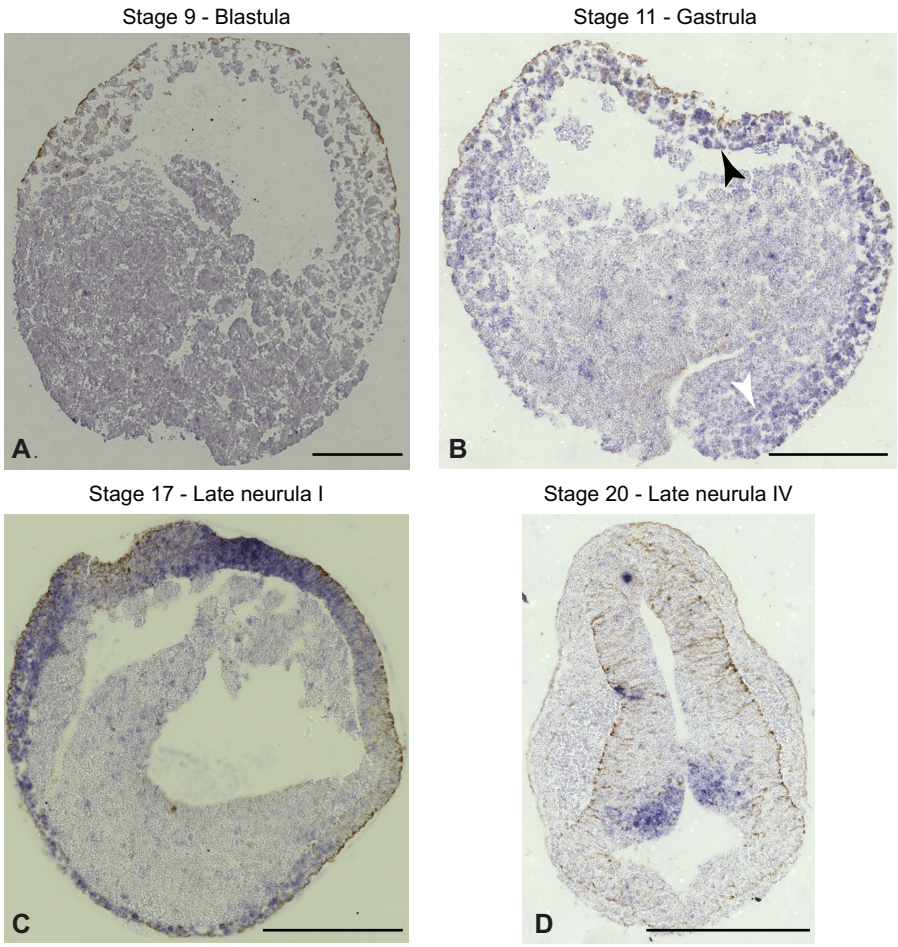

Figure 5: mRNA pattern of *Pou2* in axolotl embryogenesis
(A) *Pou2* is weakly expressed in blastula-stage embryos. **(B)** *Pou2* transcript is abundant in the ectoderm of the animal cap (black arrowhead) and the blastopore lip (white arrowhead) of an early gastrula-stage embryo **(C)** as well as in the ectoderm and mesoderm of late neurula I stage embryos. **(D)** In late neurula IV stage embryos *Pou2* expression is located in the hindbrain. Scale bars 500 μm

6.2.5 Axolotl *Oct4* and *Pou2* mRNA is expressed in gonia

Germ cell development takes place in the embryo by two different mechanisms depending on the organism. In one mechanism cells are destined to become germ cells e.g. in drosophila. The second mechanism might occur in OCT4 expressing organisms, e. g. mammals. Here, primordial germ cells are not specified at the beginning of the embryonic development. The primordial germ cells are founder cells of the gametes, and differentiate from pluripotent epiblast cells during gastrulation by mesodermal induction signals.

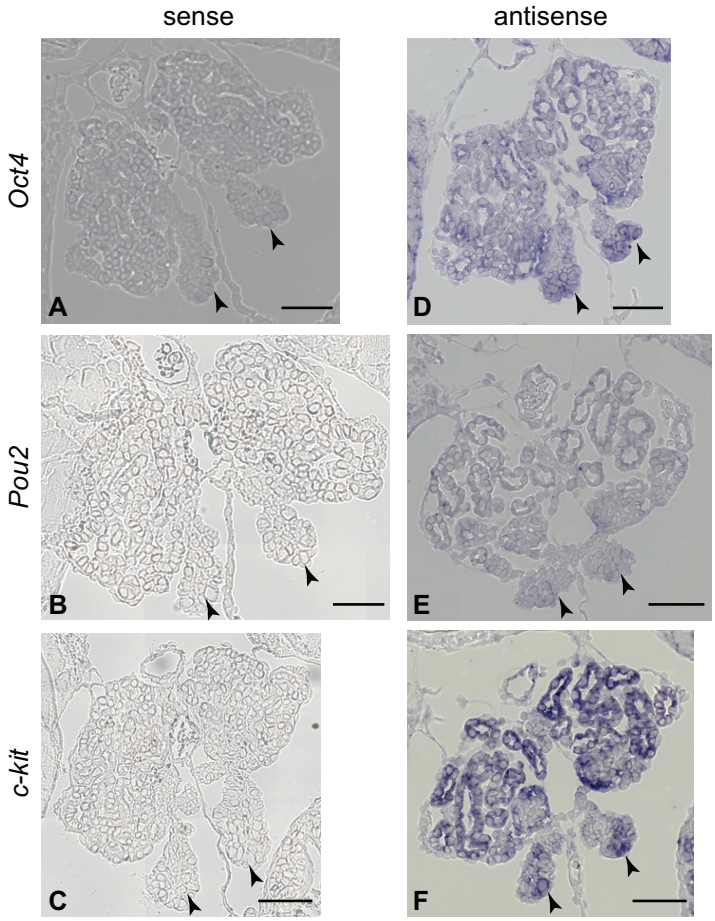

Figure 6: Localization of *Oct4, Pou2* and *c-Kit* transcripts in gonia of 3 cm axolotl larvae **(A)**, **(B)** and **(C)** show no background signal in the sense controls of *Oct4*, *Pou2* and *c-Kit* respectively. **(D)** *Oct4* **(E)** *Pou2* and **(F)** *c-Kit* shows a specific signal with the antisense probe in primordial germ cells during axolotl development. Scale bars 100 μm. Black arrowheads mark primordial germ cells.

We were interested whether also axolotl primordial germ cells express *Oct4* and whether *Pou2* is also located in this cell type. Hence, we performed *in situ* hybridization on 3 cm long axolotl larvae to investigate *Oct4, Pou2* and *c-kit* expression behavior in primordial germ cells (Figure 6). In contrast to previous experiments

(Bachvarova *et al.*, 2004) we identified *Oct4* mRNA in primordial germ cells (Figure 6 D). We could also detect weak *Pou2* in primordial germ cells (Figure 6 E). Our positive control, the transcription factor and oncogene *c-Kit* was also expressed in primordial germ cells (Figure 6 F) as was shown previously (Bachvarova *et al.*, 2004). *Oct4, Pou2* and *c-Kit* show an overlapping mRNA pattern in developing gonia which is above background level (Figure 6 A, B, C respectively).

6.2.6 Expression of axolotl *Sox2* in embryogenesis

It is well known that activation of a pluripotency target gene promoter is regulated by the interaction of the OCT4 POU domain with the SOX2 HMG domain (Ambrosetti *et al.*, 2000). Since early embryonic expression of axolotl SOX2 had not been previously described, we were interested whether *Sox2* and the pluripotency gene *Oct4* are consistent in their mRNA expression pattern in embryos. Therefore we extracted RNA from different embryonic stages and synthesized cDNA using reverse transcriptase (+ RT). We determined *Sox2* expression above background signal (- RT) during early embryogenesis from cleavage stages (stage 8) to neurula stage (stage 16) (Figure 7 A).

In situ hybridization of gastrula stage embryo showed *Sox2* expression in the ectoderm to be especially highly abundant in the pluripotent animal cap and weaker in the blastopore lip (Figure 7 B).

This shows that *Sox2* localization in the embryo is consistent with the expression pattern of *Oct4* and *Pou2*.

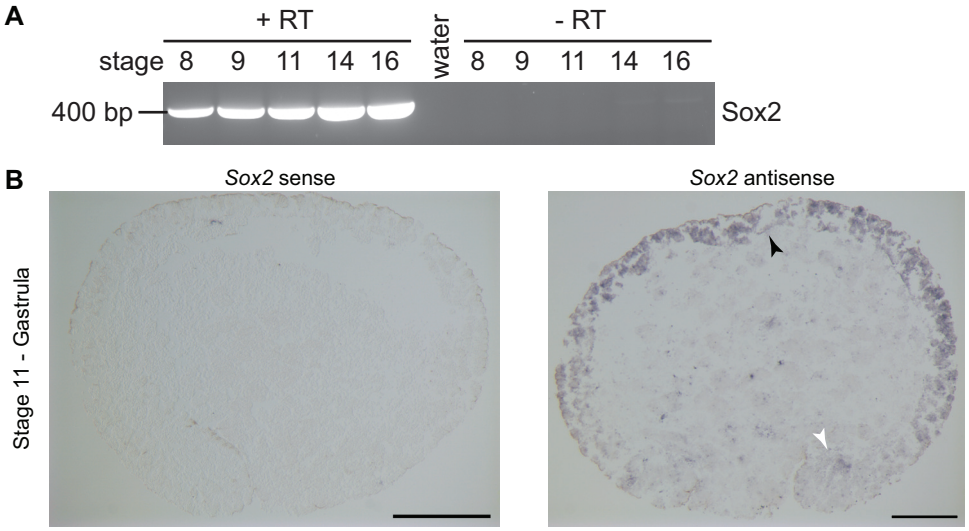

Figure 7: Localization of *Sox2* mRNA in axolotl embryos
(A) cDNA was synthesized from isolated RNA of embryonic stage 8 (cleavage), 9 (blastula), 11 (gastrula), 14 (early neurula) and 16 (late neurula) and used as template for PCR (+ RT). As negative control RNA was not treated with reverse transcriptase (- RT). Electrophorezed amplified *Sox2* product shows a significant bands at 400 bp in all stages. **(B)** *In situ* hybridization on gastrula stage embryo shows no signal in the sense control but *Sox2* is strongly present in the ectoderm of the animal cap (black arrowhead) and less abundant in the blastopore lip (white arrowhead). Scale bars 500 μm.

6.2.7 Cell reprogramming to a pluripotent state is an ancient property of *Pou2* homologs

We could show that *Oct4* and *Pou2*, as well as *Sox2* are expressed in the animal cap of gastrula stage embryos. These cells are considered to have a highly pluripotent character (Ariizumi *et al.*, 2009; Sive *et al.*, 2007). We were interested in the functional relationship of the POU orthologs and wanted to know whether factors from different species have the ability to reprogram mammalian cells and make iPS cells. We used the POU orthologs from mouse *Oct4*, human *Oct4*, axolotl *Oct4* and *Pou2*, xenopus *Pou91*, zebrafish *Pou2* and medaka *Pou2*.

For this approach we collaborated with the group from Prof. Dr. H. Schöler who performed the reprogramming experiments.

The experimental strategy is illustrated in Figure 8 A. For the reprogramming experiment we used mouse embryonic fibroblasts (MEF) which contained a green fluorescent protein (GFP) transgene driven by the mouse *Oct4* promoter (Yeom *et al.*, 1996). MEF were transduced with retroviruses carrying mouse *Sox2*, mouse *Klf4*, and mouse *c-Myc*, plus one of each different POU homologs: mouse *Oct4*, human *Oct4*, axolotl *Oct4*, axolotl *Pou2*, xenopus *Pou91*, zebrafish *Pou2* or medaka *Pou2*. After 14 days we determined the reprogramming efficiency by measuring reactivation of GFP expression and calculated the percentage of GFP expressing cells (Figure 8 B).

We showed that xenopus *Pou91*, as the only non-mammalian example, is nearly as efficient as mouse and human *Oct4* cDNAs in inducing GFP expressing cells. Also axolotl *Pou2*, axolotl *Oct4* and medaka *Pou2* showed reprogramming character, however at a much lower efficiency. In contrast, zebrafish *Pou2* is not able to establish iPS cells. This observation is fortified by Morrison and Brickman which demonstrated that zebrafish *Pou2* does not have the capacity to maintain pluripotency in mouse ES cells (Morrison and Brickman, 2006).

We wanted to make sure that there is no cross-contamination between the different POU factors. To determine this we selected two to three different iPS colonies for each of the tested homologs and genotyping the colonies (Figure 8 C). All generated iPS cells using a certain POU factor showed a clean amplified product using their respective primer, indicating that there was no cross-contamination between the different POU factors.

Furthermore, we investigated the reactivation and maintenance of GFP expression driven by the mouse *Oct4* promoter as well as alkaline phosphatase expression in the generated colonies. Therefore we performed histochemical staining on the colonies and could show that all iPS cells generated with one of the different POU factors are positive for GFP (Figure 8 D) and express alkaline phosphatase (Figure 8 E), a marker for pluripotent cells.

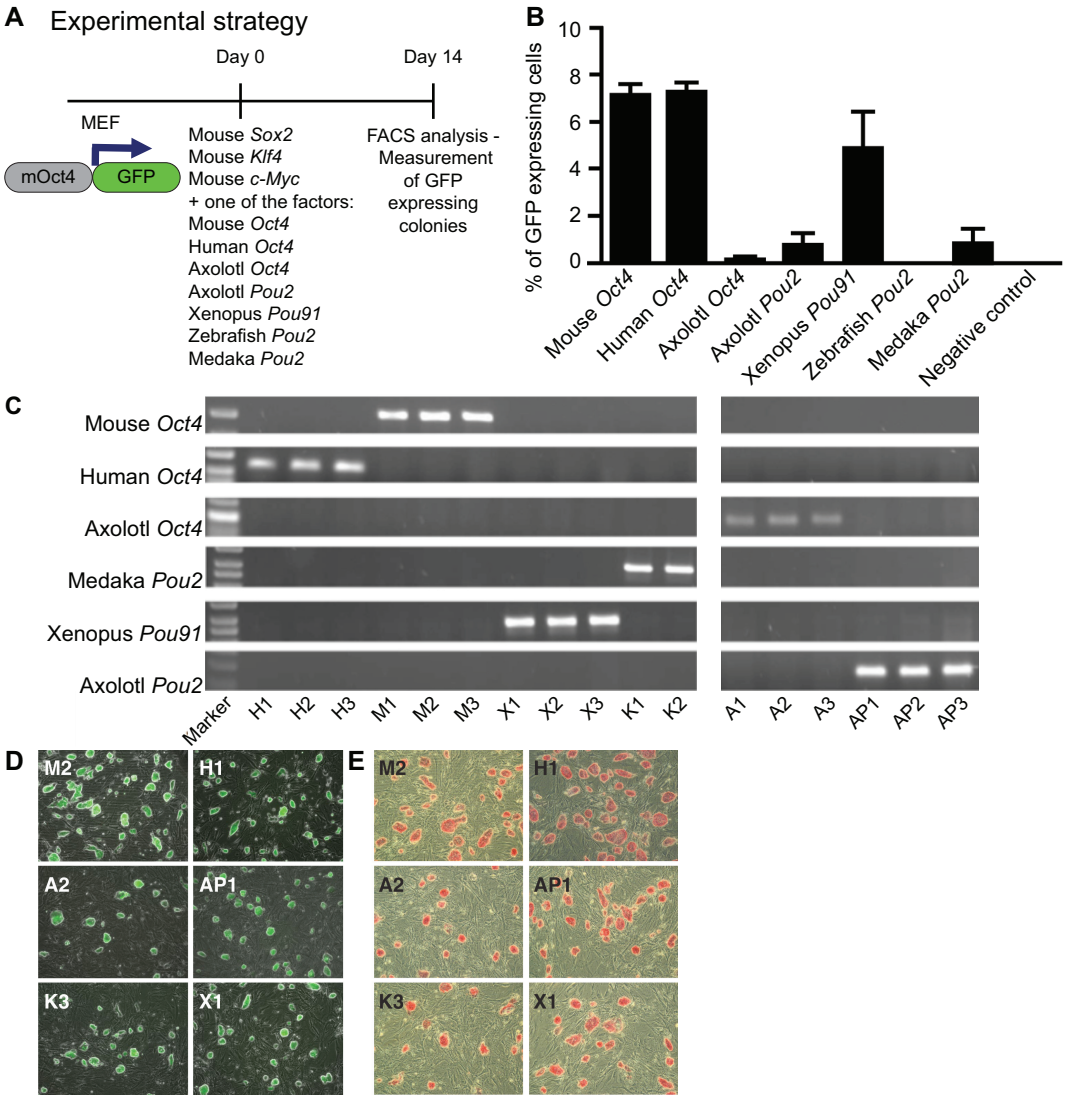

Figure 8: Generation and characterization of mouse induced pluripotent stem cells achieved by applying various POU factors
(A) Mouse embryonic fibroblasts (MEF) contain a GFP transgene driven by mouse *Oct4* promoter. On day 0 cells were transduced with pMX retroviruses coding for mouse *Sox2*, *Klf4* and *c-Myc* in addition to one of the *Pou* homologs. After 14 days the number of GFP expressing cells was measured by fluorescence-activated cell sorting (FACS). **(B)** The result is illustrated as a percentage of the total number of cells and thus indicating the reprogramming efficiency. Standard deviations were calculated from two independent experiments that were run simultaneously. **(C)** To ensure that there is no crosscontamination between the different POU factors we genotyped two to three of the derived mouse iPS cell colonies (indicated on the bottom, colony labeled with 1, 2 or 3) which were generated by using different POU factors. Primers (indicated on the left) amplify only one specific POU homolog. For each pair of primers, the clones containing the only POU homolog that can be specifically amplified are considered to be positive controls; the rest of the clones are considered to be negative controls. Amplified products for each primer pair were loaded into two different gels. **(D)** For each Pou factor, one iPS clonal cell line is depicted for GFP and **(E)** alkaline phosphatase expression, a marker for pluripotency. Generated iPS cells are marked as M, Mouse OCT4; H, Human OCT4; A, Axolotl OCT4; AP, Axolotl POU2, K, Medaka POU2; X, Xenopus POU91. The number labels each different clonal cell line established from each homolog. Experiments were performed by the collaborating group of H. Schöler.

We expect that the generated iPS cells express pluripotency markers. As further support for our hypothesis we performed quantitative RT-PCR to determine the expression of the mouse pluripotency markers *Oct4, Nanog, Fgf4, Rex1* and *Utf1* (Figure 9 A). All generated iPS cells show similar expression levels to two different mouse ES cell lines used as a positive control. In contrast, as expected the initial fibroblast cell population showed a significantly lower expression of the tested pluripotency markers.

An additional possibility to test the pluripotent character of the iPS cell is the establishing of teratomas *in vivo*. Therefore, we performed a teratoma assay where one subcutaneously inject generated iPS cells into nude athymic mice. All generated iPS cell clones differentiated into all three germ layers demonstrating its *in vivo* pluripotent capacity (Figure 9 B).

In summary, our results indicate that mouse *Oct4*, human *Oct4*, axolotl *Oct4*, axolotl *Pou2*, medaka *Pou2* and xenopus *Pou91* but excluding zebrafish *Pou2* are able to generate *bona fide* iPS cells by inducing pluripotency in mouse fibroblasts. We discovered that the inability of zebrafish *Pou2* to induce pluripotency is not characteristic of all teleost *Pou2* genes. In fact, medaka *Pou2* ortholog showed a similar potency to axolotl *Oct4*.

Our data indicate that the reprogramming ability to a pluripotent cell state is an ancient trait of *Pou2* and *Oct4* homologs.

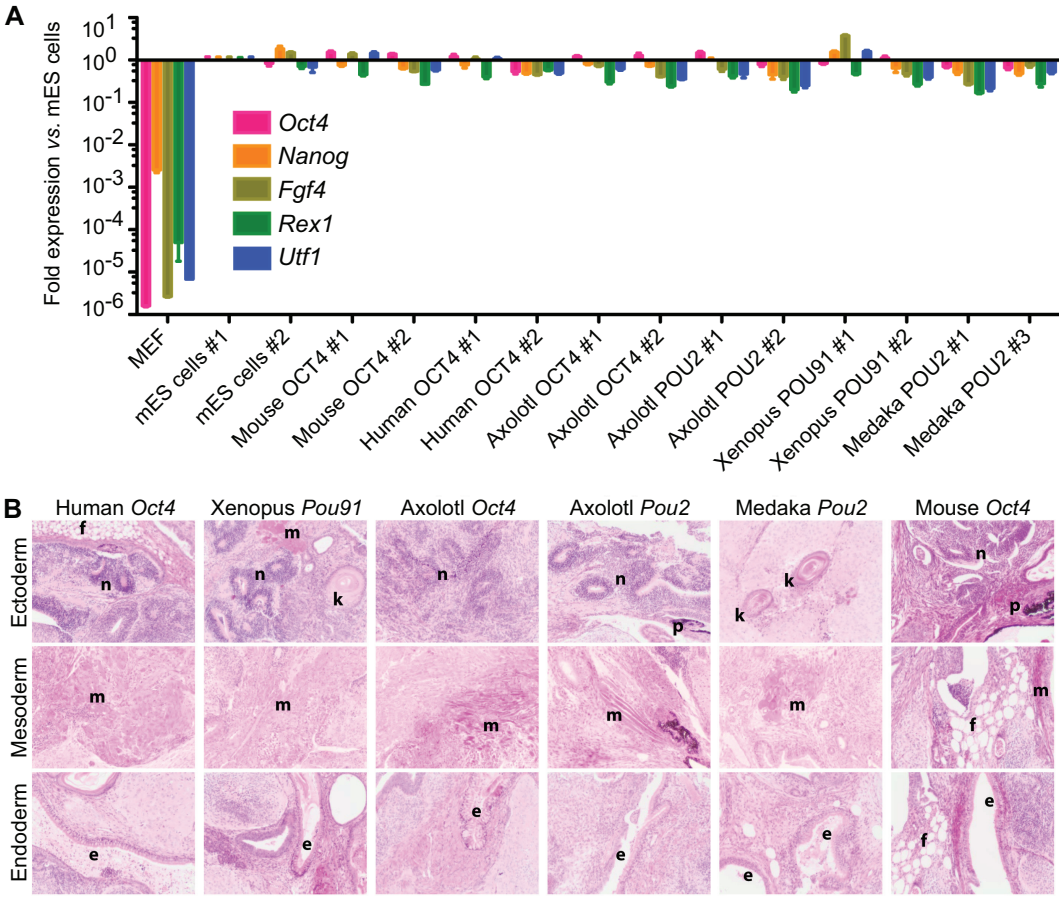

Figure 9: Expression of endogenous pluripotency markers and teratoma assay of mouse iPS cells which were generated by applying the different POU factors
(A) Expression of endogenous pluripotency markers was measured by qRT-PCR in two clonal iPS cell lines (#1, #2 or #3) established applying one of the various POU factor, in two mES cell lines and in MEF. All data are calibrated to mES cells #1, which is defined as 1 and thus plotted relatively to the mES cells #1. Error bars reflect the standard error mean based on replicates. **(B)** Teratoma assay of mouse iPS cells. Nude mice were injected subcutaneously with mouse iPS cells generated using the different POU factors. Four weeks later sections of generated teratomas were stained with hematoxylin and eosin and showed all three embryonic germ layers: endoderm (e... respiratory epithelium), mesoderm (c... cartilage, m... skeletal muscle, f... adipose tissue), ectoderm (n... neural epithelium with rosettes, p... pigmented melanocytes). Experiments were performed by the collaborating group of Schöler.

6.2.8 Axolotl *Oct4*, *Pou2* and *Sox2* reprogram human fibroblasts

Axolotl *Oct4* and *Pou2* had the potential to generate iPS cells from mouse fibroblasts. Hence, we wanted to characterize the pluripotent network in more detail in an *in vitro* study by applying axolotl *Oct4*, *Pou2* and *Sox2* to human fibroblasts, an evolutionary advanced cell type.

In mammalian ES cells *Oct4* and *Sox2* activate target pluripotency genes and both are essential genes to induce pluripotent stem cells (Yamanaka, 2007). Thus as positive control for our *in vitro* reprogramming assay in human fibroblasts we used the mammalian factors *Oct4*, *Sox2*, *Klf4* and with or without *c-Myc*. To test the pluripotent character of the axolotl *Oct4*, *Pou2* and *Sox2* we exchanged the human factors and replaced them by one or two factors from the axolotl. The tested combinations are summarized in Table 1.

Table 1: Tested combinations to reprogram human fibroblasts

Abbreviation	**Factors**
OSK	human *Oct4, Sox2, Klf4*
OSKM	human *Oct4, Sox2, Klf4, c-Myc*
osK	axolotl *Oct4, Sox2*, human *Klf4*
oSK	axolotl *Oct4*, human *Sox2, Klf4*
OsK	human *Oct4*, axolotl *Sox2*, human *Klf4*
osKM	axolotl *Oct4, Sox2*, human *Klf4, c-Myc*
oSKM	axolotl *Oct4*, human *Sox2, Klf4, c-Myc*
OsKM	human *Oct4*, axolotl *Sox2*, human *Klf4, c-Myc*
pSK	axolotl *Pou2*, human *Sox2, Klf4*
pSKM	axolotl *Pou2*, human *Sox2, Klf4, c-Myc*

Retrovirus encoding for the different factors was used to transduce two primary human fibroblast cell lines: hFib # 1 and hFib #2 (Figure 10) and thus to generate human iPS cells, termed as iPS #1 and iPS #2, respectively. We were able to establish iPS cells from all tested combinations (Table 1). A representative iPS colony which was generated with axolotl factors *Oct4* (o), *Sox2* (s) and human *Klf4* (K) is illustrated in Figure 10. The cell morphology shows a high similarity to the the human ES cell line H9 and to the iPS cells generated with only human factors (OSK).

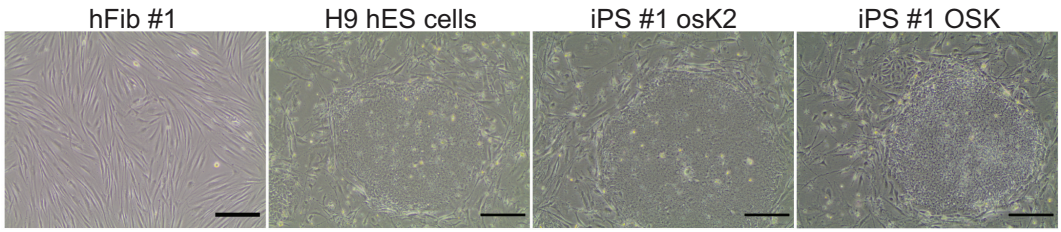

Figure 10: Generation of human induced pluripotent stem cells achieved by applying axolotl *Oct4* and axolotl *Sox2*
Panel illustrates an iPS cell colony generated by applying axolotl *Oct4* (o), *Sox2* (s) and human *Klf4* compared to the negative control, the initially used human fibroblasts (hFib #1). Positive controls were the human ES cell line H9 and the iPS cells generated with only human factors (OSK). Scale bars 100 μm. Experiments were performed by the collaborating group of H. Schöler.

6.2.9 Characterization of molecular properties of human iPS cells generated by axolotl *Oct4*, *Pou2* and *Sox2*

All generated iPS colonies were genotyped by PCR and we could verify the presence of only the applied transgenes. Figure 11 A shows genotyping of iPS cells generated with axolotl *Oct4* whereas Figure 11 B illustrates the genotyping result from iPS cells induced by axolotl *Pou2*.

The next step was the investigation of the expression of different pluripotency markers in the generated iPS cell. Therefore, we performed an immunochemical staining. Generated iPS cells using axolotl *Oct4* and *Sox2* (Figure 12 A) or *Pou2* (Figure 12 B) were stained for the pluripotency markers OCT4, NANOG, the stage-specific embryonic antigen 4 (SSEA4), and the ES cell markers TRA1-60 and TRA1-81. All of them showed a similar expression intensity as in the human ES cell line H9 and the iPS cells generated with the human factors *Oct4* (O), *Sox2* (S) and *Klf4*. iPS cells did not stain for the non-pluripotency marker stage-specific embryonic antigen 1 (SSEA1) (Figure 12 A). Human fibroblasts did not stain for the various pluripotency markers.

Next, we measured the mRNA levels of the endogenous pluripotency markers *Oct4, Sox2, Klf4, c-Myc, Nanog, Lin28, Rex1* and *Dppa4* in the generated iPS cells and compared levels to the initial fibroblast cell population and two ES cells lines (Shef3, NCL4), the positive controls. The iPS cells were generated using axolotl *Oct4* and *Sox2* in combination with the human factors, and the analysis was performed by quantitative RT-PCR and plotted relatively to Shef3 in Figure 13 A. Figure 13 B shows the relative expressing levels in iPS cells generated with axolotl *Pou2* in combination with the human factors. We could show that iPS cells generated with different sets of factors have a similar expression level of pluripotency markers as ES cells. However they are dramatically different when compared to the levels obtained from the human fibroblasts cell line.

Further, we performed microarray analysis to study global gene expression profiles of different iPS cell lines

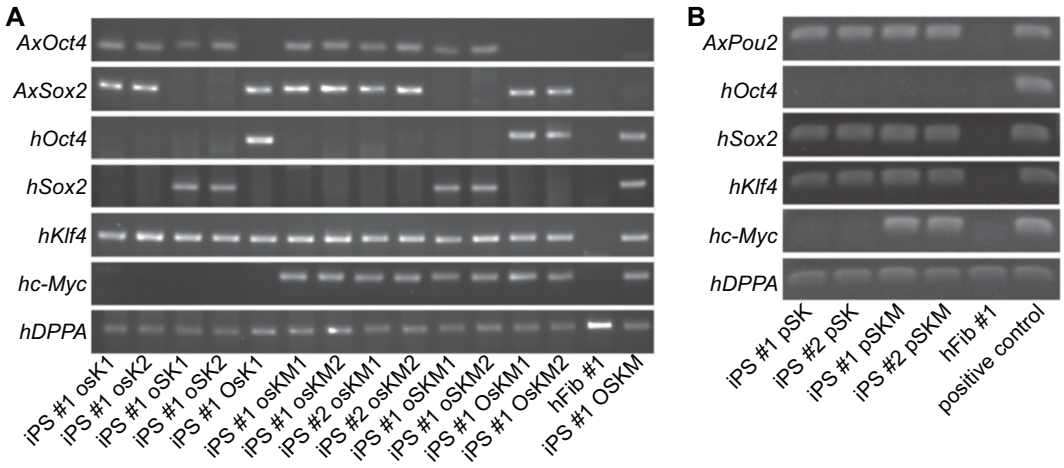

Figure 11: Genotyping of human induced pluripotent stem cells achieved by applying axolotl *Oct4*, *Pou2* and *Sox2*
(A) Genotyping of human iPS cell colonies induced by axolotl *Oct4* and/or axolotl *Sox2* and **(B)** axolotl *Pou2* in combination with the human factors. Genomic PCR was performed with specific primers for each viral vector. *DPPA4* was considered to be a loading control, hFib #1 was the negative control, while **(A)** iPS #1 generated with only human factors *Oct4* (O), *Sox2* (S), *Klf4* (K) and *c-Myc* (M) or **(B)** plasmid used in viral preparation were used as positive controls. Experiments were performed by the collaborating group of H. Schöler.

and compared it to profiles from human fibroblasts and human ES cell lines. In pairwise scatter plots we compared iPS1 osK2 cell line with the initial hFib #1 population (Figure 13 C) and the human ES cell line Shef3 (Figure 13 D). We can demonstrate that hFib #1 osK2 cells exhibit a fully reprogrammed gene expression profile which is very similar to Shef3 but distinct from that of hFib #1 cells.

Activation and inactivation of genes is regulated due to demethylation or methylation, respectively of the promoter region of a gene. To investigate whether the promoter of pluripotency genes was activated or not we performed bisulfite sequencing analysis of the *Oct4* and *Nanog* promoter regions (Figure 13 E). We detected demethylation and thus an activation of both promoters during the reprogramming process in iPS cell. In comparison, the parental hFib #1 population is highly methylated in *Oct4* and *Nanog* promoter region.

We also performed a hierarchical analysis of generated iPS cells, human ES (hES) cells and parental human fibroblasts based on gene expression profiles. We observed a clustering of diverse hES cells with iPS cells generated with a different set of factors on the same tree branch. However, this group can be distinguished clearly from human fibroblasts (Figure 13 F).

These results suggest that axolotl *Oct4* and *Pou2* are able to reprogram the fibroblast transcription network and generate a *de novo* pluripotent cell state.

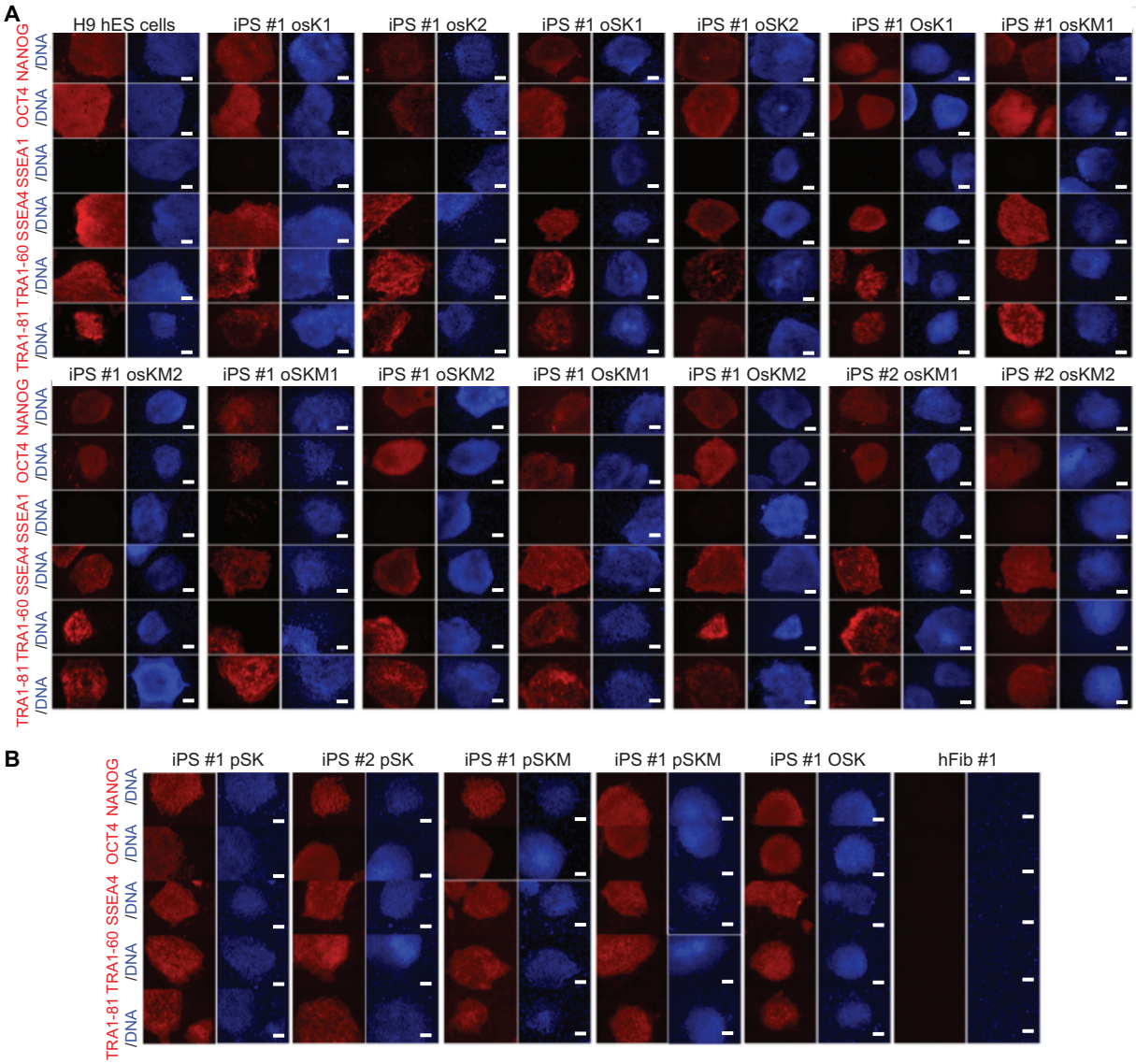

Figure 12: Immunofluorescence staining of the pluripotency markers in induced pluripotent stem cell

(A) Immunofluorescence staining of the pluripotency markers NANOG (red), OCT4 (red), SSEA4 (red), TRA1-60 (red) and TRA1-81(red) in the various iPS cells lines generated using axolotl or human *Oct4* and *Sox2*. The human ES cell line H9 and iPS cell line generated with human factors *Oct4* (O), *Sox2* (S), *Klf4* (K) were used as positive controls. Non-pluripotency marker SSEA1 does not show a staining. **(B)** Immunofluorescence staining of the pluripotency markers OCT4 (red), NANOG (red), SSEA4 (red) TRA1-60 (red) and TRA1-81(red) in the various iPS cells lines generated using axolotl *Pou2*. Human Fib #1 were considered as the negative control. Nuclei were counterstained with Hoechst (blue). Scale bars 500 μm. Experiments were performed by the collaborating group of H. Schöler.

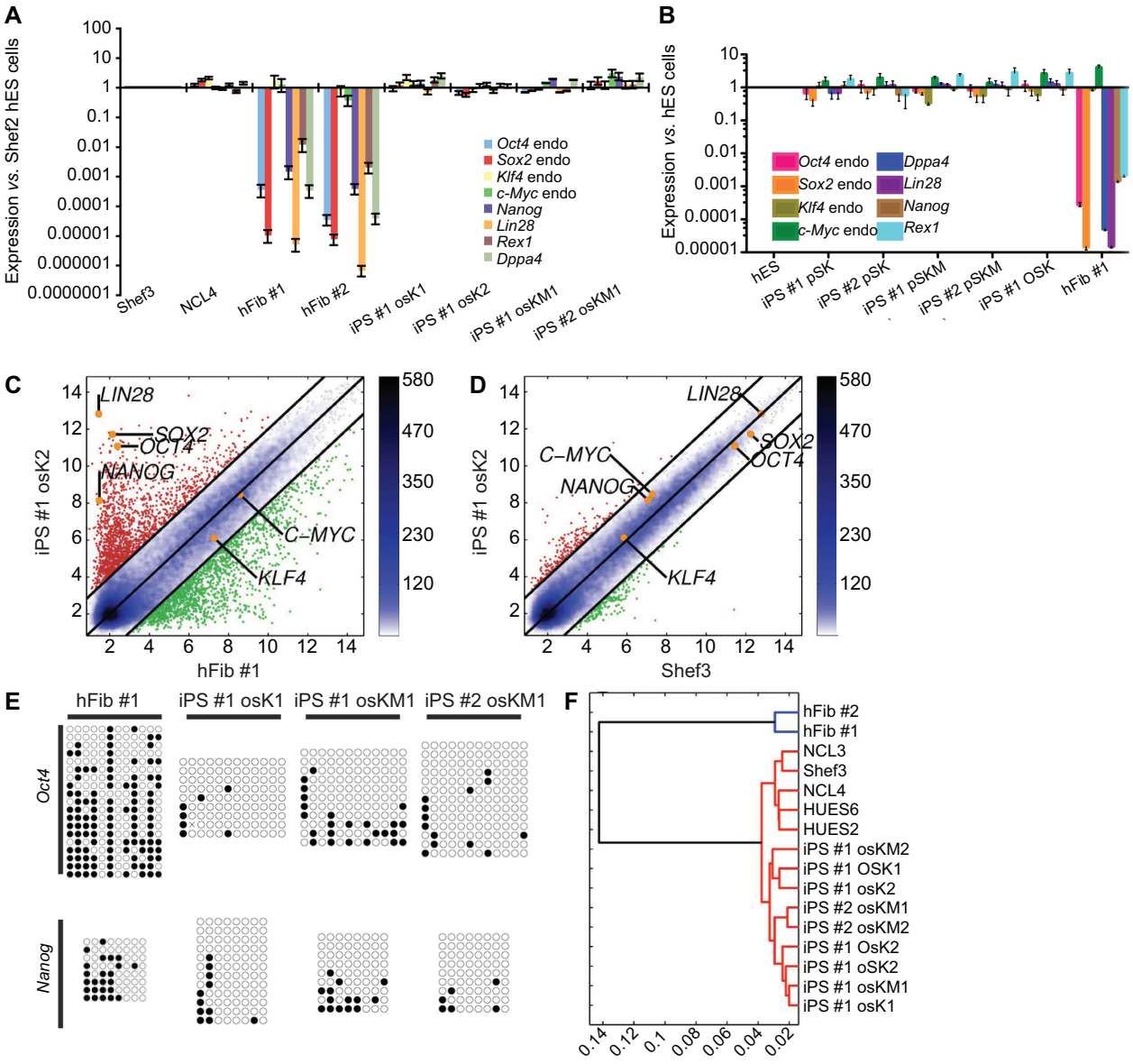

Figure 13: Molecular characterization of human induced pluripotent stem cells
Expression of the endogenous pluripotency markers *Oct4, Sox2, Klf4, c-Myc, Nanog, Lin28, Rex1* and *Dppa4* in human ES cells, human fibroblasts hFib #1, hFib #2 and iPS cells using **(A)** axolotl *Oct4* and *Sox2* or **(B)** axolotl *Pou2* in combination with the human factors was determined by qRT-PCR and plotted relative to hES cell levels. Error bars indicate standard errors based on normalization to GAPDH and ACTB. **(C), (D)** Illustrate a pairwise scatter plots of global gene expression profiles comparing iPS #1 osK2 cells with **(C)** hFib #1 cells and **(D)** Shef3 hES cell line. Black lines label a two-fold change in gene expression between paired populations. Color code on the right marks scattering density. Up- and down-regulated genes are shown by red and green dots, respectively. The position of the pluripotency markers *Oct4, Sox2, Nanog, Klf4, Lin28* and *c-Myc* is represented as orange circles. **(E)** Bisulfite sequencing of genomic *Oct4* and *Nanog* promoter regions in iPS #1 osK1, iPS #1 osKM1, iPS #2 osKM1 compared to human fibroblasts hFib #1. White and black circles display unmethylated and methylated CpGs, respectively. **(F)** Hierarchical clustering based on gene expression profile. Blue branches connect human fibroblasts and red branches connect iPS cells or human ES (hES) cells, both pluripotent cell populations. Experiments were performed by the collaborating group of H. Schöler.

6.2.10 Generated induced pluripotent stem cells are pluripotent

Further, we evaluated the pluripotent potential of the generated iPS cell lines. We performed *in vitro* studies on embryoid body formation using the hanging-drop method. Cells were induced to differentiate. To determine whether the specific cell types of all three germ layers were formed, we carried out immunofluorescence staining two weeks after induction. We observed a positive immunofluorescence staining for the endoderm marker α-FEROPROTEIN, the mesoderm marker α-SMOOTH MUSCLE ACTIN and the ectoderm marker βIII TUBULIN in the generated cells. This indicates that the iPS cells generated using axolotl *Oct4* and *Sox2* in combination with mammalian *Klf4* and with or without *c-Myc* (Figure 14 A), as well as iPS cell generated with axolotl *Pou2* and mammalian *Sox2* and *Klf4* and with or without *c-Myc* (Figure 14 B) have a pluripotent potential.

The *in vivo* differentiation potential of iPS cells generated using axolotl *Oct4* was studied by teratoma formation, a classical method for measuring the pluripotency of human ES cells. Therefore nude athymic mice were subcutaneously injected with iPS cells and 6 to 8 weeks later we analyzed whether all three germ layers had formed. Hence we did a hematoxylin and eosin staining on microsections. We observed teratoma formation from all lines analyzed (Figure 15). Teratomas contained respiratory epithelium from endoderm, cartilage and skeletal muscle formed from mesoderm and neural epithelium differentiated from ectoderm.

Our results indicate that iPS cell lines can be generated from fibroblasts of two different mammalian species using axolotl *Oct4* and axolotl *Pou2*. Furthermore, the generated iPS cells feature a pluripotent ability to differentiate into cells of the three germ layers - ectoderm, mesoderm and endoderm.

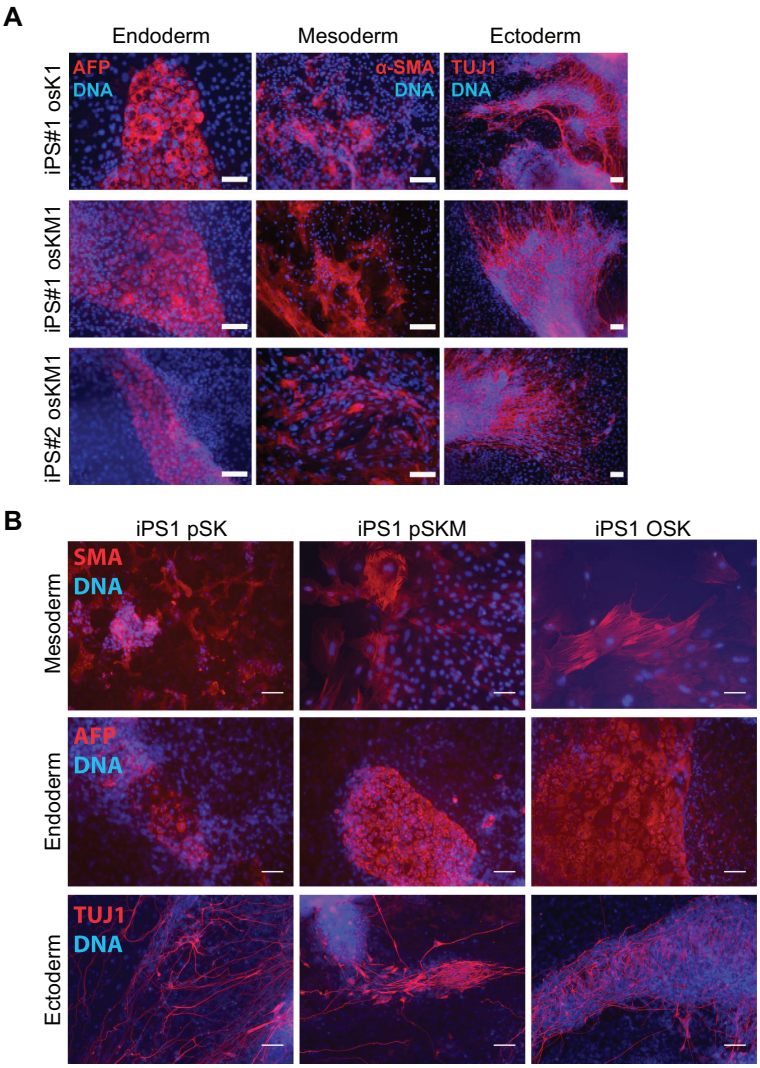

Figure 14: *In vitro* **differentiation of human iPS cells generated using axolotl factors** Human iPS cells differentiated *in vitro* into cells of all three germ layers. iPS cells were stained by immunocytochemistry. α-FEROPROTEIN (AFP) was used as endodermal marker, α-SMOOTH MUSCLE ACTIN (SMA) as mesoderm marker and βIII TUBULIN (TUJ1) as ectoderm marker. All markers are shown in red whereas nuclei were counterstained with Hoechst and are illustrated in blue. Scale bars 250 μm. Experiments were performed by the collaborating group of H. Schöler. **(A)** *In vitro* differentiation of human iPS cells generated with axolotl *Oct4* and *Sox2* in combination with mammalian *Klf4* and with or without *c-Myc*. **(B)** *In vitro* differentiation of human iPS cells generated with axolotl *Pou2* and mammalian *Sox2* and *Klf4*, and with or without *c-Myc*.

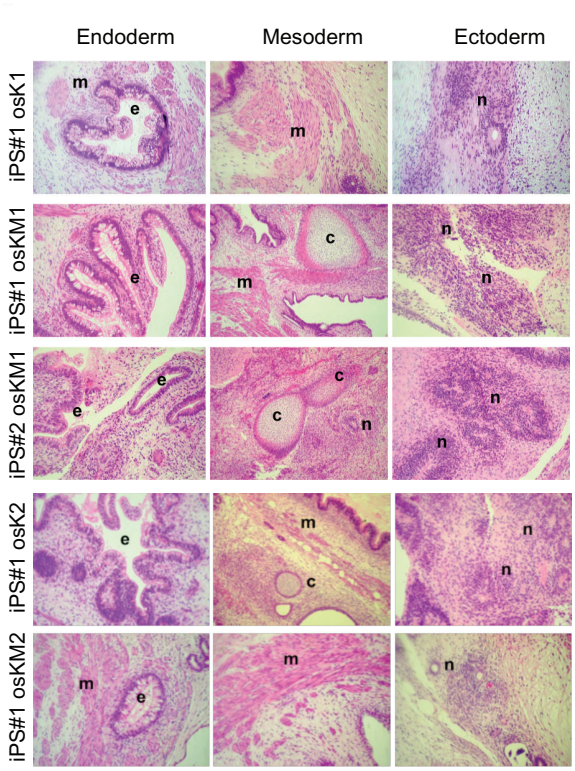

Figure 15: *In vivo* **pluripotency analysis of the human iPS cells**
Nude mice were injected with iPS cells generated using axolotl factors (*Oct4* (o), *Sox2* (s)) plus human factors (*Klf4* (K), *c-Myc* (M)). Images show microsections of hematoxylin and eosinstained teratoma after 6 to 8 weeks. Generated iPS cells have differentiated into tissues of all three germ layers: endoderm (e... respiratory epithelium), mesoderm (c... cartilage, m... skeletal muscle), and ectoderm (n... neural epithelium with rosettes). Experiment was performed by the collaborating group of H. Schöler.

6.3 Discussion

6.3.1 Evolution of POU homologs

The evolution of the ancestral class V POU gene and thus Oct4 had been discussed controvertibly in the past years (Frankenberg *et al.*, 2010; Niwa *et al.*, 2008). In our study, we could show for the first time that axolotl, a basal tetrapod, retained both POU homologs, the POU2 and the OCT4, during evolution. So far, this had been only observed in marsupials and monotreme mammals (Frankenberg *et al.*, 2010; Niwa *et al.*, 2008). *Xenopus laevis* on the other hand contains three different *Oct* genes, which are referred as *Pou* genes (*Pou25*, *Pou60*, *Pou91*) in this thesis (Cao *et al.*, 2006), but no *Oct4*, whereas humans have two splice isoforms of OCT4 (Atlasi *et al.*, 2008) but do not harbor a *Pou* gene.

Phylogenetic assembly of POU domains from different species showed a division of class V POU factors into OCT4 and POU2. In xenopus the POU class V ancestor gene duplicated in evolution, resulting in the different POU orthologs *Pou25*, *Pou60* and *Pou91*.

Axolotl POU2 shows similarities to the POU2 sequences in chicken and tammar, but it is evolutionary further distinct from zebrafish POU2. On the other hand, axolotl OCT4 clusters with sequences from lizard, tammar and different eutherian mammals like mouse. Our results indicate that axolotl *Pou2* and *Oct4* are clearly distinguishable genes. From the results of the phylogenetic, synteny analyses and the different expression pattern of *Oct4* and *Pou2* we claim that *Pou2* from axolotl is a *bona fide Pou2* and thus does not belong to the *Oct4* family.

Based on our result of the phylogenetic assembly of POU domains from different species we confirmed Frankenberg *et al.* (2010) hypothesis of an ancestral class V POU gene duplication latest in early tetrapod development.

The POU domain gene from *Hydra* seems to have characteristics of an *Oct4/Pou2* precursor gene (Millane *et al.*, 2011) which would suggest that OCT4/POU2 ancestral proteins had been present already before the evolutionary development of vertebrates.

6.3.2 Axolotl *Oct4* and *Pou2* are both expressed in pluripotent cell types and germ cells

The mRNA of axolotl *Pou2* and *Oct4* both showed a pattern in the ectoderm of gastrula stage embryos. Furthermore, we observed that the mRNA of *Sox2* is consistent in localization with the mRNA of the *Pou2* genes. All three genes were expressed in the animal cap region of gastrula stage embryos, a highly pluripotent area.

Frankenberg *et al.* (2010) showed that *Oct4* as well as *Pou2* are present in pluripotent tissues of tammar. OCT4 was expressed in gastrula stage tammar embryos whereas POU2 was present in the primitive streak stage conceptus.

These results suggest that axolotl and marsupial *Pou2* is associated with pluripotent cells of the gastrula,

and similar to *Oct4* from both species (Frankenberg *et al.*, 2001).

Tammar OCT4 was expressed in oocytes, proliferating oogonia, and migrating germ cells. They further examined the mRNA pattern of *Oct4* and *Pou2* in different tissue types of the tammar and identified an intensive *Oct4* expression in developing testis cords, the germ cells. However, *Pou2* mRNA was not detectable (Frankenberg *et al.*, 2010).

Zebrafish *Pou2* does also not show an expression in developing primordial germ cells or the adult gonads (Marlow and Mullins, 2008).

In contrast, it had been reported that medaka expresses *Pou2* during embryonic development but also in primordial germ cells, in the male germ cells the spermatogonia, in adult testis and in oocyte development (Sanchez-Sanchez *et al.*, 2011, 2010). However, its function remained unclear. Since medaka does not have an *Oct4* homolog one could assume that medaka *Pou2* has a post-embryonic function in germ line development.

In axolotl, Bachvarova *et al.* (2004) could not detected *Oct4* expression in primordial germ cells. However, our observations would indicate that axolotl *Oct4* and *Pou2* are expressed in primordial germ cells.

Interestingly, this pattern of *Oct4* and *Pou2* gene retention in different organisms correlates with the variable mechanisms of germ cell formation found among vertebrates. Fish, xenopus and chicken retained *Pou2*. In these organisms germ cell formation is determinative, meaning that germ cells are generated through the segregation of germ plasm. In contrast, axolotl and mammals retained *Oct4*. Here, the germ cell formation is inductive, meaning that germ cells are formed by induction of embryonic mesoderm (Johnson *et al.*, 2003a,b). Axolotl is the first species described which harbors both *Oct4* and *Pou2*, and both are not only expressed in the pluripotent animal cap of gastrula stage embryos but also in primordial germ cells. Our observations imply that the ancestral *Oct4/Pou2* gene could have played a role in pluripotency as well as in germ cell development. This ability was selectively lost in some species during evolution.

6.3.3 Conservation and diversification of POUV proteins

By *in vitro* studies we demonstrated that the *Oct4* and *Pou2* gene from axolotl can confer pluripotency. Surprisingly, we could show that both can confer pluripotent character and can reprogram fibroblasts from two different species, mouse and human, to generate a pluripotent cell.

In our mouse fibroblast reprogramming assay we were not able to establish iPS cell colonies using zebrafish *Pou2*. Even so we observed GFP-expressing cells after transduction. This data is strengthened by the fact that zebrafish *Pou2* is not able to maintain ES cell character when mouse *Oct4* is absent (Niwa *et al.*, 2008; Morrison and Brickman, 2006). It had been shown that zebrafish *Pou2* has a function as a mediator of endoderm induction and differentiation during gastrulation (Lunde *et al.*, 2004). However, the restricted induction potential of zebrafish *Pou2* does not apply for all *Pou2* orthologs since axolotl POU2 as well as medaka POU2 can induce pluripotent stem cells. Furthermore, using mouse fibroblasts, xenopus POU91 showed highly efficient reprogramming potential similar to the mammlian factors from mouse and human

(Figure 10 B).

In *Xenopus laevis* three POU homologs have been identified, *Pou25*, *Pou60* and *Pou91*. At that time no self-renewing ES cell lines have been generated from lower vertebrate species. Thus, it was unknown whether the mechanisms governing self-renewal were conserved. As the *Oct4* gene is an essential requirement for ES cell self-renewal, Morrison *et al.* assayed the ability of the different POU family members to substitute for *Oct4* by using an inducible *Oct4* knockout ES cell line (Morrison and Brickman, 2006). In ES cells both alleles of the endogenous *Oct4* had been inactivated, and thus OCT4 expression in these cells is maintained by a *Oct4* transgene. They assessed the OCT4 rescue by measuring alkaline phosphatase positive ES cell like colonies, the long-term self-renewal, and the expression of ES cell specific markers. They demonstrated that POU91 has the ability to maintain murine ES cells in the absence of Oct4. Xenopus POU25 and POU60 as well as axolotl OCT4 had some ability to rescue ES cell self-renewal (Morrison and Brickman, 2006). These data suggest that ES cell self-renewal is a conserved aspect of vertebrate *Oct4/Pou2*, rather than mammalian-specific.

Axolotl is an organism containing the three transcription factors *Oct4*, *Pou2* and *Sox2*. It is known that induction of mammalian adult fibroblasts to generate iPS cells requires *Oct4* and *Sox2* (Takahashi and Yamanaka, 2006). We are the first group to replace the mammalian with axolotl factors and investigating the reprogramming potential of human fibroblasts. We showed a pluripotency-related role for axolotl *Sox2*. POU2, OCT4 and/or SOX2 expression combined with the human factors generated iPS cells from human fibroblasts. This indicates that the axolotl factors do not only substitute human homologs, but can also dimerize with the human proteins.

To summarize, axolotl *Oct4* but also axolotl *Pou2* were able to reprogram human and mouse fibroblasts. This would propose that already the ancestral class V POU gene possessed a pluripotency conferring potential and this characteristic also remained after the duplication of class V POU at the base of tetrapod development. Thus, pluripotent potential is a feature for *Pou2* as well as for *Oct4*. However, at some point in evolutionary history the pluripotency conferring potential of *Pou2* expression in zebrafish disappeared while it retained and/or gained functions in somatic cells (Morrison and Brickman, 2006; Niwa *et al.*, 2008).

6.3.4 Summary I

Finally, with our study we show the first time that axolotl contains both POU homologs, the already identified *Oct4* (Bachvarova *et al.*, 2004) but also *Pou2*. Axolotl *Pou2*, *Oct4* and *Sox2* mRNA was localized in the pluripotent animal cap region of gastrula stage embryos. Furthermore, *Pou2* and *Oct4* was also present in primordial germ cells. Further we demonstrated that axolotl *Pou2*, *Oct4* and *Sox2* together with human factors are able to induce pluripotency in mouse and human fibroblasts. Thus, axolotl factors can substitute their mammalian homologs and in addition, are also able to form heterodimers with the mammalian proteins. With these observations, we are the first group to identify the role of axolotl *Sox2* expression in a pluripotency

related context. This means that human and axolotl *Oct4* and *Sox2* have a conserved activity in inducing pluripotency which suggests a highly conserved pluripotency network, and thus induced pluripotency is characteristic not only occurring in mammals, but existed already in the *Oct4/Pou2* common ancesteral vertebrates.

Intraspecies cell reprogramming has already been investigated (Huangfu *et al.*, 2008b; Wu *et al.*, 2009). However, here we show the first time that human somatic cells can be also reprogrammed with *Oct4* and *Sox2* from lower vertebrates.

7 Chapter II: Regenerating spinal cord cells are pluripotent

7.1 Introduction

7.1.1 Advantages of regeneration studies on salamanders

Most investigations in regenerative biology aiming a medical application have focused on *in vitro* studies on stem cells. However, to have a firm understanding of regenerative processes, *in vivo* studies are inevitable. Thus, one can study complicated interactions taking place between different cell types. The usage of model organisms is essential to provide the knowledge, and to eventually understand, manipulate and control regenerative properties. Understanding the regenerative mechanisms is potentially advantageous for biomedicine and future medical treatments in humans by stimulating regeneration through endogenous pathways.

It is known that some adult non-mammalian vertebrates have the potential to fully regenerate lost tissue structures in a process termed epimorphic regeneration (Brockes, 1997).

Tail regeneration in salamander might represent a natural example where differentiated somatic cells are efficiently reprogrammed to a stem cell like state. Thus, it would be interesting to study this process *in vivo*. Due to its enormous regeneration potential, salamanders like *Ambystoma mexicanum* became a very attractive regeneration model organism in the past decades. Animals can be kept and breed in colonies. Due to relatively low maintenance costs it is possible to raise a large number of animals. One mating can yield about 200 - 400 offspring. Furthermore, axolotl larvae are transparent and thus perfect for techniques like live imaging. In addition, they have a relatively short regeneration time, depending on temperature and size of the animal.

In this study, we were interested in the involved genes in pluripotency during regeneration. Comparing most gene sequences it was depicted that salamander sequences show higher similarity to xenopus than to mouse sequences. However, axolotl OCT4, as one pluripotency factor and other germ-cell associated protein sequences are more similar to mammals than to POU sequences in xenopus (Johnson *et al.*, 2003a; Bachvarova *et al.*, 2004).

In the last years, progress in molecular biotechnology and manipulations of the animal positions the axolotl as an excellent regeneration model organism. Tools like expressed sequence tags, which are used to identify gene transcripts, became available for axolotl (Habermann *et al.*, 2004). We further developed an efficient transgenesis protocol for axolotl (Sobkow *et al.*, 2006). Thus, we were able to label specific cell and tissue types and to follow gene expression in the cells of interest. Transgenic animals contain site-specific recombination sites which is necessary to turn on gene expression in either a tissue-dependent, or time-dependent manner by controlling expression of the Cre recombinase.

7.1.2 Lens regeneration in amphibians

Newts and frogs are able to regenerate the eye lens, but salamanders lost this ability. While lens regeneration in frogs only occurs before metamorphosis using cornea epithelium cells, the regenerative process in newts

takes place throughout their adult life from dorsal iris pigment epithelial cells (PEC) (Watanabe, 1978). The ventral iris PEC has no lens regeneration ability.

Hayashi *et al.* (2004) showed that the fibroblast growth factor FGF2, a protein functioning in initiating the regeneration process, induces expression of the transcription factor genes *Pax6* and *Sox2*. During normal lens regeneration, the transcription factor genes *Sox2* and *Klf4* are upregulated two days after injury, a time point when pre-existing tissues become reprogrammed and re-enter the cell cycle (Maki *et al.*, 2009). In contrast, *c-Myc* peaked at day eight after injury, a time point when the vesicle formation is establishing (Maki *et al.*, 2009). OCT4 and NANOG were not expressed in the PEC during regeneration (Maki *et al.*, 2009). Based on the expression profile, the researchers hypothesize that the newt cells do not become pluripotent.

Ito *et al.* (1999) performed regeneration studies by transplanting iris PEC into limb. They dissociated iris PEC and transplanted reaggregates of dorsal and ventral iris PEC into blastema of forelimb in newt. Lens was formed in high efficiency from dorsal PEC, in a process similar to normal lens regeneration. Ventral iris PEC on the other hand did not regenerate a lens. In addition, when reaggregates were transplanted into non-regenerating limb no lens was formed. They showed that the dorsal cells are only able to form lens. Hence, the newt cells are not pluripotent (Ito *et al.*, 1999). The transdifferentiation process is restricted.

7.1.3 The development of the vertebrate tail

The vertebrate tail is a post-anal extension along the main body axis and includes a neural tube and a notochord which is surrounded by somitic mesoderm. There were two different views about the tail development discussed amongst embryologists. The old hypothesis proposed that the tailbud develops by a blastema-like mass of mesenchymal cells (Holmdahl, 1925). After new studies were undertaken this hypothesis seems less likely. The alternative view point is that the tail arises by morphogenic processes which also shape the head and trunk during gastrulation.

To establish the bilateral symmetry of an organism, the site of gastrulation and the initiation of germ layer formation the presence of the primitive streak is necessary. The primitive streak is a structure that develops in the early avian, reptilian and mammalian embryo. The epiblast has polarized epithelial cells, which are connected to mesenchymal cells (area opaca) in the periphery, able to form extra-embryonic tissue. The inner cells (area pellucida) will give rise to the embryo (reviewed in Chuai and Weijer (2009)). Area opaca and area pellucida are separated by epithelial cells, the marginal zone. An aggregate of cells underneath the epiblast is formed at the posterior pole of the area pellucida. Mesendoderm starts forming from epiblast cells, and moves towards the midline of the embryo generating the primitive streak. The midline is the first embryonic axis established, and is the the beginning of gastrulation. The streak is formed at the posterior pole of the epiblast and then elongates towards anterior. When it is about halfway over the epiblast, cells deeper in the streak move between epiblast and hypoblast to build gut, muscles, and skeleton. In chicken, *Pou2* mRNA was localized in the epiblast of pre-primitive streak stage embryos and the later formed hypoblast. When the

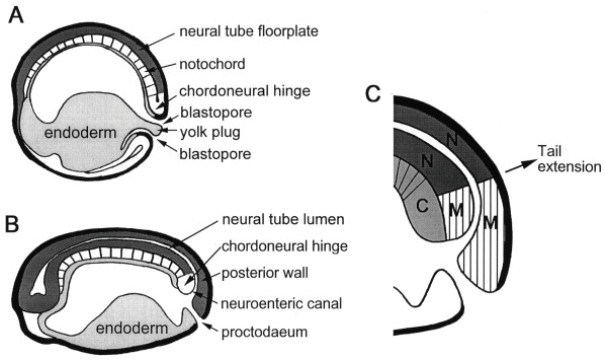

Figure 16: Scheme of xenopus tailbud development shown as sagittal section
(A) Tailbud develops after gastrulation (stage 13) by interaction of the notochord and the posterior neural plate. **(B)** In early tailbud stage (stage 22) the lateral blastopore lip grows over the blastopore and forms the posterior wall. The iniciated neuroenteric canal continues the neural tube lumen. **(C)** Magnification of posterior area "B". Positions of N (neural plate anterior to M), M (most posterior neural plate) and C (caudal notochord) regions form the tailbud. Picture from Beck and Slack (1998).

primitive streak forms, chicken *Pou2* was detected in the epiblast of the streak itself and the mesendoderm (Lavial *et al.*, 2007b). Whole mount *in situ* hybridisation on mouse embryos showed that *Sox2* mRNA was present in the primitive streak ectoderm and gut endoderm (Wood and Episkopou, 1999). Wilson *et al.* (2009) showed that the streak marker FGF8 was also expressed in the primitive streak and the tailbud (Cambray and Wilson, 2002; Chapman *et al.*, 2002; Gofflot *et al.*, 1997) of mouse and chick embryos. FGF4, an early embryonic developmental marker, is also expressed exclusively in the primitive streak during gastrulation. It was reported that a protein complex including OCT4 and SOX2 regulates FGF4 expression (Ambrosetti *et al.*, 1997; Dailey *et al.*, 1994).

Fate map studies showed that the mechanism of tail formation is highly conserved between different vertebrates (Tucker and Slack, 1995b; Kanki and Ho, 1997; Catala *et al.*, 1995). The tailbud is assumed to be a mosaic cell population with their origin more anterior in the embryo. The tailbud is a direct derivative of the late blastopore lip and has an organizer like property, attracting cells into the axis (Gont *et al.*, 1993; Tucker and Slack, 1995a). Tailbud formation starts after gastrulation with differentiation of the germ layers by an interaction of the notochord and the posterior neural plate (Figure 16 A). The chordoneural hinge, a direct derivative of the late dorsal blastopore lip assists the formation of tail notochord and spinal cord (Tucker and Slack, 1995b), (reviewed in Handrigan (2003)). Later the posterior wall forms due to covering the neural tube over the blastopore (Figure 16 B). Chordoneural hinge and the posterior wall are separated by a neurenteric canal (Gont *et al.*, 1993). Tucker and Slack (1995b) proposed the "NMC" model (Figure 16 C), which means that the tailbud formation requires a junction of the posterior neural plate (M), neural plate anterior to "M" (N) and the caudal notochord (C). Clonal analysis showed that myotomes and cells of the central nervous system (CNS) derive from a stem cell population (Mathis and Nicolas, 2000; Nicolas *et al.*,

1996). It was reported that the chordoneural hinge represents at least one stem cell population which gives rise to notochord and ventral spinal cord, and the posterior wall forms somites (Gont *et al.*, 1993; Cambray and Wilson, 2002, 2007; McGrew *et al.*, 2008), (also reviewed in Handrigan (2003)).

Recent studies analyzed the progression of lineage segregation during embryogenesis in mice (Tzouanacou *et al.*, 2009). They identified common progenitors for neural and mesodermal (N-M) lineages in the tailbud stage. These N-M progenitors supply derivatives to both tail tissues (Tzouanacou *et al.*, 2009). Cells in the chordoneural hinge give rise to the neural tube, notochord and somites (Beck and Slack, 1998; Cambray and Wilson, 2002; McGrew *et al.*, 2008).

Tzouanacou *et al.* (2009) results in mouse challenged the idea that there is a closer interaction between neurectoderm and mesoderm than between surface- and neural ectoderm. Interestingly, Downs (2008) detected OCT4 expression in mouse after gastrulation until the 16-somite stage. At headfold stage OCT4 expression was detected in the surface- and neural ectoderm of caudal node in mouse, the anterior end of the primitive streak formed in early gastrulation (Downs, 2008). Studies reported that the ventral node in mouse contains cells able to self-renew (Beddington, 1994; Tam *et al.*, 2004). Fate map studies of chick Hensen's node indicated that different parts of this complex structure give rise to multiple cell lineages like ectoderm or neural tube (Selleck and Stern, 1991).

These findings suggest that the OCT4 expressing caudal node may be a stem cell reservoir.

7.1.4 Regeneration of the tail in axolotl

Regeneration of the tail in salamanders like the axolotl is categorized in the three steps: **(i)** wound healing, **(ii)** blastema formation and **(iii)** regenerative outgrowth.

Figure 17 A shows a non-amputated fully functional tail. **(i)** Once the tail is amputated (Figure 17 B) wound closure takes place soon after, and cells from the surrounding epidermal tissue cover the amputation stump. This leads to migration of proximal cells towards the amputation plane and **(ii)** within the first days a blastema is formed (Figure 17 C).

Previously, it was thought that blastema cells are undifferentiated reprogrammed pluripotent cells and thus they would be able to form each cell type. However, in limb regeneration studies it was shown that blastema cells are a heterogenous mixture of cells which "remember" their origin and hence are limited to their lineage in regeneration (Kragl *et al.*, 2009). It could be that blastema cells in regenerating tail have a similar characteristic.

In mouse development, OCT4 was expressed in the ectoderm of the caudal node, the anterior end of the previously formed primitive streak (Downs, 2008). It would be interesting to know whether OCT4 is also expressed in regeneration of the axolotl tail, and hence the blastema cells would be in an ES cell-like state.

This transient structure of undifferentiated and proliferating blastema cells gives rise, in an origin dependent manner, **(iii)** to the different cell types necessary for the newly formed tail. Over the following days the

outgrowth of the regenerate takes place (Figure 17 D, E) until a fully functional tail is visible (Figure 17 F).

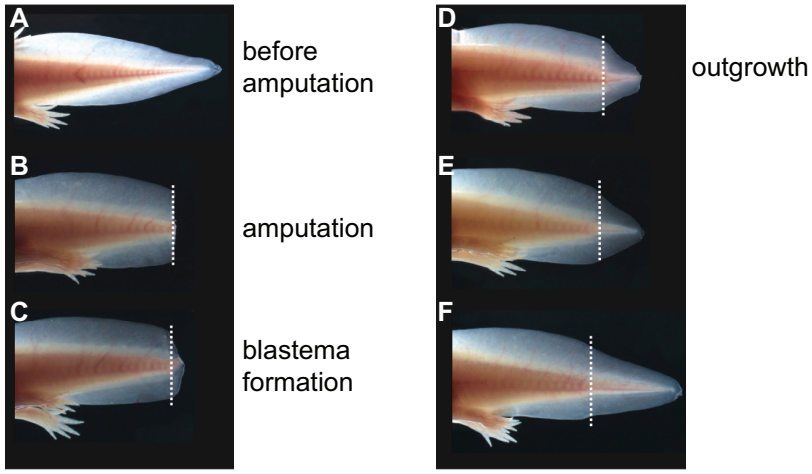

Figure 17: Regeneration of an axolotl tail over time
(A) Fully functional tail before amputation. **(B)** Amputation. **(C)** Within the first day after amputation a formation of undifferentiated and proliferating blastema cells, recruited from the mature tissue part, is visible. **(D, E)** Over the next days an outgrowth of the regenerating tail takes place until it has its **(F)** complete structure formed. Dashed line illustrates the amputation plane. (Picture adopted from Tanaka).

7.1.5 Regeneration of the spinal cord in axolotl tail

The spinal cord in the tail is the most accessible part of the vertebrate CNS and the structure is simpler than for example the complex structure of the brain. Due to these reasons, it is relatively easy to study. Like any other vertebrate, the spinal cord in axolotl is composed of grey matter in the central core which is surrounded by white matter.

In Figure 18 it is illustrated that irrespective of where the tail together with the spinal cord is amputated, cells in a 500 μm zone proximal of the amputation plane are recruited to regenerate the missing part (McHedlishvili *et al.*, 2007).

We identified this by transplanting EGFP expressing spinal cord into a non-GFP host where the spinal cord was removed (Figure 18 A, D). Tail was amputated leaving 600 μm (Figure 18 B) and 350 μm (Figure 18 E) remaining. At day 16 of regeneration we observed an entirely regenerated spinal cord derived from EGFP expressing cells when 600 μm was remaining (Figure 18 C). In contrast, only a portion of the spinal cord was EGFP expressing when leaving only 350 μm in the amputation stump remaining (Figure 18 F).

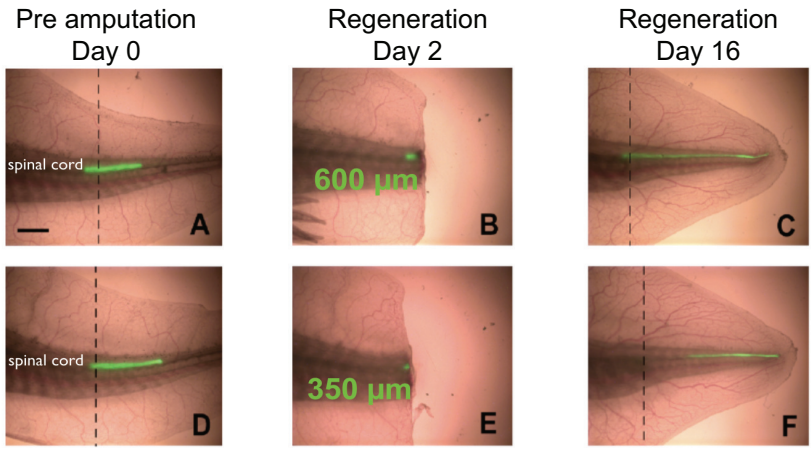

Figure 18: A zone of 500 μm in the mature spinal cord provides progenitor cells necessary in the regeneration process
A spinal cord section of 4 mm from an EGFP expressing transgenic animal was transplanted into a wild type 3.5 cm host. **(A, D)** axolotl tail harboring an implanted EGFP transgenic spinal cord 7 days after transplantation. Tail was amputated illustrated by the dashed line leaving an EGFP expressing spinal cord of **(B)** 600 μm or **(E)** 350 μm remaining in the host. **(C)** Tail at 16 days of regeneration. Entire regenerated spinal cord is derived from EGFP expressing cells. **(F)** On day 16 only about 70% of regenerated spinal cord is formed from EGFP expressing cells. Scale bar 2 mm. (Figure adopted from (McHedlishvili *et al.*, 2007))

The cells in the 500 μm zone proximal of the amputation plane have the status of progenitor cells. They increase their cell division and form an elongating neuroepithelial tube, also termed ependymal tube. The ependymal cell layer lining along the central channel of the spinal cord plays an important part in the spinal cord regeneration (Ferretti *et al.*, 2003; Chernoff *et al.*, 2003; Holder and Clarke, 1988). These cells provide neural progenitors needed in the process.

Upon amputation, the ependymal tube grows out of the cut spinal cord into the blastema. Ependymal cells proliferate, migrate and eliminate extracellular matrix and cell debris from apoptotic cells (Egar and Singer, 1972). Cells at the distal end of the growing ependymal tube form a terminal vesicle. The cells can leave the terminal vesicle and migrate into the blastema.

During spinal cord regeneration there is also axonal growth taking place. In injured animals, ependymal cells express early neural markers like vimentin and nestin, which was undetectable in non-injured urodele spinal cord (O'Hara *et al.*, 1992; Walder *et al.*, 2003). Furthermore, studies with Bromodeoxyuridine (BrdU) were performed to investigate ependymal cells in the regenerate. BrdU, a synthetic nucleoside, is an thymidine analogue and is used to label and detect proliferating cells. Thus, *in vivo* and *in vitro* studies showed that BrdU labeled ependymal cells give rise to glia cells and neurons in adult newt (Benraiss *et al.*, 1999). As well as functional replacement of spinal cord with their axons, cellular regeneration such as renewal of motor neurons is taking place. It was shown that motor neurons can be also formed in a postembryonic stages.

They occurred relatively often in small (5-7 cm long) axolotls, but only occasionally in large (7-13 cm long) animals (Holder *et al.*, 1991; Arsanto *et al.*, 1992).

7.1.6 Neurogenesis is not restricted to embryonic development

In the past it was believed that neurogenesis in CNS of mammals was limited to embryonic development and the early postnatal period, and hence in the adult would not regenerate after an injury (y Cajal, 1928). The inability of mammalian CNS to induce axonal growth and thus to regenerate was concluded from the following observations: in CNS myelin and injury-induced glia scars at the injured site, as well as in denervated axonal tracts (Okano *et al.*, 2003), there is an inability of endogenous neural stem cells in spinal cord to activate *de novo* neurogenesis after an injury (Johansson *et al.*, 1999) and insufficient factors to form a trophic environment (Widenfalk *et al.*, 2001). New research articles however revised Cajal's dogma and showed that axons are able to regenerate when there is an adequate environment at the site of injury. This was shown by transplanting peripheral nerves (Richardson *et al.*, 1980) and fetal spinal cord (Bregman, 1987) into the injured site of the spinal cord. Later articles show that neurogenesis takes also place in adult monkey and human brain (Eriksson *et al.*, 1998). Further it was demonstrated that there are neural stem cells in mature brain showing multipotency and self-renewal ability (Reynolds and Weiss, 1996, 1992; Morrison *et al.*, 1997). These cells are able to generate the three different cells types of the CNS: neurons, astrocytes and oligodendrocytes (Reynolds and Weiss, 1996). Localization of neural stem cells was performed by culturing tissue from different regions of the CNS. Stem cells could be enriched from the wall of the ventricular system in fore- and midbrain, from the hippocampus as well as the spinal cord. The wall of the ventricular system consists of a single ependymal cell layer in which Johansson *et al.* (1999) claimed that there are neural stem cells. This is supported by a similar expression and location profile of markers like NESTIN, NOTCH 1 and MUSASHI in ependymal cells and embryonic ventricular zone stem cells (Lendahl *et al.*, 1990; Sakakibara and Okano, 1997; Weinmaster *et al.*, 1992).
In addition, ependymal cells in lizard and newt are able to generate new neurons after injury (reviewed in Chernoff (1996)). Hence, studies of spinal cord regeneration in amphibians are a fundamental contribution to determine requirements necessary for a successful CNS regeneration also in higher (amniote) vertebrates like humans.

7.1.7 Fusion of cells

In the past, the fate of adult cells had been regarded as restricted to their tissue origin. However, the observation that these cells could be reprogrammed and express differentiated cell type markers was quite unexpected. Surprisingly, transplantation of adult bone marrow cells generated muscle cells (Ferrari *et al.*, 1998), liver cells (Petersen *et al.*, 1999; Theise *et al.*, 2000; Lagasse *et al.*, 2000), brain cells (Brazelton *et al.*, 2000; Mezey *et al.*, 2000) and others (Krause *et al.*, 2001). Weimann *et al.* (2003) showed that cells of the

human adult bone marrow contributes to cells in adult human brain. They analyzed cerebellar tissues from female patients after bone marrow transplantation. In patients receiving male marrow, Purkinje neurons diploid cells (Mann *et al.*, 1978; Manuelidis and Manuelidis, 1974; Mares *et al.*, 1973), were found which harbor X and Y chromosome. Furthermore, there were also Purkinje neurons observed with more than a diploid number of sex chromosomes. This would suggest that the neurons, which are only generated during early brain development in embryogenesis, were formed from bone marrow cells. Weimann *et al.* (2003) claim that the generation of Purkinje neurons takes place either *de novo* from marrow-derived cells or by fusion of bone marrow-derived cells with recipient Purkinje neurons. Cell fusion has been previously suggested as a mechanism of bone marrow contribution to tissue (Blau, 2002). Bone marrow cells could fuse with damaged cells and provide them an intact nucleus (Weimann *et al.*, 2003).

Barnabe-Heider *et al.* (2010) have assessed the origin of new cells in adult spinal cord of mice by genetic fate mapping. They analyzed oligodendrocytes, astrocytes and ependymal cells in intact and injured spinal cord. In the uninjured situation, ependymal cells and astrocytes are limited to self-duplication. Oligodendrocyte progenitors on the other hand self-renew but also generate more mature oligodendrocytes. After a spinal cord injury all three cell types are recruited. Astrocytes and ependymal cells generate the largest number of cells and ependymal cells show multilineage potential of the progeny (Barnabe-Heider *et al.*, 2010). However, the researchers did not investigate how ependymal cells changed their fate. In fact they claim that the ependymal cells are a quiescent stem cell population that is recruited after injury.

Spontaneous generation of tetraploid hybrid cells was observed *in vitro* when progenitor cells of the CNS from mouse were co-cultured with pluripotent ES cells (Ying *et al.*, 2002). ES cells used were male and where a female fetus as brain cell source had been used, the sex chromosome complement was XXXY. This observation can be only explained by formation of cell hybrids between ES and CNS cells. In addition, the tetraploid cells featured a pluripotent character, including multilineage contribution to chimaeras.

Terada *et al.* (2002) claim that interleukin-3 plays a role in cell fusion. In *in vitro* studies they demonstrated that mouse bone marrow-derived, embryonic stem-like cells fused spontaneously with ES cells when interleukin-3 was present in culture. So far, they do not know which cell fraction in the bone marrow is responsible for the fusion. Monocytes and macrophages might be involved in cell fusion. In culture, macrophages are able to fuse spontaneously and form giant multinucleated cells (Parwaresch *et al.*, 1986; Chiozzi *et al.*, 1997; Falzoni *et al.*, 1995). *In vitro* studies showed that this process is enhanced by cytokines like interleukin-3 (Enelow *et al.*, 1992).

To determine cell fate changes is challenging. Spontaneously fused cells can subsequently adopt the phenotype of the recipient cell which could be easily misinterpreted as "dedifferentiation" or "transdifferentiation". Hence stringent analyzing criteria have to be used. Criteria for establishing the occurrence of cell fate changes are intensively reviewed by Blau *et al.* (2001) and are summarized here.

I) Demonstration that a previously silent gene specific for the new cell type becomes expressed in the cell of interest. To observe whether proteins are co-expressed in the same cell, laser scanning confocal or deconvolution microscopy are indispensible. These methods allow analysis of optical sections less than 1 μm. Tracking of cells needs genetic markers having non endogenous counterparts, such as GFP or the Y-chromosome when male donor cells are introduced into female recipients.
II) Determination that the cell is well integrated into the tissue structure and thus morphologically indistinguishable from the host-neighboring cells.
III) Demonstration of cell fate change by a functional assay using a genetically deficient animal that is rescued from lethality or a disease related deficit.
Taken together, cells do not usually convert directly into other cell types but rather cell fusion seems be the mechanism used to lower the barriers between different cell identities.

7.1.8 The goal of this project

In axolotl, *Oct4* mRNA is highly abundant during embryonic development until gastrulation (Bachvarova *et al.*, 2004), to provide a pluripotent state of the cells. Studies in mouse showed that OCT4 is even expressed in the caudal node of embryos having 16 somites (Downs, 2008). In mouse tailbud there are progenitors giving rise to neural and mesodermal lineage (Tzouanacou *et al.*, 2009). This suggests that the OCT4 expressing caudal node might be a stem cell reservoir.
Our previous *in vitro* study showed that axolotl OCT4, POU2 and SOX2 confer a pluripotent character and can reprogram mammalian cells. Hence, we were interested in the involvement of the pluripotency genes *Oct4*, *Pou2* and *Sox2* in regenerating axolotl spinal cord. We observed expression of OCT4 and SOX2 in regenerating spinal cord cells. To determine whether the spinal cord cells have also a pluripotent character *in vivo* we transplanted EGFP labeled spinal cord into somite stage embryos and showed muscle cell formation.

7.2 Results

During embryogenesis it is known that *Oct4, Sox2* and *Fgf4* are present in the primitive streak and tailbud (see chapter 7.1.3).

It had been reported, that a protein complex including OCT4 and SOX2 regulates FGF4 expression (Ambrosetti *et al.*, 1997; Dailey *et al.*, 1994; Yuan *et al.*, 1995; Pan *et al.*, 2002).

Prior to my work A. Tazaki performed whole mount *in situ* hybridizations of a day-7 regenerating axolotl tail, and determined *Sox2* and *Fgf4* mRNA expression pattern (Figure 19 A). *Sox2* mRNA showed a strong staining in the mature as well as the regenerating spinal cord, named also ependymal tube. *Fgf4* on the other hand was determined in the epidermis and more interestingly in the terminal vesicle, the tip of the regenerating spinal cord with pluripotent character.

Developmental processes and regeneration share many similarities. For this reason we were interested in the expression of the pluripotency factor OCT4 during spinal cord regeneration. In case OCT4 is expressed we wanted to know whether the regenerating spinal cord progenitor cells have the ability to reprogram *in vivo*, and thus can form a different cell type apart from neural cells.

7.2.1 *Oct4, Pou2* and *Sox2* mRNA are present in mature and regenerating spinal cord

Prior to my work, an axolotl blastema cDNA library was screened and *Oct4* was identified. Hence, this gene should be present in regenerating tissue. We were interested whether *Oct4* together with *Pou2* and *Sox2* plays a role in spinal cord regeneration, and further whether the proteins confer a reprogramming capability to spinal cord cells.

Hence, the aim of the first experiment was to examine the mRNA pattern of *Oct4, Pou2* and *Sox2* in non-amputated and regenerating spinal cord using *in situ* hybridization. We performed cross sections through the tail of 3 cm larvae and compared non-amputated with day-6 regenerated tails.

In non-amputated mature tails (Figure 19 B) we detected *Oct4* mRNA in spinal cord and partially in mesenchyme, whereas *Pou2* and *Sox2* were located in spinal cord only. In contrast to this in day-6 regenerating tail sections (Figure 19 C) *Oct4* and *Pou2* were identified in spinal cord as well as blastema cells whereas *Sox2* mRNA was limited to spinal cord only. Furthermore, *Pou2* seemed to be upregulated in the regenerating compared to non-amputated tail.

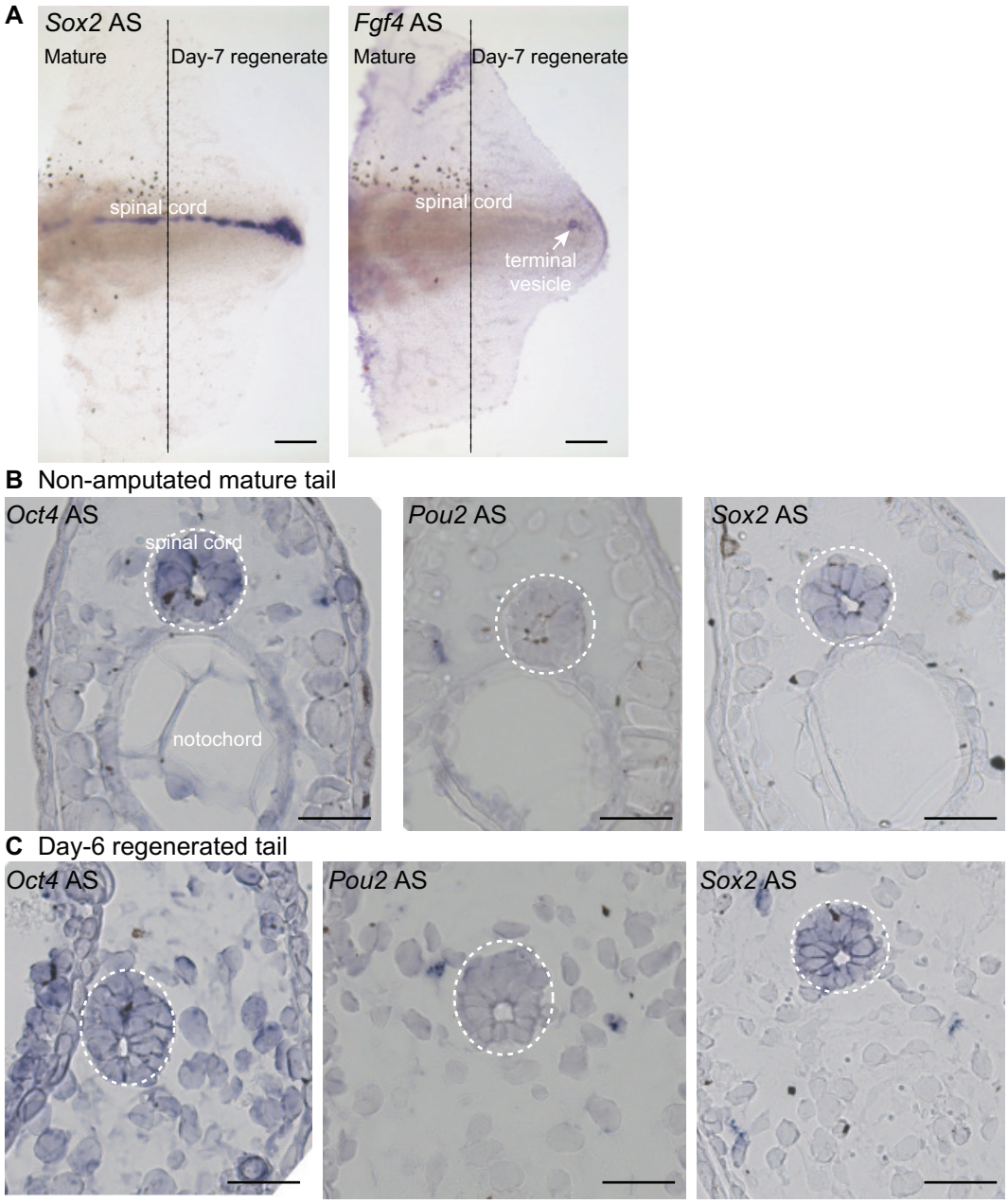

Figure 19: *Oct4, Pou2* **and** *Sox2* **mRNA are present in mature and regenerating spinal cord** **(A)** Whole mount *in situ* hybridization on axolotl tails collected seven days post amputation. *Sox2* mRNA is present in mature as well as in regenerating tail whereas *Fgf4* mRNA is restricted to the terminal vesicle and ectoderm. Dashed lines show the amputation plane. Scale bar 500 μm. AS = anti sense probe. Experiment was performed by A. Tazaki. **(B)** *In situ* hybridizations was performed on non-amputated mature (n=3 each) and **(C)** regenerating tails six days post amputation (n=3 each). Scale bars 100 μm. AS = anti sense probe. **(B)** In non-amputated mature tail *Oct4* is located in spinal cord and partially in mesenchyme, whereas *Pou2* and *Sox2* are restricted to spinal cord only. **(C)** In day-6 regenerating tail *Oct4* and *Pou2* are detectable in spinal cord as well as blastema cells whereas *Sox2* transcript is limited to spinal cord only.

7.2.2 Characterization of the OCT4 antibody specificity

In addition to the determination of *Oct4* and *Sox2* mRNA, we were interested in the protein expression of OCT4 and SOX2. Since there was no commercially available antibody against OCT4 working in axolotl we had to generate them ourselves with the help of the facilities in the institute. We produced three different polyclonal OCT4 antibodies, two against different variable regions of the C-terminus and one against the entire highly variable N-terminus. We performed a number of immunohistochemical stainings to assess specificity and validity of the staining pattern with the OCT4 antibodies.

To determine the specificity of the antibody, we carried out immunofluorescence stainings on sections of gastrula stage embryos. We observed nuclear OCT4 staining in the ectoderm including the animal pole, tissue that was shown to be positive for *Oct4* mRNA (Figure 4 A).

We observed a similar staining pattern of N- and C-terminal purified antibodies but stainings using the N-terminal OCT4 antibody (Figure 4 B) were stronger. Thus, we performed all following experiments with OCT4 N-terminal antibody.

For a further characterization of the OCT4 antibody we performed *in vitro* knockdown experiments by Oct4-morpholino. *Oct4* plasmid, nuclear EGFP plasmid as electroporation control, and either standard control morpholino or Oct4-morpholino were mixed with newt A1 myoblasts and electrically shocked to transfer DNA and morpholino into the cells. Figure 20 A illustrates the experimental set-up. Three days later fixed cells were stained for OCT4 with the OCT4 antibody.

We observed a strong OCT4 staining in the cells treated with standard control morpholino indicating, that the control morpholino did not influence OCT4 overexpression in the cells (Figure 20 B). Co-electroporation of a *Oct4* plasmid and Oct4-morpholino however, reduced the OCT4 overexpression in newt A1 cells dramatically, and was visible as a weak OCT4 staining (Figure 20 C).

Our results suggest that the N-terminal OCT4 antibody reliably detects OCT4 protein and hence could be used for further experiments.

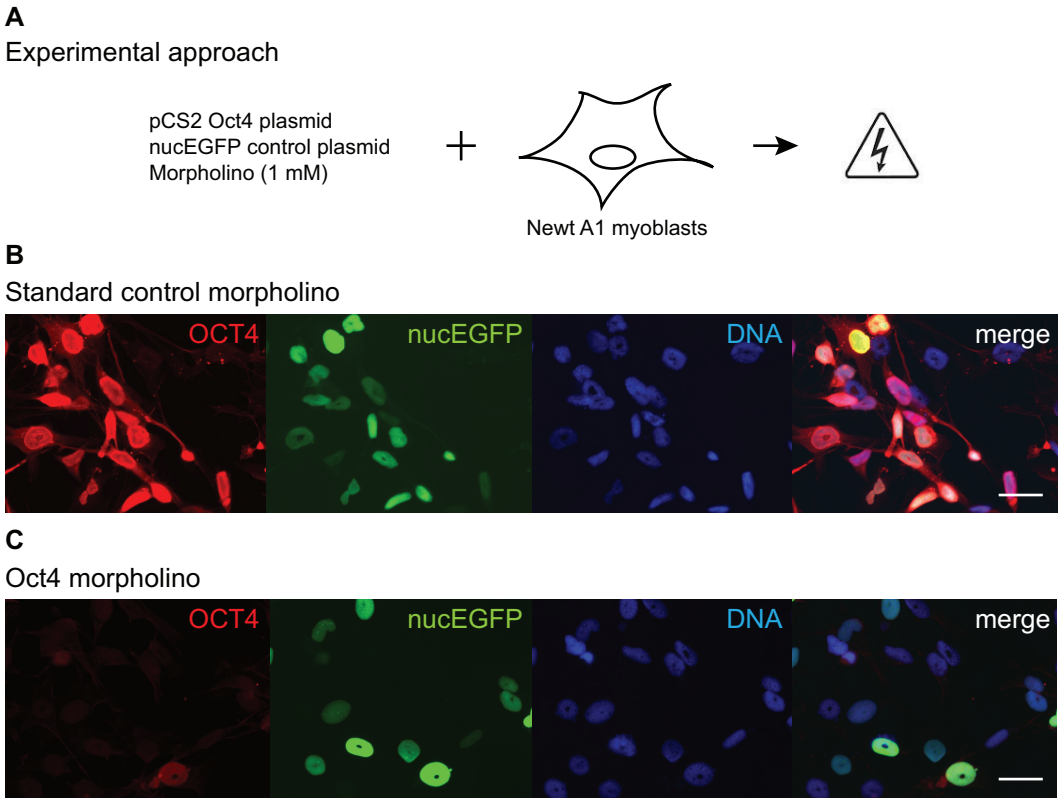

Figure 20: Oct4-morpholino downregulates OCT4 overexpression in electroporated newt A1 myoblasts
(A) Experimental set-up. Newt A1 myoblasts were mixed with pCS2 *Oct4* plasmid for exogenous overexpression of OCT4, nucEGFP as a control plasmid to determine electroporation efficiency (green) and 1 mM of either standard control morpholino or Oct4-morpholino. Three days later cells were fixed and OCT4 expression was detected by immunostaining with a polyclonal OCT4 antibody (red). DNA was counterstained with Hoechst 33342 (blue). **(B)** Strong OCT4 immunofluorescence staining (red) in the cells treated with standard control morpholino. **(C)** Co-electroporation of Oct4-morpholino and *Oct4* plasmid reduced OCT4 overexpression in newt A1 cells dramatically visible as a weak OCT4 staining (red). Scale bars 100 μm.

7.2.3 OCT4 and SOX2 are expressed in non-amputated and regenerating spinal cord, with OCT4 being upregulated in the regenerate

After detection of *Oct4* and *Sox2* mRNA in non-amputated and 6-day regenerating tails we also expected OCT4 and SOX2 protein expression in these tissues. To prove that, we performed immunohistochemical staining on sections of non-amputated and 6-day regenerating tails obtained from 3 cm larvae. We compared the staining in proximal and distal tissue sections, with the proximal section investigating protein expression in the mature spinal cord and the distal section the tip of the spinal cord. In samples of 6-day regenerating tails the proximal section is about 2 mm proximal of the amputation plane and thus in a region which does not contribute to the regeneration process. The distal section in 6-day regenerating sample however is the regenerating tissue part and thus a major area of our interest.

In proximal sections of non-amputated tails, SOX2 was present in the dorsal root ganglion, which lies along the spinal cord (Figure 21 A). More interestingly, SOX2 was expressed at a strong intensity in the proximal (Figure 21 A) and similarly the distal (Figure 21 B) part of the spinal cord progenitor cells. In contrast, we observed a low OCT4 expression in the proximal (Figure 21 C) and the distal (Figure 21 D) part of non-amputated spinal cord sections. Further, low levels of OCT4 were detected in some cells of the mesenchyme. Magnified images of the spinal cord in a rainbow look-up table showed the low expression levels of OCT4 at the proximal (Figure 21 C') and the distal (Figure 21 D') part of the spinal cord.

In 6-day regenerating tails, SOX2 showed a strong expression similarly in the proximal (Figure 22 A) and the distal (Figure 22 B) section of the progenitor cells in the spinal cord. OCT4 is expressed at a low level in the proximal (Figure 22 C) region of the spinal cord. Magnified images of the spinal cord in a rainbow look-up table showed the low OCT4 expression at the proximal (Figure 22 C') part of the spinal cord in more detail. The expression level is similar to non-amputated tail. In contrast, OCT4 is strongly upregulated in the distal part towards the terminal vesicle, the tip of the spinal cord (Figure 22 D). Furthermore, OCT4 is not only restricted to the spinal cord but also expressed in the mesenchyme of the regenerate. Magnified images of the spinal cord illustrated in a rainbow look-up table shows the high OCT4 expression in the distal part of the spinal cord and the mesenchyme (Figure 22 D').

Our results show that *Sox2* mRNA and protein as well as *Oct4* mRNA and OCT4 protein are localized in non-amputated and 6-day regenerating spinal cord, with OCT4 being upregulated in the spinal cord and mesenchyme of the regenerate.

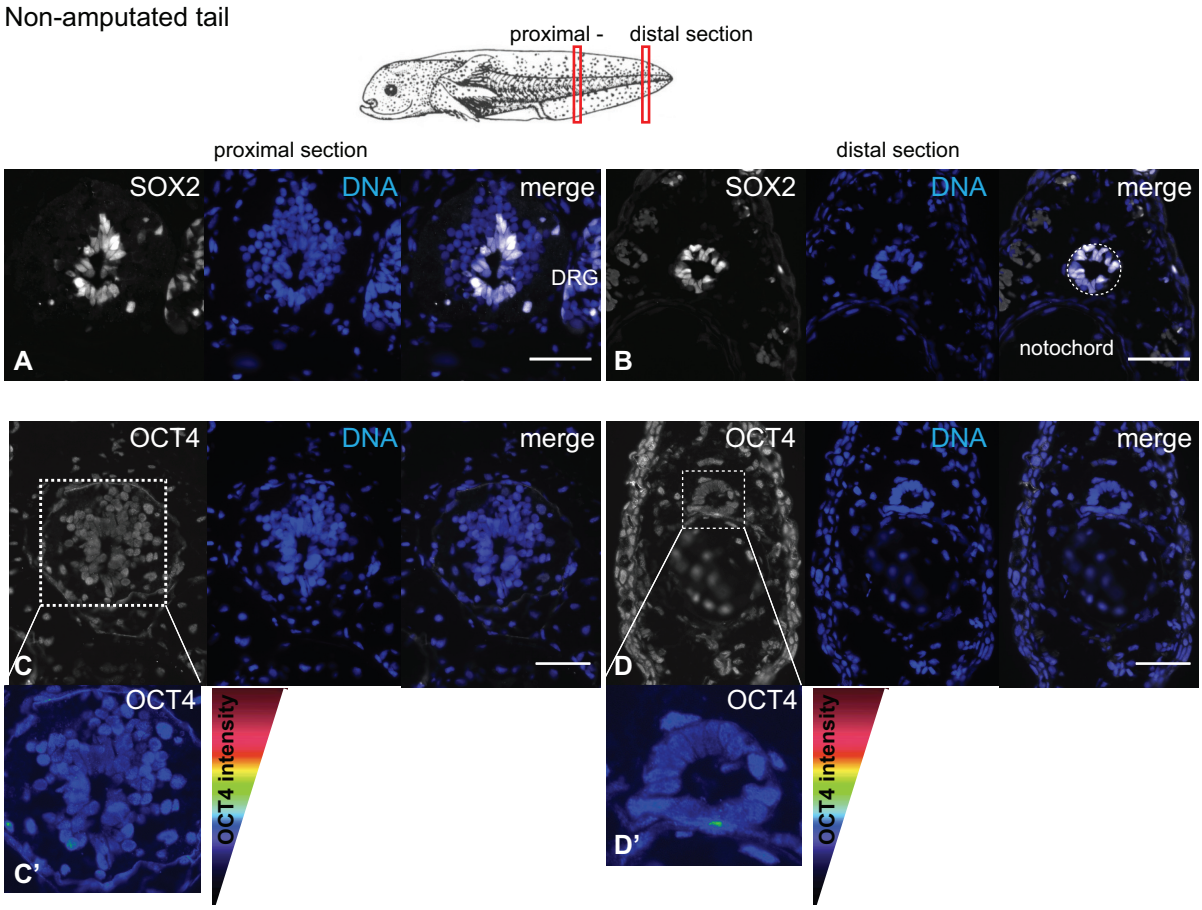

Figure 21: The transcription factors SOX2 and OCT4 are expressed in spinal cord of a non-amputated tail
Axolotl juveniles of about 3 cm from snout to tip of the tail were used for immunohistochemical staining with SOX2 or OCT4 antibody (white) (n=3 each). DNA was counterstained with Hoechst 33342 (blue). Scale bars 100 μm. SOX2 is strongly expressed in the progenitor cells of spinal cord in a **(A)** proximal as well as in **(B)** a distal tissue section of a non-amputated tail. Dashed circle shows the spinal cord. DRG... dorsal root ganglion. **(C)** OCT4 is expressed at a low level in proximal region and **(D)** distal part of the spinal cord. **(C')** Higher magnification of OCT4 expression level in the spinal cord in a rainbow look-up table at a proximal tissue section. **(D')** Higher magnification of OCT4 expression level in the spinal cord in a rainbow look-up table of a distal section. In the rainbow look-up table the expression level is illustrated as a gradient from black to red, indicating a low to strong expression, respectively.

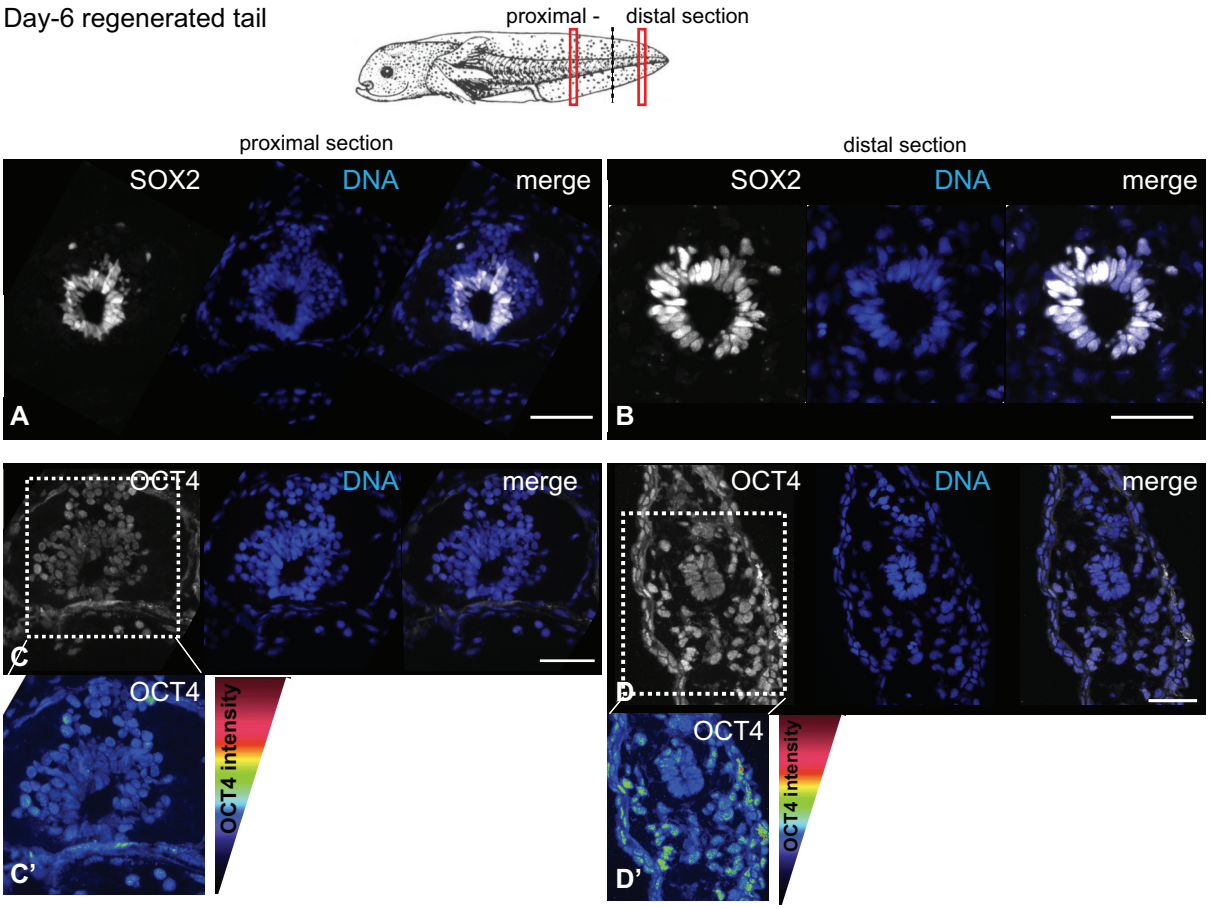

Figure 22: The transcription factors SOX2 and OCT4 are expressed in spinal cord of a day-6 regenerating tail
Axolotl juveniles of about 3 cm from snout to tip of the tail were used for immunohistochemical staining with SOX2 or OCT4 antibody (white) (n=3 each). Dashed line in the cartoon shows the amputation plane. DNA was counterstained with Hoechst 33342 (blue). Scale bars 100 μm. SOX2 is strongly expressed in the progenitor cells of the spinal cord in **(A)** a proximal as well as in **(B)** a distal tissue section of a day-6 regenerating tail. **(C)** OCT4 is expressed at low level in proximal spinal cord **(D)** but is upregulated in the spinal cord and mesenchyme of distal regenerating tail. **(C')** Higher magnification of OCT4 expression level in the spinal cord in a rainbow look-up table at a proximal tissue section. **(D')** Higher magnification of OCT4 expression level in the spinal cord and mesenchyme in a rainbow look-up table of a distal regenerating section. In the rainbow look-up table the expression level is illustrated as a gradient from black to red, indicating a low to strong expression, respectively.

7.2.4 Knockdown of OCT4 leads to a shorter regenerating spinal cord and to a decrease of cycling cells

We showed that *Sox2* and *Oct4* mRNA and protein are expressed in non-amputated and 6-day regenerating spinal cord, with OCT4 being upregulated in the regenerating spinal cord. This suggests that OCT4 is involved in spinal cord regeneration. Hence, we were interested in the effect of downregulating OCT4. The only possibility to knockdown expression of a protein in axolotl is by injecting morpholino, a short oligonucleotide complementary to the mRNA and thus inhibiting protein expression. We decided for morpholinos blocking translation of OCT4, SOX2 and POU2. We also used a standard control morpholino. When Oct4-, Sox2- and Pou2-morpholino were used together, they were mixed in a volume ration of 1:1:1. All morpholinos are fluorescein isothiocyanate (FITC)-labeled and thus detectable with fluorescence light.

We injected the spinal cord of 3 cm larvae (snout to tail tip) with 3 μl of 1 mM morpholino and electroporated immediately (Figure 23 A). Four days later we amputated the tail where the amputation plane went through the highest amount of morpholino positive cells visible in a dissecting microscope. A high efficiency of morpholino positive cells was the main criteria for this experiment. To determine this we sectioned the amputated tail close to the amputation plane, and assessed the amount of morpholino positive cells.

The distribution of morpholino into the cells was not equal and thus there were animals having zero or only a few cells showing morpholino uptake (Figure 23 B). By contrast, other animals had weak positive and strong morpholino positive progenitor cells in the spinal cord. An example using standard control morpholino or Sox2-morpholino injected into spinal cord is shown in Figure 23 C and Figure 23 D, respectively. We only performed further analyzes on animals showing more than 50% of morpholino positive progenitor cells in the spinal cord.

Six days after amputation the length of the regenerated spinal cord was measured and result plotted in Figure 23 E. We observed a significant reduction in spinal cord regeneration of OCT4 knocked down animals compared to animals injected with standard control morpholino ($p < 0.005$). However, we did not detect any difference when POU2 expression was knocked down. Spinal cord regeneration was reduced in SOX2 knocked down animals but to a lesser extent than in OCT4 knock downs. Regenerated spinal cord in animals injected with Oct4-, Sox2- and Pou2-morpholino together was longer than with Oct4- or Sox2-morpholino injected alone, but shorter than when POU2 is knocked down. This effect is probably due to the fact that morpholinos were used in a volume ration of 1:1:1, which led to a lower amount of each morpholino in a cell.

Further, we determined whether morpholino weak and strong positive spinal cord cells were able to proliferate. Therefore we performed tail sections of three regenerating animals and stained regenerate and mature spinal cord, maximally 500 μm proximal to amputation plane, for Proliferating Cell Nuclear Antigen (PCNA) a marker for proliferating regenerating cells. From the staining results we calculated the percentage of PCNA expressing progenitor spinal cord cells which had a weak and strong standard control-, Sox2- and Oct4-

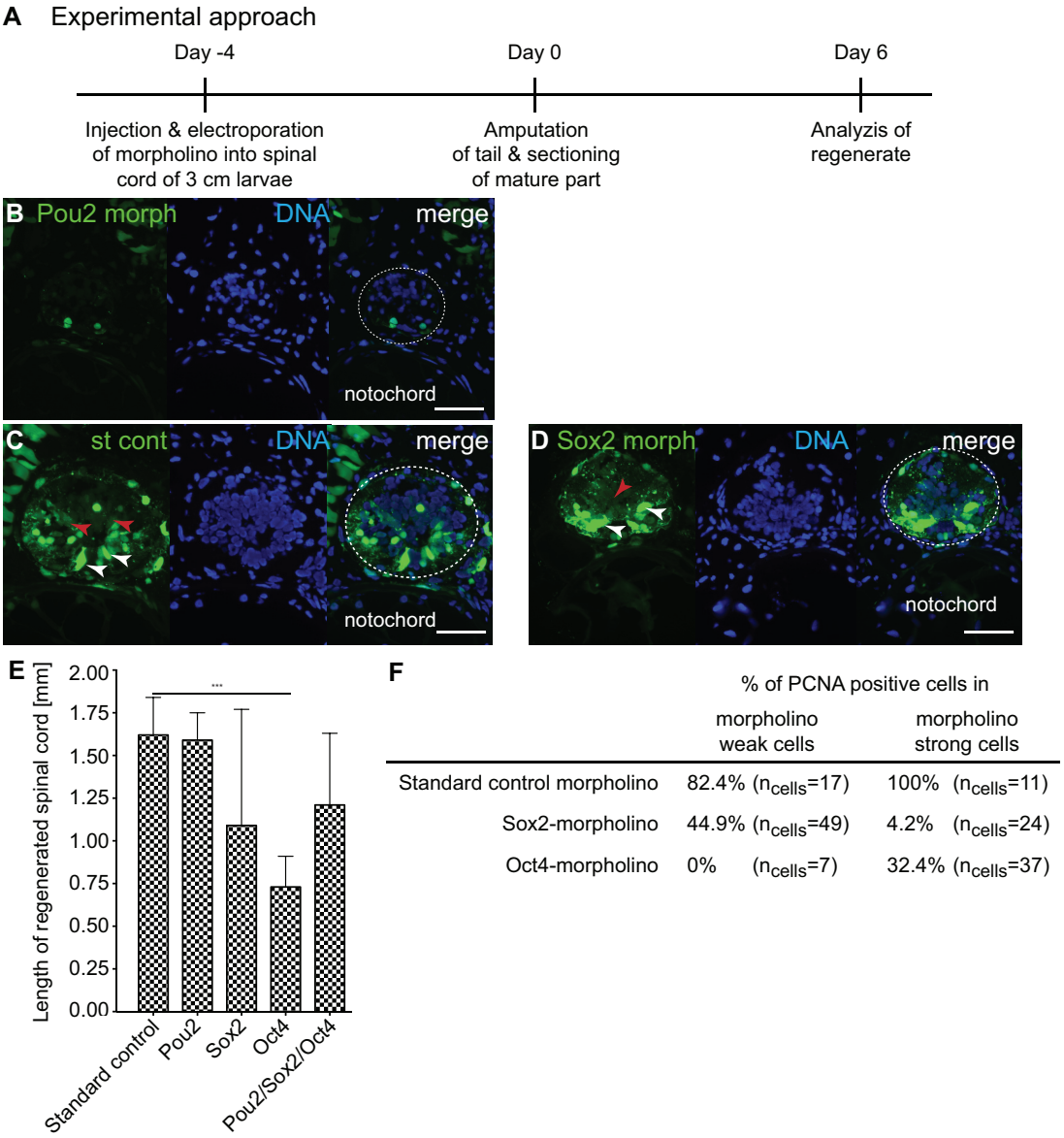

Figure 23: OCT4 and SOX2 knockdown results in a shorter regenerating spinal cord
(A) Axolotl juveniles of about 3 cm were injected with morpholino (standard control n=8, Pou2 n=10, Sox2 n=10, Oct4 n=9, Pou2/Sox2/Oct4 (v/v 1:1:1) n=10) and electroporated four days before tail amputation. Amputated tail close to the amputation plane was sectioned to determine the amount of morpholino positive cells. On day-6 length of regenerated spinal cord was measured and tissue was used for staining. **(B)** Example of low morpholino uptake. Only a few cells are Pou2-morpholino positive (green). Animals were not used for further procedure. **(C)** Example of higher standard control and **(D)** Sox2-morpholino (green) uptake in spinal cord close to amputation plane. Red arrowheads indicate weak, white strong morpholino positive cells. Animals were used for further procedure. DNA was counterstained with Hoechst 33342. Scale bars 100 μm. Dashed circles mark spinal cord. **(E)** length of the regenerating spinal cord on day-6 after amputation. Compared to standard control morpholino regenerating spinal cord length is significantly reduced in OCT4 knocked down animals ($p < 0.005$). POU2 knocked down does not have an effect on regenerated length while SOX2 knock down phenotype is stronger than POU2. **(F)** Day-6 regenerate was stained for PCNA and percentage of PCNA expressing progenitor spinal cord cells with a weak and strong standard control-, Sox2- and Oct4-morpholino uptake was calculated. Remaining cells were PCNA negative.

morpholino uptake.

We found that 82% to 100% of the standard control morpholino positive cells were PCNA positive (Figure 23 F). However, SOX2 knockdown led to a dramatic decrease of PCNA expression in spinal cord progenitors. Only 45% of weak Sox2-morpholino positive cells expressed PCNA. PCNA is even more repressed in strong Sox2-morpholino positive cells (4%). Compared to control we observed a drastic PCNA downregulation in OCT4 knock down cells. Only max. 34% of cells injected with Oct4-morpholino expressed PCNA.

7.2.5 Lineage tracing of SOX2 expressing cells from regenerating spinal cord is not efficient using *Sox2* reporter transgenic strain

From our OCT4- and SOX2 knock down experiment we have learnt that spinal cord cells show reduced proliferation, and the regenerated length is shorter. This would indicate that *Oct4* and *Sox2* play a role in regenerating spinal cord. Further we showed that SOX2 in the spinal cord is only expressed in progenitor cells while OCT4 expression is not restricted to just spinal cord. With lineage tracing experiments, where SOX2 expressing cells are labeled, we wanted to follow OCT4 and SOX2 positive cells from regenerating spinal cord.

Toward this aim, we used a technique based on the Cre/LoxP recombination, with which one can turn gene expression on and off in a specific tissue or cell types (Sauer, 1998). We created a transgenic reporter system that would allow us to identify, isolate and follow SOX2 expressing cells from the regenerating spinal cord. Figure 24 A shows the strategy of this experiment. In our laboratory we have generated a number of lines of germline transgenic animals harboring the LoxP reporter construct where the ubiquitous CAGGs promoter expresses a floxed EGFP - 3-Poly-Adenylation site followed by the *Cherry* gene. In addition, we produced several lines of animals where the axolotl *Sox2* genomic sequence drives an inducible Cre-recombinase-ERT which should specifically induce recombination of the LoxP construct in all SOX2 expressing cells, leading to CHERRY expression in all SOX2 positive cells.

We injected 4-OH-Tamoxifen to induce CRE expression into the progeny. We observed conversion from EGFP to a strong CHERRY expression in the brain of the animals. However, we did not see any conversion in the spinal cord of the tail. To trigger SOX2 expression in the spinal cord and thus to increase the conversion we amputated a part of the tail from the offspring and injected them with 4-OH-Tamoxifen. However, the conversion efficiency in the tail was very low. By immunofluorescence staining we observed a few CHERRY expressing cells in the mature spinal cord (Figure 24 B), but none in the regenerate.

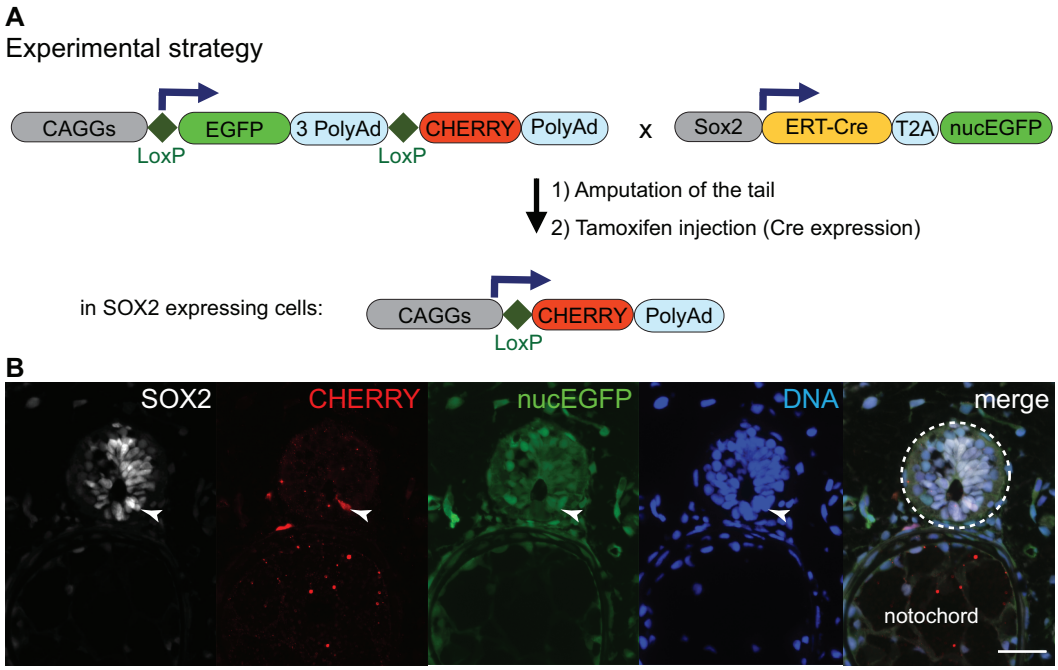

Figure 24: Transgenic reporter animals for lineage tracing of SOX2 expressing cells from spinal cord

(A) Experimental approach. A mating of a CAGGs-LoxP-EGFP-LoxP-Cherry with a Sox2-ERT-CRE-nucEGFP animal was set up (grey boxes show the promoter). The tail of the EGFP expressing offsprings was amputated and 6 days later injected with tamoxifen to induce CRE expression under the control of the *Sox2* promoter. CRE recombinase excises LoxP-EGFP. All SOX2 expressing cells would express CHERRY under the *CAGGs* promoter. **(B)** Immunohistochemical staining to determine conversion of LoxP reporter in the mature part of an amputated, tamoxifen-injected tail. SOX2 (white) is expressed in the spinal cord, CHERRY conversion is shown in red indicated by an arrowhead. EGFP (green) is ubiquitously expressed including the spinal cord. DNA was counterstained with Hoechst 33342. The merge image shows the overlay of all four channels. Dashed line indicates the spinal cord. Scale bar 100 μm.

7.2.6 Transplanting neural ectoderm labels SOX2 spinal cord cells used for lineage tracing

Due to the low efficiency of conversion in the reporter line we performed embryonic transplantations to label spinal cord cells. Therefore, we used neurula stage embryos and grafted a cell cluster of about 4 to 10 cells from neural plate ectoderm of a CAGGs-EGFP donor onto a non-GFP host of the same stage (Figure 25 A). Transplantation of only a small cell cluster compared to the entire section of the neural plate responsible for spinal cord formation allows us to cleanly label only spinal cord cells. However, because of the low number of these cells it is not possible to label the entire spinal cord.

All transplanted animals we screened for GFP expression in the spinal cord after hatching. Figure 25 B shows an example of a transplanted animal expressing GFP in a spotted manner in the spinal cord. The amount of GFP labeled spinal cord cells is limited when only a small cell cluster was transplanted. This can be abolished when we amputate the tissue through the GFP expressing cells (see dashed line in Figure 25 B). It led to an elongation of the GFP labeled spinal cord. On day-6 we observed GFP expression in regenerating spinal cord (Figure 25 C). This method ensures that we minimize contamination and label only spinal cord cells.

To determine GFP expression in the spinal cord we performed immunofluorescence staining on cross sections and could identify a co-localization with the spinal cord progenitor marker SOX2 (Figure 25 D). Further GFP was expressed in neurons of the spinal cord, the cell bodies and also in the outgrowing axons (Figure 26 A). Immunofluorescence staining with βIII TUBULIN (Figure 26 B), a microtubule protein exclusively expressed in neurons, showed co-localization (Figure 26 D). Confocal images document this observation in more detail. Co-localization of GFP (Figure 26 A') and βIII TUBULIN (Figure 26 B') is visible in Figure 26 D'.

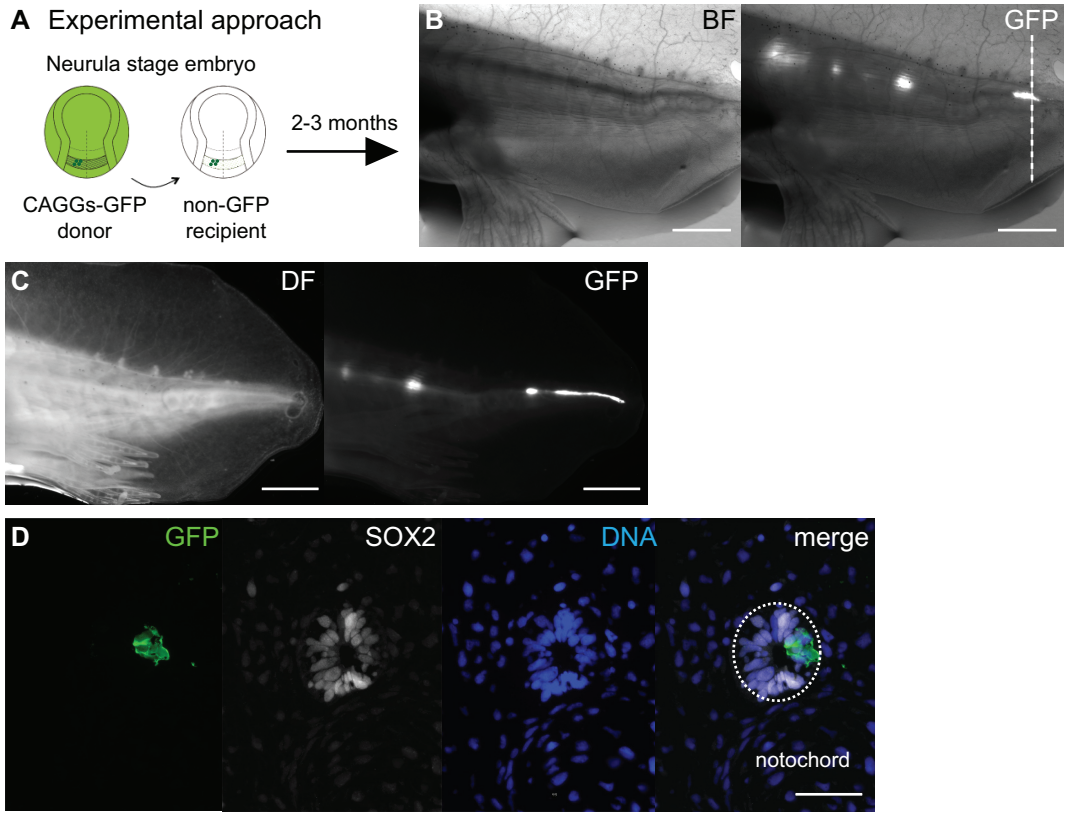

Figure 25: Embryonic transplantation to label spinal cord cells for lineage tracing studies of SOX2 positive cells
(A) A mating of CAGGs-EGFP donor with non-GFP host animals was set up. Offsprings were used for grafting experiments. A small ectodermal cell cluster from CAGGs-GFP donor of a neurula stage embryo was transfered to the same position in a non-GFP recipient. After hatching animals were screened for GFP expression in the spinal cord with a dissecting microscope. **(B)** Tail of a grafted animal in brightfield (BF) and GFP channel. Scale bar 2 mm. GFP is expressed in a spotted pattern in the spinal cord. Amputation (dashed line) through GFP expressing cells **(C)** elongated GFP labeled spinal cord. Regenerating tail six days after amputation in darkfield (DF) and GFP channel. Scale bar 2 mm. **(D)** Immunohistochemical staining of a cross section of the regenerating tail. Spinal cord is partially GFP labeled which co-localizes with SOX2. DNA was counterstained with Hoechst 33342. Merged image shows the overlay of all three channels. Dashed circle marks spinal cord. Scale bar 100 μm.

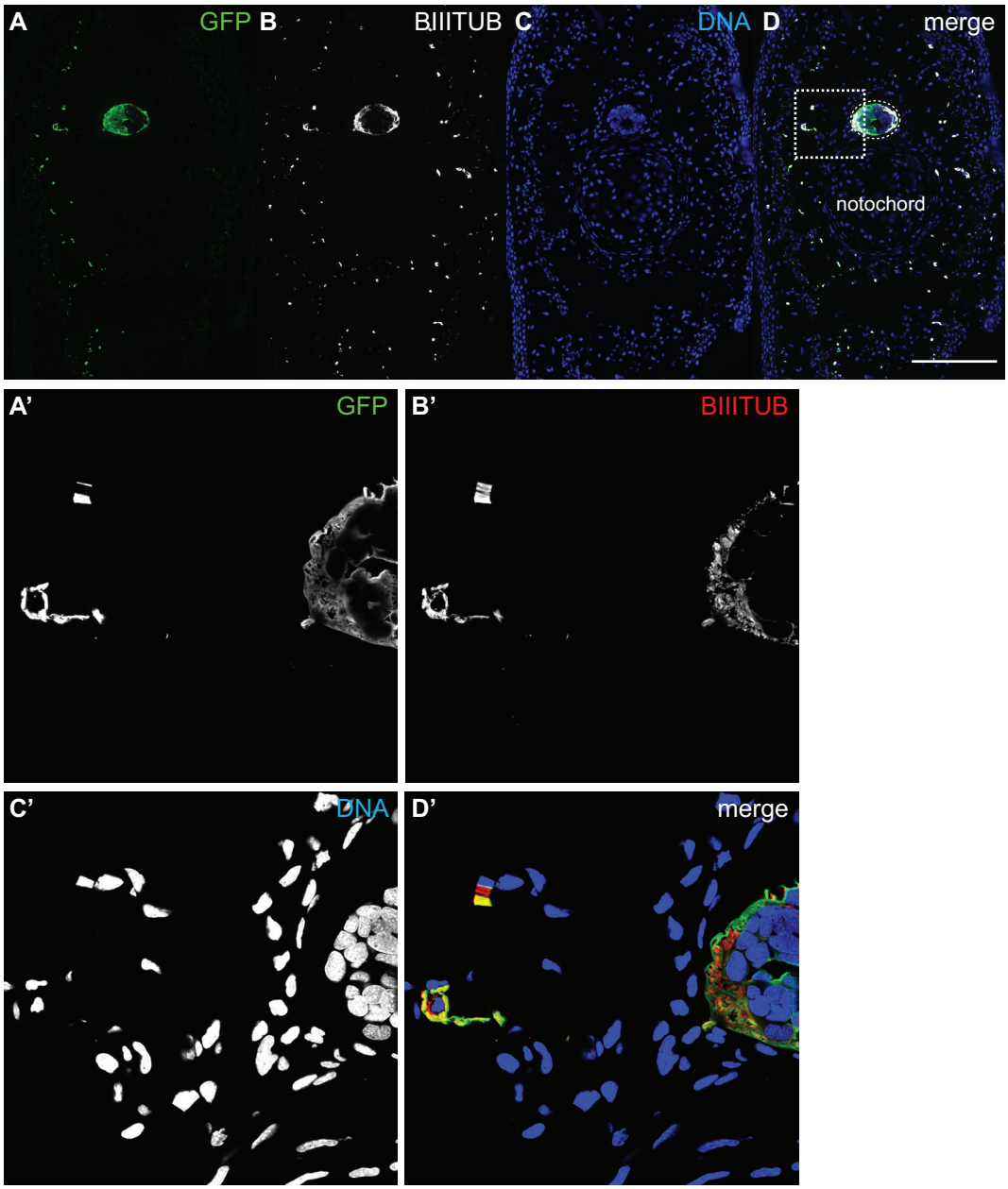

Figure 26: GFP labeled animals due to ectodermal transplantation express GFP in cells of the neural system
Immunohistochemical staining of a cross section from the mature part of the tail. DNA was counterstained with Hoechst 33342 ((**C**), (**C'**)). Scale bar 100 μm. **(A)** Shows expression of GFP in spinal cord and cells of the neural system. **(B)** Staining for βIII TUBULIN a neural cell marker. Dashed square is magnified and shown by the confocal images. **(A')** GFP expression co-localizes with βIII TUBULIN **(B')**. Merged images show the overlay of all three channels ((**D**), (**D'**)).

We wanted to confirm that due to the transplantation and amputation of the tail no muscle cells were labeled. Hence we stained sections of the regenerating tail with the muscle marker myosin heavy chains (MHC) and calculated the percentage of double positive GFP/MHC expressing cells, indicating muscle formation and compared it to cells double positive for GFP/βIII TUBULIN indicating neurons. The result is shown in Table 2. Transplantation of GFP neural ectoderm cluster to one side of the neural plate ectoderm led to about 55% GFP expressing spinal cord cells per tissue section. We determined about 43% of GFP/βIII TUBULIN expressing neurons outside the spinal cord. There were no cells expressing GFP/MHC. Figure 27 shows an example of distinct cells expressing GFP and MHC. This shows that animals obtained by transplantation show only GFP expression in spinal cord and neurons but not in muscle tissue, and thus can be used for further cell tracking experiments.

Table 2: Embryonic transplantation labels spinal cord including neurons, but no muscle cells

% of GFP labeled spinal cord cells	**% of GFP/βIII TUBULIN expressing cells**	**% of GFP/MHC expressing cells**
54.8% (+/- 9.1%) (n_{cells}=851)	43.1% (+/- 11.3%) (n_{cells}=551)	0% (n_{cells}=209)

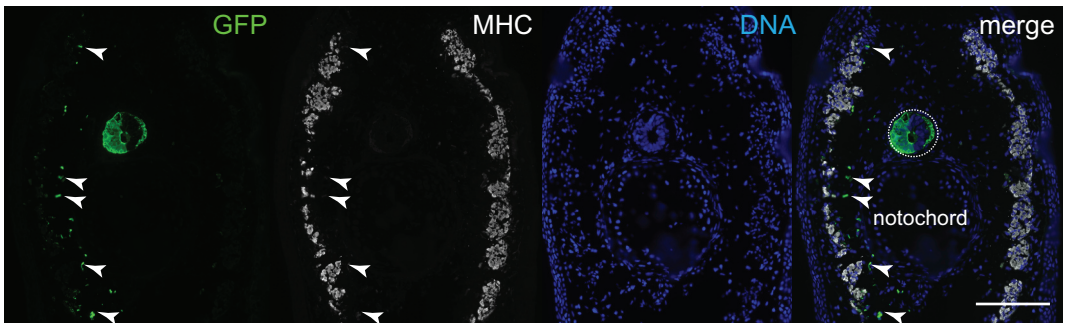

Figure 27: No co-localization of muscle cells and GFP-labeled cells from the spinal cord Immunohistochemical staining of a cross section in the mature region. GFP is expressed in the spinal cord and axons due to transplantation in neurula stage embryos. GFP does not show co-localization with myosin heavy chains (MHC) indicated by arrowheads. DNA was counterstained with Hoechst 33342. Merged image shows the overlay of all four channels. Dashed circle marks spinal cord. Scale bar 100 μm.

7.2.7 In an embryonic context pluripotent spinal cord cells form muscle

With our final experiment we wanted to investigate whether regenerating spinal cord cells, expressing OCT4 and SOX2 have a pluripotent character. Hence we performed *in vivo* studies and transplanted regenerating spinal cord cells into somites of an embryo. Spinal cord developed from the ectoderm during embryogenesis. In contrast, somites are mesodermal cells and form skeletal muscle, dermis and the vertebrae. By transplanting spinal cord cells into the niche of muscle forming tissue we have the ability to judge whether spinal cord cells form another cell type and hence are pluripotent.

For the experiment we used spinal cord of a day-6 regenerating tail since OCT4 is upregulated compared to non-amputated and very proximal mature tissue. The animal we used was obtained from embryonic transplantation (see chapter 7.2.6). Evaluation of the transplanted animals showed that cells of the spinal cord are GFP expressing, but muscle cells did not. Hence, we used this animal for lineage tracing of spinal cord cells when transplanted into somites. We dissected mature spinal cord close to the amputation plane and the regenerating spinal cord six days after amputation. To disrupt the cell-cell contact we incubated the spinal cord in a papain ovomucoid mixture and transplanted the disrupted cells into somites of a somite stage axolotl embryo (Figure 28 A). We performed 12 transplantation experiments.

Figure 28 B shows an example of GFP labeled spinal cord cells into somites of an axolotl. After hatching we identified GFP expression in ten out of twelve transplanted animals using a dissecting microscope. We sectioned the tissue of the ten animals and stained for GFP (Figure 28 C) and MHC (Figure 28 D). Interestingly, in all cases we observed co-localization of GFP and MHC, shown in Figure 28 F. Confocal images illustrate this observation in more detailed way (Figure 28 C', D', E', F').

This result suggests that regenerating axolotl spinal cord cells are pluripotent and can give rise to muscle cells when brought into an embryonic context.

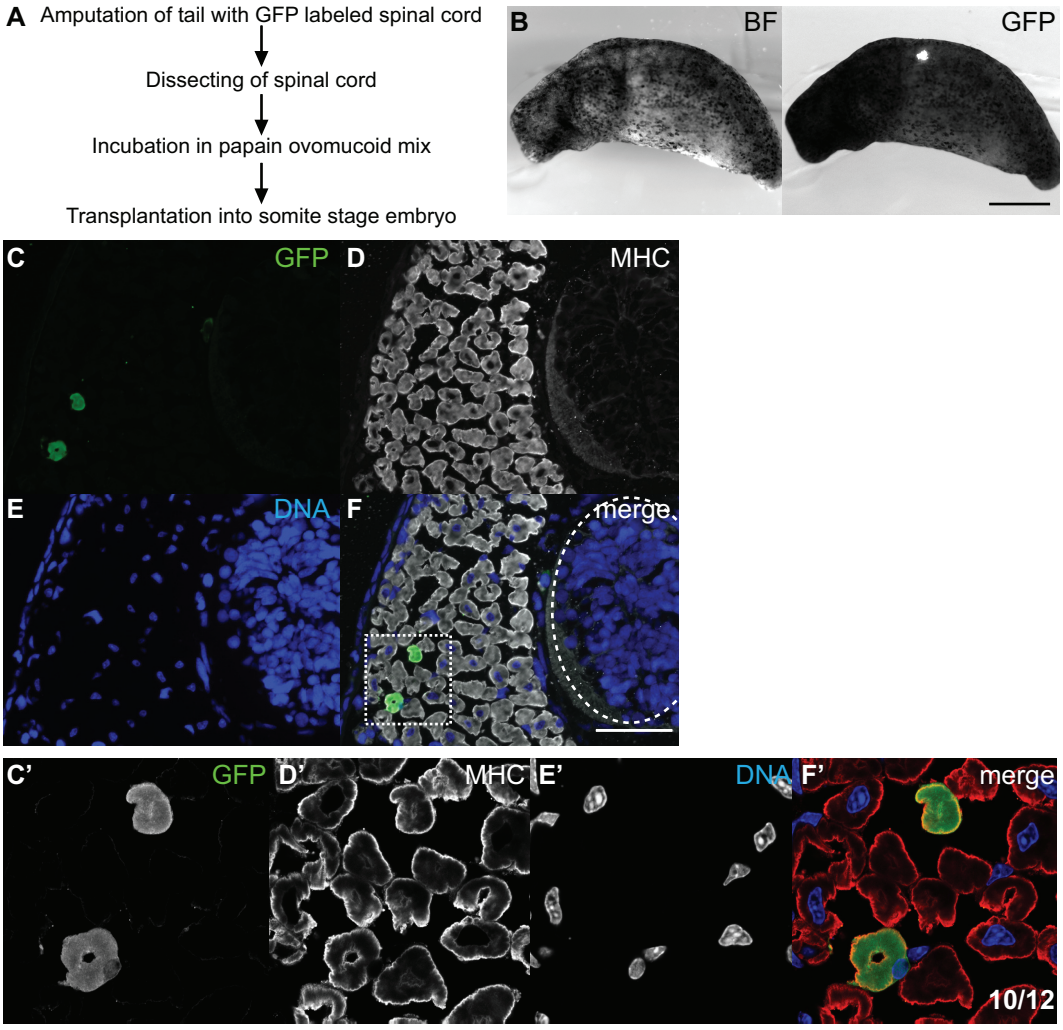

Figure 28: In an embryonic context spinal cord cells can form muscle
(A) Experimental approach. Day-6 regenerating spinal cord was dissected from a host with GFP labeled cord. Cell clump was treated in papain ovomucoid mix for a better cell disruption before transplanting GFP expressing cells it into somites of an axolotl embryo. **(B)** Transplantation of GFP labeled spinal cord cells into somites. Scale bar 1 mm. BF... brightfield. Hatched animals were checked for GFP expression using a dissecting microscope. Positive animals (10/12) were sectioned and stained for GFP **(C)** and **(D)** MHC. **(E)** DNA was counterstained with Hoechst 33342. **(F)** Overlay of the different channels, indicates co-localization of GFP and MHC. Dashed circle illustrates the spinal cord. Magnification of the GFP and MHC expressing cells (indicated with a dashed rectangle) is shown in the confocal images. **(C')** GFP (green), **(D')** MHC (red), **(E')** DNA (blue) and **(F')** merge. Scale bar 100 μm.

7.3 Discussion

In the present study we characterized of the transcription factors *Oct4, Pou2* and *Sox2* in spinal cord regeneration after axolotl tail amputation. Furthermore, we traced SOX2/OCT4 expressing spinal cord cells in axolotl embryos after transplantation. We could show for the first time that spinal cord cells have an *in vivo* potential to form muscle cells in an embryonic context.

7.3.1 Axolotl OCT4 and SOX2 play a key role in spinal cord regeneration

From mammalian systems as well as amphibians it is known that the transcription factor *Oct4* is expressed during cleavage stages in embryo development and is an essential key player for the differentiation process of blastocysts (Nichols *et al.*, 1998; Bachvarova *et al.*, 2004). Later, OCT4 expression becomes restricted to the inner cell mass and epiblast, and after gastrulation OCT4 is expressed in primordial germ cells (Nichols *et al.*, 1998; Morrison and Brickman, 2006; Downs, 2008). In mouse, Downs (2008) detected OCT4 in distinct epiblast-derived embryonic and extraembryonic tissue up to a developmental stage of 16-somite pairs.

In our study on axolotl we found that *Oct4* is not only restricted to germ cells but also present in somatic cells. We identified an upregulation of *Oct4* and *Pou2* mRNA in spinal cord and mesenchymal cells of a day-6 regenerate compared to non-amputated tail. OCT4 protein showed an identical expression pattern. SOX2 expression was highly abundant but restricted to progenitor cells of the spinal cord without a significant change between non-amputated tail and regenerate. In contrast, in xenopus tail amputation leads to a global increase in SOX2, and a proliferation of SOX2 expressing cells (Gaete *et al.*, 2012). By overexpressing a dominant negative form of SOX2, Gaete *et al.* (2012) showed a decrease in proliferation of spinal cord cells which affected tail regeneration. This suggests that xenopus SOX2 is necessary for the process of spinal cord regeneration. We had a similar result in axolotl. To study the loss of a gene function in axolotl, the use of a morpholino, blocking mRNA translation to protein is necessary. SOX2 was required for spinal cord regeneration but to a lesser extent than OCT4, which decreased the regenerated length significantly compared to control. Even though, with Sox2-morpholino we did not observe the phenotype of a significantly shorter regenerated spinal cord, about 45% of SOX2 knocked down cells were no longer cycling and proliferating. This would indicate that axolotl SOX2 has an effect in regeneration. One may be able to prove that by applying a higher amount of Sox2-morpholino to spinal cord cells by either using higher morpholino concentration, injecting and electroporating the tail over several days before amputation, or changing the electroporation conditions to improve the number of Sox2-morpholino positive cells.

In zebrafish *Pou2* and *Sox2* were expressed before and during fin regeneration, suggesting that both are required for the regeneration process. However, none of the factors was upregulated in regenerating fin tissue compared to non-regenerating tissue (Christen *et al.*, 2010). POU2 knockdown in one or two day blastema cells reduced dorsal fin outgrowth by 40%, while SOX2 was also required for fin regeneration but to a lesser

extent (Christen *et al.*, 2010). The researchers claimed that *Pou2* is a crucial gene in fin regeneration.
We could also show that Oct4- and Sox2-morpholino electroporated cells are less proliferating. PCNA expression is diminished to at least 33% and 45% of the cells, respectively. Further, OCT4 knockdown animals regenerated a shorter spinal cord. Taken together, this would indicate that *Oct4* and to a lesser degree also *Sox2* are important in spinal cord regeneration of the axolotl.

7.3.2 Cell lineage tracing studies require an efficiently labeled cell type of interest

From previous studies it was known that cells keep the memory of their tissue origin during axolotl limb regeneration (Kragl *et al.*, 2009). However, it remained unclear whether progenitor cells from the spinal cord are restricted in their lineage of neural cells or whether they have the ability to form other cell types in a different environment. We therefore carried out lineage tracing experiments. One of the standard methods to perform long-term cell fate tracing is to develop transgenic axolotls.
We used germline transgenic animals harboring the LoxP reporter construct with the ubiquitous CAGGs promoter expressing a floxed EGFP - 3-Poly-Adenylation site followed by the *Cherry* gene. In addition, we have other animals where the axolotl *Sox2* genomic sequence drives an inducible Cre-ERT which would induce recombination of the LoxP construct in all *Sox2* positive cells. However, the efficiency of the conversion from EGFP to CHERRY in the spinal cord by injecting 4-OH-Tamoxifen to the progeny was very low.
One reason for the low conversion might be that the *Sox2* promoter fragment is a genomic sequence which was isolated from the axolotl genomic phage library. Thus, it might not have all required elements and enhancers necessary for an expression in spinal cord. But it might have the regulatory elements that give strong expression in brain.
It is known that chick *Sox2* has eight distinct enhancers (Uchikawa *et al.*, 2003). The different enhancers control different expression pattern in the chick embryo (Saigou *et al.*, 2010; Uchikawa *et al.*, 2003). The enhancer element N4, downstream of *Sox2* is active in mesencephalon, spinal cord, lateral head and ectoderm in chick embryos before stage 20. In later stages spinal cord *Sox2* is activated by the enhancer elements N1 and N4 as well as by a conserved block SC2. SOX2 expression in the brain however, is regulated by the upstream enhancer elements N3 and N2, and the downstream ones N5 and N4 (Uchikawa *et al.*, 2003). This might be an explanation why we had such a weak conversion in the spinal cord of our transgenic animals. To increase the conversion efficiency it would be necessary to create a construct containing a longer downstream sequence of *Sox2* including all enhancer elements necessary for SOX2 expression in the spinal cord.

7.3.3 Pluripotent spinal cord cells form muscle when brought in an embryonic context

Even though transgenic animals would be a much cleaner source for cell fate studies, the conversion efficiency was at a very low rate and thus this strategy was not possible to use for lineage tracing experiments. Thus, it was necessary to label cell types by transplantation. We transplanted ectodermal cells from neural plate

constantly expressing GFP (Sobkow *et al.*, 2006) into the same position of a non-GFP recipients and observed GFP expression in the spinal cord and axons. Due to the fact that GFP cells were only transplanted to one half of the neural plate only about 55% of spinal cord cells were GFP labeled. When the tail of the animal is amputated, the GFP labeled spinal cord cells will only form spinal cord during the regeneration process in agreement with Kragl *et al.* (2009). Hence our studies coincide with the result from axolotl limb regeneration studies where cells keep their memory. This restriction however, depends on the environment of the spinal cord cells. We showed for the first time that OCT4/SOX2 expressing spinal cord cells have the potential to change their fate in an embryonic context when one changes the environment. We obtained muscle formation when these spinal cord cells were transplanted into somites, the niche for muscle development. However, our data do not indicate whether muscle is formed directly from the spinal cord or whether spinal cord cells fuse to developmental myoblasts, a cell type of embryonic progenitors, which give rise to muscle cells.

Studies on mouse showed that progenitor cells of the CNS are able to generate non-neural derivatives (Ying *et al.*, 2002). The investigators used cells from mouse brain and co-cultured them with pluripotent ES cells, showing that brain cells do not generate directly ES cells, but the conversion takes place through generation of tetraploid hybrid cells by spontaneous fusion of ES cells and cells from the CNS (Ying *et al.*, 2002). Further, it has been reported that stem cells from the CNS can give rise to the haematopoietic cell lineage (Bjornson *et al.*, 1999), but more interestingly also to muscle when co-cultured with skeletal myoblasts (Galli *et al.*, 2000). It had been further discussed that stem cells of the nervous system change fate during co-culturing with differentiating ES cells, when forming multinucleated myotubes (Clarke *et al.*, 2000). Also other studies show that in mouse stem cells derived from adult bone marrow are able to repair liver tissue via fusion to the host liver cells (Wang *et al.*, 2003; Vassilopoulos *et al.*, 2003). These reports all indicate that cell fusion is able to remove some of the barriers for one cell type to become another.

Our experimental approach lacks of the possibility to detect fusion of the spinal cord cells with muscle cells. As markers we used the cytoplasmic GFP in the spinal cord, and the cytoplasmic myosin heavy chain marker for muscle cells. Since none of the marker labels the nuclei we can not exclude cell fusion. Thus, it would be better to use transgenic animals having spinal cord cell labeled nuclear GFP and transplant them into somites. The staining should be performed using a muscle nuclei specific marker, like the nuclear transcription factor myocyte-specific enhancer factor 2C, also called Mef2c. Since in this case the nuclei would be labeled, one would be able to detect multinucleated cells, and thus obtain evidence about cell fusion.

To clearly define whether regenerating OCT4/SOX2 expressing spinal cord cells have a pluripotent character it would be necessary to transplant cells into endoderm for example. Endodermal cells give rise to cells of the gastrointestinal tract, respiratory tract, endocrine glands, to auditory and urinary system, but not to muscle. Further it would be interesting to determine whether spinal cord cell of the very mature part would have the same capacity as the spinal cord cells from the regenerating tail. Another experimental approach

to determine the pluripotent character of OCT4 expressing spinal cord cells should be the transplantation of OCT4 knocked down spinal cord cells. We can knock down OCT4 expression in spinal cord using morpholino. We showed that these animals have a deficiency in spinal cord regeneration. Further, OCT4 knockdown cells showed decreased cell proliferation, as indicated by lower number of PCNA expressing cells. This means that cells are less proliferative, and maybe also less pluripotent if OCT4 were the main factor.

7.3.4 Summary II

Our results demonstrate, that *Pou2, Oct4* and *Sox2* are present in the spinal cord of non-regenerting and regenerating spinal cord. Further, OCT4 was upregulated in regenerating spinal cord and mesenchymal cells. Knockdown of OCT4 showed a significantly shorter regenerated spinal cord compared to control, whereas SOX2 knockdown resulted in a slight decrease of the regenerated length only. This indicates that OCT4 plays a role in the process of epimorphic regeneration. To determine the pluripotent potential of regenerating SOX2/OCT4 expressing spinal cord cells *in vivo* we transplanted cells into somites of embryos and observed muscle formation. However, we cannot exclude fusion of spinal cord and muscle cells. This can be resolved by labeling the nuclei of spinal cord and muscle. Thus, cell fusion with its multinucleated cells could be detected. To clearly state whether regenerating OCT4 expressing spinal cord cells are pluripotent we have to perform OCT4 knock down in spinal cord and transplant these less proliferating cells into embryos, observing their cell fate.

8 GENERAL DISCUSSION AND CONCLUSION

In this thesis we have studied the characteristics of the two pluripotency related genes *Oct4* and the newly identified *Pou2*, both belong to the group of *PouV* genes, as well as *Sox2* from axolotl. All three genes are present in the pluripotent animal cap cells during embryonic development and in spinal cord regeneration.

By *in vitro* we investigated whether axolotl POU2 and OCT4 expression have conferred a potent character to cells like POU orthologs do in mammals. We could show that axolotl POU2 and OCT4 in combination with the human or axolotl factors SOX2, c-MYC and/or KLF4 are able to reprogram mouse or human fibroblasts and hence generate an iPS cell. Our results demonstrate that the axolotl factors can substitute human orthologs as well as dimerize with the human proteins to initiate reprogramming. This would propose that the ancestral class V POU already possessed a pluripotency conferring potential and this characteristic also remained after the duplication of class V POU at the base of tetrapod development. Thus, the pluripotent potential is a feature for *Pou2* and *Oct4*. However, not all *Pou* orthologs from various species are able to reprogram cells. Zebrafish POU2 did not show reprogramming ability. This means that at some point in evolutionary history the pluripotency conferring potential of *Pou2* in zebrafish disappeared (Morrison and Brickman, 2006; Niwa *et al.*, 2008).

By *in vivo* studies we characterized the transcription factors OCT4, POU2 and SOX2 in spinal cord regeneration after axolotl tail amputation. All three factors are present in regenerate. Knockdown of OCT4 and SOX2 result in a shorter regenerated spinal cord. Further, the morpholino containing cells proliferate less. This indicates that OCT4 and SOX2 play a key role during the regeneration process. Lineage tracing studies showed that after amputation of the tail the cells from the spinal cord only form spinal cord again. This observation is supported by studies on limb regeneration in axolotl. The lineage tracing experiments showed that cell keep their memory of origin and hence the regeneration potential of the cells is restricted (Kragl *et al.*, 2009).

The restricted potential of the spinal cord cells expressing OCT4 and SOX2 however, depends on the environment of the spinal cord cells. We showed that OCT4/SOX2 expressing spinal cord cells have the potential to change their fate when brought into an embryonic context. We obtained muscle formation when these spinal cord cells were transplanted into somites, the niche for muscle development. Our observation is supported by results from embryonic development. There it was reported that the chordoneural hinge, a tissue posterior to the developing notochord during tailbud extension, represents at least one stem cell population which gives rise to myotomes and cells of the CNS (Mathis and Nicolas, 2000; Nicolas *et al.*, 1996; Gont *et al.*, 1993; Cambray and Wilson, 2002, 2007; McGrew *et al.*, 2008) (also reviewed in Handrigan (2003)).

However, with our experimental approach we could not observe whether muscle cells are formed directly from the spinal cord or whether spinal cord cells fuse to developmental myoblasts, which give rise to muscle. Our data indicate that somatic cells from the axolotl tail spinal cord have the ability to dedifferentiate *in vivo* to

become a more pluripotent cell. These cells are then able to re-differentiate and can form another cell type.

9 MATERIALS AND METHODS

9.1 Axolotl care

9.1.1 Breeding

Ambystoma mexicanum (axolotl) used for our experiments were bred in the facilities of the MPI-CBG, BioTec and the CRTD where they were kept in aquariums (Aquarienbau Schwarz) filled with 18 °C tap water. Juvenile animals (2-5 cm) were fed daily with freshly prepared *Artemia salina* (Fimö Aquaristik GmbH), and larger animals (above 5 cm) were fed 2-3 times per week with fish pellets (AXOBALANCE, Aquaterratec).

9.1.2 Anesthetization of animals

For surgery and live microscopy, animals were anesthetized in tap water containing 0.01% ethyl-p-benzoate (Sigma).

9.1.3 Dejelling of embryos

The embryos were transfered to a sieve, washed with tap water followed by 70% ethanol before rinsing it with sterile water. The embryos were then collected in a petridish filled with 1x Steinberg's (3.4 g/l NaCl, 0.05 g/l KCl, 0.205 g/l $MgSO_4$ x 7 H_2O, 0.56 g/l Tris, 0.08 g/l $Ca(NO_3)_2$ x 4 H_2O; pH 7.4) including 1x Anti-Anti (Gibco), an antibiotic-antimycotic mixture and 1.5 ml/l of the antibiotic Ciprobay 200 (Bayer). Embryos were staged according to Bordzilovskaya (1989) and dejellied using two sharp forceps at least 24 h prior to use in further experiments.

9.2 Axolotl manipulation

9.2.1 Injection of tamoxifen

Powdered 4-Hydrotamoxifin (Sigma) was dissolved in DMSO (Sigma) (10 mg/ml), aliquoted and stored in liquid nitrogen. For each set of injections a fresh aliquot mixed with Fast green (Sigma) dye was used. The anesthetized animal was weighted and 50 μg 4-Hydrotamoxifin per 1 g of body weight was injected intraperitoneally using a syringe (Hamilton Messtechnik GmbH). The animal was kept in a hydration chamber for 20 min before returning it to water.

9.2.2 Microinjection and electroporation of morpholino into axolotl spinal cord

Borosilicate glass capillaries (1.2 mm O.D. x 0.94 mm I.D., Harvard Apparatus) were clamped into the Flaming/Brown Micropipette Puller (Model P97, Sutter Instrument CO.) and pulled (heat: 485, pull: 80, velocity: 120, time: 80).

FITC-labeled morpholinos (GeneTools) (Table 3) were dissolved in distilled water to a final molar concentration of 1 mM, mixed with Fast green (Sigma) in a ratio of 25:1 and transfered into the glass capillary.

Table 3: Morpholinos

Morpholino name	**Sequence 5' - 3'**
Axolotl Oct4	TCTCCTGTCCCAAATGCCCAGCCAT
Axolotl Pou2	CACGGTATCTCTTCCGAGCATCGGC
Axolotl Sox2	CGGTCTCCATCATGCTGTACATGGC
Standard control	CCTCTTACCTCAGTTACAATTTATA

The capillary was fixed in the injection stage connected to the PV830 Pneumatic PicoPump (WPI). The anesthetized animal (3 cm snout to tip of the tail) was placed on the injection stage under a dissecting microscope, and morpholino was injected into the spinal cord.
Injected animal was immediately transfered to a 2% agarose dish filled with ice cold 1x phosphate-buffered saline (PBS) which was cut out to hold the animal in place for the electroporation. Electroporation was fulfilled using stainless steel tweezer electrodes (BTX Harvard Apparatus). Pulses (50 V, 50 ms, 5 pulses, 1 s interval, bidirectional, 7 mm distance of electrodes) were generated by Electro Square Porator^{TM} ECM830 (BTX Harvard Apparatus).

9.2.3 Transplantations

Cells of the spinal cord were labeled by transplantations. Matings using non-GFP and a GFP animal were set up, whereas non-GFP neurula stage embryos were used as hosts. The transgenic donor expressed GFP under the control of the ubiquitous CAGGS promotor (Sobkow *et al.*, 2006) and was at the same stage as the recipient embryo. A scheme is shown in Figure 29.

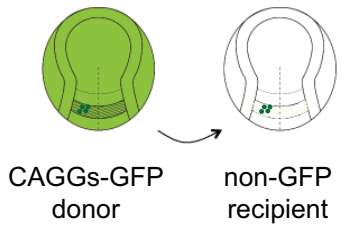

Figure 29: Scheme of ectodermal transplantion
Ectoderm of CAGGs-GFP donor from neural plate is transplanted into non-GFP host. A cell cluster of about 4-10 cells was grafted into a non-GFP recipient to label spinal cord cells.

Petri dishes with a diameter of 3 cm filled with 2% agarose prepared in 1x Steinberg's (for recipe see chapter 9.1.3) were flamed and filled with 1x Steinberg's including 1x Anti-Anti (Gibco) and 1.5 ml/l Ciprobay 200 (Bayer). All following procedures were carried out using sterile conditions.
Dejellied wild type embryo was transfered to the petri dish, and transparent membrane around the embryo was removed using forceps. The embryo was fixed by placing in a mold cut into the agarose. A small area

of the ectoderm from the neural plate was removed and a cluster of about 4-10 GFP labeled ectodermal cells was transfered by mouth pipetting. GFP labeled ectoderm cells were isolated as follows: To avoid cell attachment a drop of 1% bovine serum albumin (BSA) was placed on the bottom of three different petri dishes. Two of the dishes were filled with CMF-NT, and one with NT-solution (Niu, 1953) (for recepies see Table 4 and 5). The donor was transfered to the dish filled with CMF-NT, and cells from the ectoderm of the neural plate were scraped off with a tungsten needle and a forceps. Any mesodermal cells attached to the ectoderm were removed. Ectodermal cells were transfered by mouth pipetting using a BSA coated glass capillary to the second dish filled with CMF-NT. Cells were dissociated so that only clusters of about 4-10 cells remained. Immediately cells were transfered to NT-solution and used for transplantation into the donor. Between two to four days after transplantation, embryos were transfered to a fresh agarose dish filled with 1x Steinberg's including 1x Anti-Anti and 1.5 ml/l Ciprobay 200.

All six solutions for preparing CMF-NT and NT-solution (Table 4 and 5) were autoclaved separately. After cooling component A, B and C of CMF-NT solution as well as NT solution were mixed in a ratio of 2:1:1. To both solution 1.5 ml/l Ciprobay 200 (Bayer) and the antibiotic-antimycotic mixture Anti-Anti (stock 100x, Gibco) to 1x final was added.

Table 4: CMF-NT solution used in transplantation

Component A	**Amount**
NaCl	3.40 g
KCl	0.05 g
$Ca(NO_3)_2$ x 4 H_2O	0.08 g
$Mg(SO_4)$ x 7 H_2O	0.10 g
Distilled water	500 ml
Component B	**Amount**
Na_2HPO_4	0.11 g
KH_2PO_4	0.02 g
Distilled water	250 ml
Component C	**Amount**
$NaHCO_3$	0.20 g
Distilled water	250 ml

Table 5: NT solution used in transplantation

Component A	**Amount**
NaCl	2.943 g
KCl	0.05 g
Distilled water	500 ml
Component B	**Amount**
Na_2HPO_4	1.30 g
KH_2PO_4	0.115 g
Distilled water	250 ml
Component C	**Amount**
$NaHCO_3$	0.20 g
Distilled water	250 ml

9.3 Microscopy

9.3.1 Dissecting microscopy

Embryos or anesthetized animals were transfered to a petridish and imaged using the Olympus SZX16 with the SDF PLAPO 1xPF objective (Olympus). Images were taken using the F-View camera (Olympus) and Cell^F Soft imaging software.

9.3.2 Microscopy of tissue sections

To visualize fluorescence or bright field, digital images of axolotl tissue sections were taken on the Zeiss Observer Z1 microscope. Images were taken using a 10x Plan-Neofluar (Numerical aperture (NA) 0.3 Ph1, Zeiss) or a 20x Plan-Apochromat objective (NA 0.8, Zeiss) with an AxioCam MRm camera (Zeiss) for black/white images or AxioCam MRc (Zeiss) for color images under the control of the AxioVision software. Mosaic images were assembled using AxioVision program.
Confocal images were taken on Leica CRT 4000 using the 40.0x ACS APO (NA 1.15, Leica) oil objective.

9.3.3 Image processing

Measurements of fluorescence intensities were analyzed using the Fiji program.

9.4 Molecular Biology

9.4.1 Agarose gel electrophoresis

Agarose gels were prepared from agarose (Serva) disolved in 1x TBE (0.9 M Tris (Serva), 0.9 M Boric acid (VWR), 10 mM EDTA (Merck)) by boiling. After allowing the solution to cool down, it was poured into the chamber and Ethidium bromide (3,8-Diamino-5-ethyl-6-phenylphenanthridiniumbromid (Roth)) was added directly to the agarose solution. DNA samples were mixed with 6x loading dye (30% (v/v) glycerol

(VWR), 0.25% (w/v) bromophenol blue (Sigma Aldrich), 0.25% (w/v) xylene cyanol FF(Sigma Aldrich)) and electrophorezed in 1x TBE at 120 V for 20 to 60 min. When purified DNA was required, DNA was extracted using the agarose gel extraction kit (Qiagen) following the manufacturers instructions.
RNA samples were electrophorezed for 15 min at 130 V to avoid degradation of the samples.

9.4.2 Polymerase chain reaction

PCR were carried out in a total volume of 20 μl. The reaction contained 0.5 μl 40 mM dNTPs (10 mM each, Bioline), 2 μl 10x reaction buffer (MPI-CBG), 0.2 μl of forward and reverse primer (stock 100 mol/l) (Sigma) and 5 units of *Taq* or *Taq-Pfu* polymerase mix (MPI-CBG). For amplification of axolotl *Oct4* from gastrula stage cDNA, 1x CES (for 5x CES use 2.7 M betaine, 6.7 mM DTT, 6.7% DMSO, 55 μg/ml BSA) (Ralser *et al.*, 2006) was added to the reaction mix. Either 5 μl of cDNA or 50 ng of plasmid DNA was used as a template. Depending on the annealing temperature of the primers and the length of the generated product, 30 cycles with 30 s at 95 °C, 30 s at 55-70 °C and 30-90 s at 72 °C were performed. Primers used for PCR to amplify *Sox2* are shown in Table 6. All other primers are summarized in Table 7. The PCR amplified products were electrophorezed in an agarose gel or purified using PCR purification kit (Qiagen) according to the protocol the company provided.

Table 6: Primers used for PCR to amplify *Sox2*

Primer name	**Sequence 5' - 3'**
Sox2-5UTR-RT-F	AAATAATAACCCGAAATCAGTGAAGAA
Sox2-5UTR-RT-R	TGTAAAGTCACTTCAGTCTTTTGGAG

9.4.3 RNA extraction

The extraction of total RNA from axolotl tissue was performed according to Mini RNeasy kit (Qiagen) using the protocol "Purification of total RNA from animal tissue". Briefly, frozen tissue was transfered to a 5 ml tube and Buffer RLT was added. Tissue was disrupted and homogenized using a blender. Total RNA was eluted in 30 μl of RNase free water and RNA concentration determined on the NanoDrop (Thermo Scientific). RNA was kept in liquid nitrogen.

9.4.4 cDNA preparation from total RNA

Total RNA samples of 500 ng to 1 μg were DNase treated by adding 1 μl 10x DNase I reaction buffer, 1 μl DNase I (1 U/μl, Invitrogen) and made up to 10 μl with RNase free water. Reactions were incubated for 15 min at 25 °C. The enzyme was heat inactivated for 10 min at 65 °C and sample chilled on ice. Each sample was divided into two. To one part RT III superscript enzyme will be added to generate cDNA. To the other half RT III will be omitted and thus will be a negative control. Oligo d(T)-12-18 primer (1 μl, Invitrogen), 1

μl of 40 mM dNTP mix (Bioline), 4 μl 5x first strand buffer (Invitrogen), 2 μl 50 mM $MgCl_2$ (Invitrogen), 2 μl 0.1 M DTT (Invitrogen) and 1 μl RNase OUT (40 U/μl, (Invitrogen)) were added and made up to 19 μl with RNase free water. The reaction was heated for 2 min at 42 °C and 1 μl of SuperScript III (Invitrogen) was added to one set of the samples. The sample was mixed and reverse transcription was performed for 1 h at 42 °C. The enzyme was heat inactivated at 70 °C for 15 min, and the samples then cooled down on ice and stored at −20 °C.

9.4.5 Preparation of *in situ* hybridization probe

Sense and antisense probes were prepared from DNA templates either by PCR or the plasmid was linearized using one restriction enzyme. Template was purified using PCR purification kit (Qiagen) according to provider's protocol. Concentration of the purified DNA was measured on a photometer (NanoDrop) and 1 μg of DNA was used for *in vitro* transcription. DNA was mixed with 2 μl 10x transcription buffer (Roche), 2 μl DIG RNA labeling kit (Roche), 1 μl 0.1 M DTT (Invitrogen), 1 μl RNase OUT inhibitor (Invitrogen) and 2 μl of an RNA polymerase (Sp6, T7) (MPI-CBG), and incubated for 2-3 h at 37 °C. RNA cleanup was performed using RNeasyMini kit (Quiagen) following the manual provided. Probe was eluted using two 30 μl distilled water additions and used at a dilution between 1:800 to 1:1200 in hybridization buffer. Probes were stored at −20 °C and a samples was electrophorezed in an agarose gel before using to determine whether the probe is still intact.

9.4.6 Identification of axolotl *Pou2*

An assembly of axolotl sequences derived from Sanger sequences (Habermann *et al.*, 2004; Putta *et al.*, 2004), 454 published sequences (Monaghan *et al.*, 2009) and 454 unpublished sequences was performed using MIRA 3.0.

To identify a close paralog of the axolotl *Oct4* sequence the contig assembly was checked using BLAST. This resulted in the detection of axolotl *Pou2* sequence fragment. When this fragment was BLAST searched to NCBI RefSeq set, *Pou2* sequences from different organisms were referred as the closest ortholog.

9.4.7 Axolotl *Oct4, Pou2, Sox2*, xenopus *Pou91*, medaka *Pou2* and zebrafish *Pou2* amplification and cloning into retroviral vector

The different *Pou* orthologs were cloned into the pMX retroviral vector (Cell biolabs) by standard methods using restriction enzymes and its buffers from the NEB company. For primer sequences see Table 7.

Axolotl *Pou2* was isolated by PCR from our long-insert cDNA library using primers designed from the identified contig sequence. Two PCR reactions were performed using Axolotl-Pou2 Fw1 and the vector primer M13 Rv, and Axolotl-Pou2 Rv1 with M13Fw. The amplified products were sequenced, and the coding sequence was amplified by PCR (Axolotl-Pou2fl-BamHI-Fw, Axolotl-Pou2-NotI-Rv) and directionally cloned into the pMXs vector using *BamH*I and *Not*I restriction sites.

Table 7: Primers used for cloning reactions

Primer name	**Sequence 5' - 3'**
Axolotl-Pou2 Fw1	AACGAGGCCGAGAACACAGACAACATG
Axolotl-Pou2 Rv1	AGGCTGAGGTCCTCTGCGATCTGAGA
M13 Rv	GGAAACAGCTATGACCATG
M13 Fw	TGTAAAACGACGGCCAGT
Axolotl-Pou2fl-BamHI-Fw	ACTGGATCCATGCTCGGAAGA
Axolotl-Pou2-NotI-Rv	AGAGCGGCCGCTTAGCTAATGCTG
Zebrafish-EcoRI-Fw	ATCGAATTCATGACGGAGAGAGC
Zebrafish-T-A-Rv	CCAAGCTGGTCCTTCGTTTTC
Zebrafish-T-A-Fw	GAAAACGAAGGACCAGCTTGG
Zebrafish-XhoI-Rv	TCGCTCGAGTTAGCTGGTGAGATG
Zebrafish-EcoRI-Fw	ATCGAATTCATGACGGAGAGAGC
Zebrafish-XhoI-Rv	TCGCTCGAGTTAGCTGGTGAGATG
Xenopus-BamHI-Pou91-Fw	ATCGGATCCATGTATAACCAACAG
Xenopus-XhoI-Pou91-Rv	TCGCTCGAGCTAGTTGCCTTGG
Medaka-Pou2-HindIII-Fw	GCACAAGCTTATGTCTGACAGG
Medaka-Pou2-NCBI-Rv	CTGTTGAAAGGTTCTCCTCCTCAGAGTCGC
Medaka-Pou2-NCBI-Fw	GCGACTCTGAGGAGGAGAACCTTTCAACAG
Medaka-Pou2-XhoI-Rv	TCGCTCGAGTCATCCTGTCAGGT
Oct4-RT-Fw3	GAGGCTGCAGCTGGAATTAG
Oct4-RT-Rv2	TATTCCAGGTATGGTGCAATAAAGT
Sox2-D-Fw1	ATGAAYGCITTYATGGTITGG
Sox2-D-Rv1	CRRTGCATIGGYTGCATYTG
Sox2-sRv1	AGCTGTCCATCCGCTGGCTGGAGTTCAT
Sox2-sFw2	GGCTACGGCATGATGCAGGAGCAGCT
Sox2-full-Fw	TTTCAAAAAAGTCTCCCGGAGTTGTCAAAA
Sox2-full-Rv	CGCTTAATCTCCTCTGTACAAAAATAGTCC

The vector pME18S-FL3 containing zebrafish *Pou2* was obtained from imaGenes. However, this clones had a point mutation compared to the sequence in the NCBI database. To eliminate this point mutation, *Pou2* was amplified as two fragments (Zebrafish-EcoRI-Fw and Zebrafish-T-A-Rv, Zebrafish-T-A-Fw and Zebrafish-XhoI-Rv). PCR fragments were purified (Qiagen) and used as template for a further PCR reaction with Zebrafish-EcoRI-Fw and Zebrafish-XhoI-Rv primer. The PCR product was purified, and *Pou2* excised using *EcoR*I and *Xho*I, and ligated into the same sites within the vector pMXs.

The xenopus *Pou91* gene in the vector pCS2 was a kind gift from the Knöchel lab (University of Ulm). The *Pou91* sequence was amplified (Xenopus-BamHI-Pou91-Fw, Xenopus-XhoI-Pou91-Rv), the PCR product was purified, *Pou91* excised using *BamH*I and *Xho*I, and ligated into the same sites within pMXs vector.

The medaka *Pou2* gene was amplified as two fragments (Medaka-Pou2-HindIII-Fw and Medaka-Pou2-NCBI-Rv, Medaka-Pou2-NCBI-Fw and Medaka-Pou2-XhoI-Rv). PCR fragments were purified from an agarose gel and used as template for the final PCR reaction with Medaka-Pou2-HindIII-Fw and Medaka-Pou2-XhoI-Rv primer set. The product was purified from an agarose gel. Medaka *Pou2* was digested with *Hind*III and

*Xho*I, and ligated into the same sites within pMXs viral vector.

Axolotl *Oct4* cDNA was PCR amplified from gastrula stage (stage 11) embryonic cDNA using Oct4-RT-Fw3 and Oct4-RT-Rv2 primers designed from a published sequence (Johnson *et al.*, 2003b). Axolotl *Oct4* was digested using *BstX*I and cloned into pMXs vector.

Axolotl *Sox2* cDNA fragment was PCR amplified from a day-6 tail blastema cDNA using Sox2-D-Fw1 and Sox2-D-Rv1 primer. 5'RACE and 3'RACE were performed with Gene Racer Kit (Invitrogen) using primers Sox2-sRv1 and Sox2-sFw2, respectively. The full-length axolotl Sox2 sequence was amplified from the day-6 tail blastema cDNA using Sox2-full-Fw and Sox2-full-Rv primer. Finally, axolotl *Sox2* was cloned into pMXs vector using *BamH*I and *Xho*I restriction enzymes.

9.5 Phylogenetic and synteny analysis

9.5.1 Phylogenetic analysis of POU orthologs and axolotl *Oct4* and *Pou2* synteny analysis

The analysis was carried out by R. Voss. In brief, phylogentic results were achieved with MRBAYES 3.2 using Bayesian Inference to develop consensus phylogenetic trees with the posterior probabilities estimated by Markov chain Monte Carlo methods (Ronquist *et al.*, 2011).

First, an alignment of the entire sequences of *Oct1, Oct4, Oct6* and *Pou2* genes across different species and the zebrafish *Brn3c* gene as an outgroup was created. *Gblocks* was used to determine the most suitable conserved region for the analysis. This was the DNA binding domain. Analysis using both the alignment of the entire sequence and that of the DNA binding domain was carried out and we did not observe major differences between the two consensus trees.

The criterion for the outgroup was a single sequence from a different class of POU factors. Jones model (Jones *et al.*, 1992) for amino acid substitutions was applied with the rate heterogeneity modeled by a gamma distribution. Each consensus tree was calculated from two independent runs (four chains per run with one cold and three heated chains), of 500000 tree generations each (samples taken every 1000), after excluding 25% of samples. The convergence was measured by the standard deviation of split frequencies, and the value for the presented tree was between 0.000 and 0.0677. Sequences used for alignment and tree building are indicated in Table 8.

Genetic linkage mapping was performed according to a previous method (Voss *et al.*, 2011). Primers were designed to amplify DNA fragments from axolotl *Pou2* and *Oct4* that contained diagnostic single nucleotide polymorphisms that were informative for mapping using a primer extension genotyping method (Smith *et al.*, 2005). Markers were mapped using MultiPoint 2.2 (Korol, 2003) and the Kosambi (Kosambi, 1944) mapping function.

Table 8: Sequences used for alignment and tree building

Species	Accession Number	Species	Accession Number
Brn3c Zebrafish	Q90435 / NP_571353.1	Oct1 Human	P14859-1 / NP_002688.3
Oct1 Swine	F1S265 / NP_999429.1	Oct1 Mouse	P25425-1 / NP_035267.2
Oct1 Chick	P15143 / NP_990803.1	Oct1 Opossum	F7GF90 / -
Oct1 X. Laevis	P16143-1 / NP_001095255.1	Oct1(A) Zebrafish	O42276 / NP_571513.1
Oct1(B) Zebrafish	A4IFW4 / NP_001082798.1	Oct6 Human	Q03052 / NP_002690.3
Oct6 Rat	P20267 / NP_620193.1	Oct6 Mouse	P21952 / NP_035271.1
Oct6 Chicken	O73861 / AAC18592.1	Oct6(A) X. Laevis	P31363 / NP_001158054.1
Oct6(B) X. Laevis	Q561L5 / NP_001096655.1	Oct6 Zebrafish	Q90482 / NP_571236.1
Oct4 Human	Q01860-1 / NP_002692.2	Oct4 Chimpanzee	Q7YR49 / NP_001238970.1
Oct4 Macaque	Q5TM49 / NP_001108427.1	Oct4 Cat	D3U664 / NP_001166912.1
Oct4 Dog	E2QTW5 / XP_538830.1	Oct4 Elephant	G3T5K8 / XP_003422494.1
Oct4 Rabbit	A2ICN2 / NP_001093427.1	Oct4 Swine	Q9TSV5 / NP_001106531.1
Oct4 Bovine	O97552 / NP_777005.1	Oct4 Rat	Q6MG27 / NP_001009178.1
Oct4 Vole	A0MPW0 / ABK34451.1	Oct4 Mouse	P20263 / NP_038661.2
Oct4 Tammar	D2EA24 / ACZ54717.1	Oct4 Platypus	A7X5W5 / NP_001229656.1
Oct4 Lizard	- / XP_003228387.1	Oct4 Axolotl	Q5J1Q2 / AAT09163.1
Oct4 Bullfrog	C1C4W5 / ACO52025.1	Oct25 X. Laevis	Q7T103 / NP_001079832.1
Oct25 X. Tropicalis	B3DM25 / NP_001123406.1	Oct60 X. Laevis	Q91989 / NP_001081583.1
Oct60 X. Tropicalis	B3DM23 / NP_001123836.1	Oct91 X. Laevis	B7ZQA9 / NP_001081342.1
Oct91 X. Tropicalis	F6TLT1 / XP_002942017.1	Pou2 Tammar	D2EA25 / ACZ54718.1
Pou2 Opossum	- / XP_003339690.1	Pou2 Stickleback	G3PZT5 / -
Pou2 Platypus	- / XP_001520175.1	Pou2 Chicken	A7Y7W2 / NP_001103648.1
Pou2 Medaka	Q6DVF4 / NP_001098339.1	Pou2 Carp	D3YBA7 / ADC96616.1
Pou2 Cod	Q2I0F8 / ABC84854.1	Pou2 Zebrafish	Q90270-1 / NP_571187.1
Pou Hydra	Reference Millane *et al.*, 2011		

9.6 Biochemistry

9.6.1 Protein expression for antibody production

Antibody against axolotl OCT4 was generated against amino acid sequence 1-161 of axolotl OCT4 protein. The axolotl SOX2 antibody was raised against the amino acid sequence 1-44 of the SOX2 protein. Sequences used for generation of the antibodies are shown in Table 9. Two fusion constructs, one to maltose binding protein (MBP) another one to glutathione S-transferase (GST), were generated for each axolotl protein. The protein was expressed in BL21(DE3) *E.coli* cells, induced with isopropyl-β-D-thiogalactopyranosid (IPTG) and purified (MPI-CBG, Protein Expression and Purification facility).

GST-fusion constructs were used to inject the rabbit for polyclonal antibody production. The animal was immunized followed by three boosts after several days (200 μg protein each time). The MBP-fusion construct was used for affinity chromatography to purify the antibody from the serum (section 9.6.2).

Table 9: Protein sequences of OCT4 and SOX2 used for antibody production

Protein	**Protein sequence**
OCT4	M A G H L G Q E I G R A A Y G F G A Q A L H L G A G G L E A G G P G F L S E S Y G P Y A G F K A L E Y A H G G A E G E G R P G A H G L A R A W Y P F S E A W G P V Y G Q S G A G A G F E S S R V E V K V E R P D K E A G Y G Q Q H Q Q A W A G Y F V P Q L A V P A R S P A S V A S G G Q V P A A P A S P S D D S P H S S T A S S S S
SOX2	M Y S M M E T D L K P P A P Q Q T S T N P G S N N N S S N A K N S P D R V K R P M N A F

9.6.2 Antibody purification

MBP-Sox2 and MBP-Oct4 were stored in 1x PBS (MBP-Sox2, MBP-Oct4). The buffer was exchanged using a PD10 desalting column (GE Healthcare) equilibrated with 100 mM HEPES pH 8.0, 500 mM NaCl, 10 mM Maltose. Afterwards $CaCl_2$ was added to a final molarity of 80 mM to the protein.

Polyclonal SOX2 and OCT4 antibodies (MPI-CBG) produced in rabbit were purified in an affinity chromatography procedure using 1 ml NHS HiTrap columns (GE Healthcare) and a peristaltic pump (Gilson) with a flow rate of 1.5 ml/min. The column was washed with 3 column volumes (CV, 1 CV = 1 ml) of ice cold and freshly prepared 1 mM HCl. A protein concentration of 0.5 mg/ml MBP-Sox2 or MBP-Oct4 was used for an antigen recirculation (30 min, room temperature (RT)) to bind the MBP-fusion protein to the resin. Unreacted NHS groups were blocked by adding 6 CV blocking buffer (0.5 M ethanolamine, 0.5 M NaCl). The circulation was stopped and the column incubated for 30 min at RT. The column was washed using 8 CV for each of the following solutions: 10 mM Tris pH 8.0, 100 mM glycine pH 2.6, 10 mM Tris pH 8.0, 100 mM triethylamine pH 11.5. This washing step was repeated before adding 22 CV 1x PBS.

Serum was thawed and diluted with an equal volume of sterile 2x PBS. NaN_3 was added to a final concentration of 0.1%. Filtered serum (0.22 μm Millex GP, Millipore) was recirculating over the column overnight at room temperature. Unbound proteins were removed by washing with 90 CV of wash buffer (1x PBS, 0.5 M NaCl, 0.1% Triton® X-100 (Serva)) followed by 30 CV 1x PBS and 12 CV 10 mM Tris pH 8.0. The antibody was eluted with 0.1 M glycine pH 2.6 and collected in twenty 900 μl fractions. The pH value of the fractions was neutralize immediately using 100 μl of 2 M Tris HCl pH 7.0. The column was then washed with 12 CV 10 mM Tris pH 8.0 and an elution using 0.1 M triethylamine pH 11.5 was performed. The elution was collected as twenty 900 μl fractions. The pH value of the fractions was neutralize immediately using 100 μl of 2 M Tris HCl pH 7.0. The IgG concentration of the separate fractions were measured, and protein containing samples pooled and dialyzed in Slide-A-Lyzer Dialysis Cassettes 10K (10000 MWCO, Pierce) against 1x PBS at 4 °C. Antibody aliquots were stored at −20 °C and −80 °C.

The column was finally washed with 18 CV 10x PBS, 18 CV storage buffer (55% glycerol (v:v) in 1x PBS)

and stored at 4 °C.

9.7 Histology

9.7.1 Fixation and embedding of tissue

For *in situ* hybridizations axolotl embryos were staged, dejellied, and fixed overnight in MEM-FA (100 mM MOPS, pH 7.4, 2 mM EGTA, 1 mM $MgSO_4$, 3.7% formaldehyde) at 4 °C.
Tail tissue was fixed for 3 days at 4 °C in MEM-FA prepared with 3.7% formaldehyde, washed in 1x PBS, dehydrated in an ethanol (VWR) series, incubated in xylol (Roth), and embedded in paraffin (Roth). Tail tissue and embryos were sectioned with a thickness of 10 μm on a rotation microtome (Leica RM2125RT).
For immunohistochemistry procedures tissue was fixed at RT for 4 h or at 4 °C overnight, dependent on the size of the sample, in MEM-FA prepared with 1% formaldehyde, washed in 1x PBS and transfered to embedding solution (20% sucrose in 1x PBS). Samples were incubated at 4 °C overnight while shaking, and embedded in Tissue Tek (O.C.T. compound; Sakura) using molding containers (Polysciences). Tissue was sectioned using a cryostat (Microm HM 560). The thickness of the section was max. 10 μm.
Newts A1 myoblasts were fixed for 15 min at RT in MEM-FA prepared with 1% formaldehyde before washing with 1x PBS. Cells were directly used for immunohistochemistry.

9.7.2 *In situ* hybridization on sections

Cross-sections 10 μm thick were washed in xylol, rehydrated in an ethanol series, washed three times for 10 min in 1x PBS/0.1% Tween 20 (Sigma) and transferred to hybridization buffer (Table 10) containing digoxigenin (Roche) labeled probe (see chapter 9.4.5) and hybridized overnight at 70 °C.

Table 10: Recipe for hybridization puffer

Component	**Amount**
Dextran (Sigma)	5 g
DEPC treated distilled water	4 ml
20 x SSC (Table 11)	12.5 ml
Formamide (VWR)	25 ml
10% Tween 20 (Sigma)	0.5 ml
Yeast RNA (Sigma)	1 ml (stock 50 mg/ml)
Heparin (Sigma)	1 ml (stock 5 mg/ml)
Denhardt's solution (Sigma)	1 ml (stock 50x)
CHAPS (Sigma)	0.5 ml (stock 10%)
EDTA (Merck)	1ml (stock 0.5 M)

Sections were washed several times in 5x SSC washing solution (500 ml formamide, 250 ml 20x SSC, 10 ml 10% Tween 20, filled up to 1 l with distilled water) followed by 2x SSC washing solution (500 ml formamide, 100 ml 20x SSC, 10 ml 10% Tween 20, filled up to 1 l with distilled water), equilibrated in MAB (100 mM

Table 11: Recipe for 20x SSC

Component	Amount
NaCl (VWR)	175.3 g/l
Sodium citrate (VWR)	88.2 g/l
DEPC	0.1% final

maleic acid (Sigma) pH 7.5, 150 mM NaCl, 0.1% Tween 20), blocked in 1% blocking reagent (Roche) in MAB for 1 h at RT and incubated with sheep anti-digoxigenin-alkaline phosphatase Fab fragments antibody (Roche) 1:5000 diluted (2 h, RT). Excessive antibody was removed with MAB. Sections were washed in AP buffer (100 mM Tris pH 9.5 (Sigma), 50 mM $MgCl_2$ (Merck), 100 mM NaCl, 0.1% Tween 20), overlaid with BM purple (Roche) for colorimetric detection, incubated for 30 min up to 3 days at 37 °C, stopped with 1x PBS/1 mM EDTA and imaged.

9.7.3 Immunohistochemistry

Sections were washed with 1x PBS/0.3 % Triton® X-100 and treated with quenching buffer (200 mM glycine/0.3 % Triton® X-100, 1x PBS), followed by citrate pH 6 (Dako) diluted in aqua. dest., and blocking in 10% goat serum for 1 h. Sections were incubated overnight with primary antibody (Table 12). Following PBS washes, sections were incubated with Alexa Fluor labeled secondary antibody (Invitrogen) for 1 h at RT (Table 13). Nuclei were counterstained with Hoechst 33342 (Sigma). Digital images were taken.

Table 12: Primary antibodies

Antibody	obtained from	Comments	Host species	Antigen species	Dilution
GFP	Rockland	1.02 mg/ml	Rabbit		1:500
GFP	Invitrogen	2 mg/ml, IgG	Rabbit	*A. victoria*	1:400
MHC	provided by S. Hughes	7.3 mg/ml, clone 4A1025	Mouse		1:1460
Neuron-specific β-III TUBULIN	R&D Systems ®	Monoclonal IgG_{2A}, clone TuJ-1	Mouse		1:300
OCT4	MPI-CBG	1.1 mg/ml, M3433 - 6ABD, N-ter.	Rabbit	Axolotl	1:5000
PCNA	Santa Cruz	200 μg/ml,IgG_{2A}	Mouse	Rat	1:400
SOX2	MPI-CBG	2.73 mg/ml, M2518 - 4DE8	Rabbit	Axolotl	1:500

Table 13: Secondary antibodies

Antibody	**obtained from**	**Comments**	**Host species**	**Antigen species**	**Dilution**
Alexa Fluor® 488	Invitrogen	IgG (H+L)	Donkey	Rabbit	1:200
Alexa Fluor® 555	Invitrogen	IgM (μ chain)	Goat	Mouse	1:200
Alexa Fluor® 555	Invitrogen	IgG (H+L)	Goat	Rabbit	1:200
Alexa Fluor® 647	Invitrogen	IgG (H+L)	Donkey	Rabbit	1:200
Alexa Fluor® 647	Invitrogen	IgG (H+L)	Donkey	Rabbit	1:200

9.8 Tissue culture

9.8.1 Passaging of newt A1 myoblasts

Newt A1 myoblasts were cultured on 175 cm^2 gelatin (Sigma) coated flasks (NUNC) in 25 ml High serum - Amphibian MEM (HS-AMEM) (62.5% MEM (Invitrogen), 10% fetal bovine serum (Perbio), 1x penicillin/streptomycin (Gibco), 1x glutamine (Gibco), 1x insulin (Gibco)) at 25 °C and 2% CO2. Cells were passaged once a week whereas one confluent flask was split into three new flasks. After aspirating off the medium cells were rinsed with 7 ml APBS (0.8x PBS). In order to detach cells 6 ml TE (1x trypsin-EDTA (Gibco), APBS) was added and the flask was incubated until cells came off. This procedure was monitored in a microscope. Trypsinization was stopped with 3 ml of HS-AMEM and cells were centrifuged in a 15 ml tube (Corning) (3 min, 1000 x g). The cell pellet was resuspended by adding 6 ml of fresh HS-AMEM. Cells were split equally into three gelatin coated flasks, filled with 25 ml HS-AMEM and incubated at 25 °C and 2% CO2.

9.8.2 Electroporation of newt A1 myoblasts

Electroporation was carried out according to the providers protocol using Neon® Transfection System and the Microporation MP-100 (Peqlab). Briefly, A1 myoblasts were harvested (section 9.8.1) and counted in a Neubauer chamber. For one electroporation reaction about $1.2x10^5$ cells were resuspended in 12 μl solution R (Peqlab), mixed with 1.3 μg DNA (pEGFPnuc, pCS2 Oct4 plasmid was a kind gift from J. Brickman), morpholino up to 1 mM final and transfered to a 10 μl Gold tip (Peqlab). The pipette with the cells in the tip was placed into the microporator pipette station (Peqlab) filled with 1x Steinberg's and electroporated (600 V, 35 ms, 3 pulses). After the pulse cells were transfered to a gelatine coated HS-AMEM filled Lab-Tek™ Chamber Slide™ System (Nunc) and incubated at 25 °C and 2% CO_2. One day later HS-AMEM was replaced by fresh medium and cells were further incubated at 25 °C and 2% CO_2.

9.8.3 Human cell culture

Culturing of cells was performed by the collaborators from the group of H. Schöler. Their protocol is summarized briefly here. Primary human skin fibroblasts used here were isolated from two Caucasian women - 48-year-old (hFib #1) and 33-year-old (hFib #2) - and cultivated for several passages in fibroblast medium, composed of DMEM high glucose, supplemented with 10% fetal bovine serum, 1% sodium pyruvate, 2 mM L-glutamine and penicillin/streptomycin (all PAA), on gelatin-coated culture dishes until infection. Human ES cells and iPS cells were cultured on mitomycin C-treated CF1 mouse feeder layers (Millipore) in human ES cell medium, composed of Knockout^{TM} DMEM (Invitrogen), 20% Knockout^{TM} serum replacement (Invitrogen), 1% nonessential amino acids (PAA), 0.10 mM β-mercaptoethanol (PAA), 2 mM L-glutamine and penicillin/streptomycin, supplemented with 5 ng/ml human basic fibroblast growth factor (Peprotech), and passaged as described previously (Huangfu *et al.*, 2008a). Mouse embryonic fibroblasts (MEF) were isolated from 13.5-dpc OG2 embryos (Yeom *et al.*, 1996) and cultured in fibroblast medium as described above. Mouse ES cells and iPS cells were cultured on irradiated MEF in mouse ES cell medium, composed of Knockout^{TM} DMEM (Invitrogen), 20% Knockout^{TM} serum replacement (Invitrogen), 1% nonessential amino acids (PAA), 0.10 mM β-mercaptoethanol, 2 mM L-glutamine and penicillin/streptomycin, supplemented with leukemia inhibitory factor.

9.8.4 Induction of pluripotent stem cells

This experiment was performed by our collaborators from the group of H. Schöler. Their protocol is summarized briefly here.

The moloney-based (pMXs) retroviral vectors with the cDNAs for either human *Oct4*, mouse *Oct4*, xenopus *Pou91*, zebrafish *Pou2*, medaka *Pou2*, axolotl *Oct4*, axolotl *Pou2* or axolotl *Sox2*, as well as human and mouse *Sox2*, *Klf4*, and *c-Myc* were cotransfected with packaging helper plasmids into human embryonic kidney 293T cells using Fugene 6 transfection reagent (Roche) to produce vesicular stomatitis virus G proteinpseudotyped virus as previously described (Huangfu *et al.*, 2008b; Takahashi *et al.*, 2007). Viral supernatants were collected 48 h later, filtered, and used directly for infection. Human fibroblasts were transfered to gelatin-coated 6-well plates at a density of 50000 cells per well one day before the first infection. Fibroblasts were incubated twice with viral supernatants containing combinations of equal amounts of each virus and supplemented with 6 μg/ml protamine sulfate (Sigma Aldrich) for 24 h. One day after the second infection, fibroblasts were reseeded at a density of 25000 or 50000 cells per well on gelatin-coated 6-well plates in human fibroblast medium. One day later, the medium was exchanged to human ES cell medium supplemented with 1 mM valproic acid (Sigma Aldrich). Valproic acid was withdrawn once human ES cell-like colonies were visible. iPS cell colonies were isolated within three to seven weeks of infection and were replated and maintained on CF1 mouse embryonic fibroblast (MEF) feeder cells (Millipore) in human ES cell medium.

The axolotl *Oct4* human iPS cell reprogramming experiment was repeated twice using two different fibroblast cell lines (marked as human Fibroblast #1 hFib #1 and human Fibroblast #2 hFib #2) each time. The axolotl *Pou2* human iPS cell reprogramming experiment was carried out once using both hFib #1 and hFib #2 to demonstrate its reproducibility. Mouse iPS cells using all different *Pou* factors were generated as previously described (Takahashi and Yamanaka, 2006). Two independent experiments using duplicates for each *Pou* factor were performed. The percentage of mouse reprogrammed GFP-positive cells was determined using a FACSAria cell sorter (BD Bioscience) two weeks after infection. After sorting, GFP-positive cells were plated on irradiated MEF from which single cell colonies were picked and expanded.

9.8.5 Characterization of induced pluripotent stem cells

These experiments were performed by our collaborators from the group of H. Schöler. Alkaline phosphatase staining, immunohistochemical staining for NANOG, OCT4, SSEA1 and SSEA4, quantitative real-time (qRT)-PCR, genotyping, *in vivo* teratoma formation, hematoxylin - eosin staining and bisulfite sequencing were carried out as already described (Kim *et al.*, 2009a,b, 2008). Clonal iPS cell lines were characterized at passage 5.

9.8.6 *In vitro* differentiation of human induced pluripotent stem cells

This experiment was performed by our collaborators from the group of H. Schöler. Their protocol is summarized briefly here.
Embryoid bodies were generated from human iPS cells using the hanging-drop method in MEF-conditioned medium, supplemented with 10 μM ROCK inhibitor Y27632 (Ascent Scientific), for 5 days (1000 cells/30 μl drop). Embryoid bodies were plated on gelatin-coated plates and cultured for 14 days in different media. The following media were used to direct differentiation into specific lineages. Endodermal lineage: DMEM low glucose, 10% FCS, and 2 mM L-glutamine and penicillin/streptomycin. Mesodermal lineage: IMDM, 20% FCS, 2 mM L-glutamine and penicillin/streptomycin, 1% nonessential amino acids, 0.05 mM β-mercaptoethanol, and 0.004% ALPHA-thioglycerol (Sigma Aldrich). Ectodermal lineage: N2B27 medium without retinoic acid, supplemented with 5 μM SB431542 activin A receptor inhibitor (Sigma Aldrich).

References

Aasen, T., Raya, A., Barrero, M., Garreta, E., Consiglio, A., Gonzalez, F., Vassena, R., Bilic, J., Pekarik, V., Tiscornia, G., Edel, M., Boue, S., and Belmonte, J.I. Efficient and rapid generation of induced pluripotent stem cells from human keratinocytes. *Nat Biotechnol*, 26(11):1276–84, Nov 2008. doi: nbt.1503[pii]10.1038/nbt.1503. URL `http://www.ncbi.nlm.nih.gov/entrez/query.fcgi?cmd=Retrieve&db=PubMed&dopt=Citation&list_uids=18931654`.

Abeyta, M., Clark, A., Rodriguez, R., Bodnar, M., Pera, R., and Firpo, M. Unique gene expression signatures of independently-derived human embryonic stem cell lines. *Hum Mol Genet*, 13(6):601–8, Mar 2004. doi: 10.1093/hmg/ddh068ddh068[pii]. URL `http://www.ncbi.nlm.nih.gov/entrez/query.fcgi?cmd=Retrieve&db=PubMed&dopt=Citation&list_uids=14749348`.

Akimenko, M., Johnson, S., Westerfield, M., and Ekker, M. Differential induction of four msx homeobox genes during fin development and regeneration in zebrafish. *Development*, 121(2):347–57, Feb 1995. URL `http://www.ncbi.nlm.nih.gov/entrez/query.fcgi?cmd=Retrieve&db=PubMed&dopt=Citation&list_uids=7768177`.

Alvarado, A.S. and Tsonis, P. Bridging the regeneration gap: genetic insights from diverse animal models. *Nat Rev Genet*, 7(11):873–84, Nov 2006. doi: nrg1923[pii]10.1038/nrg1923. URL `http://www.ncbi.nlm.nih.gov/entrez/query.fcgi?cmd=Retrieve&db=PubMed&dopt=Citation&list_uids=17047686`.

Ambrosetti, D., Basilico, C., and Dailey, L. Synergistic activation of the fibroblast growth factor 4 enhancer by sox2 and oct-3 depends on protein-protein interactions facilitated by a specific spatial arrangement of factor binding sites. *Mol Cell Biol*, 17(11):6321–9, Nov 1997. URL `http://www.ncbi.nlm.nih.gov/entrez/query.fcgi?cmd=Retrieve&db=PubMed&dopt=Citation&list_uids=9343393`.

Ambrosetti, D., Scholer, H., Dailey, L., and Basilico, C. Modulation of the activity of multiple transcriptional activation domains by the dna binding domains mediates the synergistic action of sox2 and oct-3 on the fibroblast growth factor-4 enhancer. *J Biol Chem*, 275(30):23387–97, Jul 2000. doi: 10.1074/jbc.M000932200M000932200[pii]. URL `http://www.ncbi.nlm.nih.gov/entrez/query.fcgi?cmd=Retrieve&db=PubMed&dopt=Citation&list_uids=10801796`.

Ariizumi, T., Takahashi, S., Chan, T., Ito, Y., Michiue, T., and Asashima, M. Isolation and differentiation of xenopus animal cap cells. *Curr Protoc Stem Cell Biol*, Chapter 1:Unit 1D 5, Apr 2009. doi: 10.1002/9780470151808.sc01d05s9. URL `http://www.ncbi.nlm.nih.gov/entrez/query.fcgi?cmd=Retrieve&db=PubMed&dopt=Citation&list_uids=19382122`.

Arsanto, J., Komorowski, T., Dupin, F., Caubit, X., Diano, M., Geraudie, J., Carlson, B., and Thouveny, Y. Formation of the peripheral nervous system during tail regeneration in urodele amphibians: ultrastructural

and immunohistochemical studies of the origin of the cells. *J Exp Zool*, 264(3):273–92, Dec 1992. doi: 10.1002/jez.1402640307. URL http://www.ncbi.nlm.nih.gov/entrez/query.fcgi?cmd=Retrieve&db=PubMed&dopt=Citation&list_uids=1431787.

Atlasi, Y., Mowla, S., Ziaee, S., Gokhale, P., and Andrews, P. Oct4 spliced variants are differentially expressed in human pluripotent and non-pluripotent cells. *Stem Cells*, Sep 2008. doi: 2008-0530[pii]10.1634/stemcells.2008-0530. URL http://www.ncbi.nlm.nih.gov/entrez/query.fcgi?cmd=Retrieve&db=PubMed&dopt=Citation&list_uids=18787205.

Bachvarova, R., Masi, T., Drum, M., Parker, N., Mason, K., Patient, R., and Johnson, A. Gene expression in the axolotl germ line: Axdazl, axvh, axoct-4, and axkit. *Dev Dyn*, 231(4):871–80, Dec 2004. doi: 10.1002/dvdy.20195. URL http://www.ncbi.nlm.nih.gov/entrez/query.fcgi?cmd=Retrieve&db=PubMed&dopt=Citation&list_uids=15517581.

Badis, G., Berger, M., Philippakis, A., Talukder, S., Gehrke, A., Jaeger, S., Chan, E., Metzler, G., Vedenko, A., Chen, X., Kuznetsov, H., Wang, C., Coburn, D., Newburger, D., Morris, Q., Hughes, T., and Bulyk, M. Diversity and complexity in dna recognition by transcription factors. *Science*, 324(5935):1720–3, Jun 2009. doi: 1162327[pii]10.1126/science.1162327. URL http://www.ncbi.nlm.nih.gov/entrez/query.fcgi?cmd=Retrieve&db=PubMed&dopt=Citation&list_uids=19443739.

Barnabe-Heider, F., Goritz, C., Sabelstrom, H., Takebayashi, H., Pfrieger, F., Meletis, K., and Frisen, J. Origin of new glial cells in intact and injured adult spinal cord. *Cell Stem Cell*, 7(4):470–82, Oct 2010. doi: S1934-5909(10)00436-4[pii]10.1016/j.stem.2010.07.014. URL http://www.ncbi.nlm.nih.gov/entrez/query.fcgi?cmd=Retrieve&db=PubMed&dopt=Citation&list_uids=20887953.

Beck, C. and Slack, J. Analysis of the developing xenopus tail bud reveals separate phases of gene expression during determination and outgrowth. *Mech Dev*, 72(1-2):41–52, Mar 1998. doi: S0925-4773(98)00015-X[pii]. URL http://www.ncbi.nlm.nih.gov/entrez/query.fcgi?cmd=Retrieve&db=PubMed&dopt=Citation&list_uids=9533951.

Beddington, R. Induction of a second neural axis by the mouse node. *Development*, 120(3):613–20, Mar 1994. URL http://www.ncbi.nlm.nih.gov/entrez/query.fcgi?cmd=Retrieve&db=PubMed&dopt=Citation&list_uids=8162859.

Belting, H., Hauptmann, G., Meyer, D., Abdelilah-Seyfried, S., Chitnis, A., Eschbach, C., Soll, I., Thisse, C., Thisse, B., Artinger, K., Lunde, K., and Driever, W. spiel ohne grenzen/pou2 is required during establishment of the zebrafish midbrain-hindbrain boundary organizer. *Development*, 128(21):4165–76, Nov 2001. URL http://www.ncbi.nlm.nih.gov/entrez/query.fcgi?cmd=Retrieve&db=PubMed&dopt=Citation&list_uids=11684654.

Benraiss, A., Arsanto, J., Coulon, J., and Thouveny, Y. Neurogenesis during caudal spinal cord regeneration in adult newts. *Dev Genes Evol*, 209(6):363–9, Jun 1999. doi: 92090363.427[pii]. URL http://www.ncbi.nlm.nih.gov/entrez/query.fcgi?cmd=Retrieve&db=PubMed&dopt=Citation&list_uids=10370118.

Bjornson, C., Rietze, R., Reynolds, B., Magli, M., and Vescovi, A. Turning brain into blood: a hematopoietic fate adopted by adult neural stem cells in vivo. *Science*, 283(5401):534–7, Jan 1999. URL http://www.ncbi.nlm.nih.gov/entrez/query.fcgi?cmd=Retrieve&db=PubMed&dopt=Citation&list_uids=9915700.

Blau, H. A twist of fate. *Nature*, 419(6906):437, Oct 2002. doi: 10.1038/419347a. URL http://www.ncbi.nlm.nih.gov/entrez/query.fcgi?cmd=Retrieve&db=PubMed&dopt=Citation&list_uids=12374136.

Blau, H., Brazelton, T., and Weimann, J. The evolving concept of a stem cell: entity or function? *Cell*, 105 (7):829–41, Jun 2001. doi: S0092-8674(01)00409-3[pii]. URL http://www.ncbi.nlm.nih.gov/entrez/query.fcgi?cmd=Retrieve&db=PubMed&dopt=Citation&list_uids=11439179.

Bordzilovskaya, N. Developmental-stage series of axolotl embryos. *Developmental Biology of the Axolotl edited by J.B. Armstrong and G.M. Malacinski. Oxford University Press*, pages 201–219, 1989.

Boyer, L., Lee, T., Cole, M., Johnstone, S., Levine, S., Zucker, J., Guenther, M., Kumar, R., Murray, H., Jenner, R., Gifford, D., Melton, D., Jaenisch, R., and Young, R. Core transcriptional regulatory circuitry in human embryonic stem cells. *Cell*, 122(6):947–56, Sep 2005. doi: S0092-8674(05)00825-1[pii]10.1016/j.cell.2005.08.020. URL http://www.ncbi.nlm.nih.gov/entrez/query.fcgi?cmd=Retrieve&db=PubMed&dopt=Citation&list_uids=16153702.

Brandenberger, R., Khrebtukova, I., Thies, R., Miura, T., Jingli, C., Puri, R., Vasicek, T., Lebkowski, J., and Rao, M. Mpss profiling of human embryonic stem cells. *BMC Dev Biol*, 4:10, Aug 2004. doi: 10.1186/1471-213X-4-101471-213X-4-10[pii]. URL http://www.ncbi.nlm.nih.gov/entrez/query.fcgi?cmd=Retrieve&db=PubMed&dopt=Citation&list_uids=15304200.

Brazelton, T., Rossi, F., Keshet, G., and Blau, H. From marrow to brain: expression of neuronal phenotypes in adult mice. *Science*, 290(5497):1775–9, Dec 2000. doi: 9028[pii]. URL http://www.ncbi.nlm.nih.gov/entrez/query.fcgi?cmd=Retrieve&db=PubMed&dopt=Citation&list_uids=11099418.

Bregman, B. Spinal cord transplants permit the growth of serotonergic axons across the site of neonatal spinal cord transection. *Brain Res*, 431(2):265–79., 1987.

Brockes, J. Amphibian limb regeneration: rebuilding a complex structure. *Science*, 276(5309):81–7, Apr 1997. URL http://www.ncbi.nlm.nih.gov/entrez/query.fcgi?cmd=Retrieve&db=PubMed&dopt=Citation&list_uids=9082990.

Brockes, J. and Kumar, A. Plasticity and reprogramming of differentiated cells in amphibian regeneration. *Nat Rev Mol Cell Biol*, 3(8):566–74, Aug 2002. doi: 10.1038/nrm881nrm881[pii]. URL http://www.ncbi.nlm.nih.gov/entrez/query.fcgi?cmd=Retrieve&db=PubMed&dopt=Citation&list_uids=12154368.

Burgess, S., Reim, G., Chen, W., Hopkins, N., and Brand, M. The zebrafish spiel-ohne-grenzen (spg) gene encodes the pou domain protein pou2 related to mammalian oct4 and is essential for formation of the midbrain and hindbrain, and for pre-gastrula morphogenesis. *Development*, 129(4):905–16, Feb 2002. URL http://www.ncbi.nlm.nih.gov/entrez/query.fcgi?cmd=Retrieve&db=PubMed&dopt=Citation&list_uids=11861474.

Cambray, N. and Wilson, V. Axial progenitors with extensive potency are localised to the mouse chordoneural hinge. *Development*, 129(20):4855–66, Oct 2002. URL http://www.ncbi.nlm.nih.gov/entrez/query.fcgi?cmd=Retrieve&db=PubMed&dopt=Citation&list_uids=12361976.

Cambray, N. and Wilson, V. Two distinct sources for a population of maturing axial progenitors. *Development*, 134(15):2829–40, Aug 2007. doi: dev.02877[pii]10.1242/dev.02877. URL http://www.ncbi.nlm.nih.gov/entrez/query.fcgi?cmd=Retrieve&db=PubMed&dopt=Citation&list_uids=17611225.

Cao, Y., Siegel, D., and Knochel, W. Xenopus pou factors of subclass v inhibit activin/nodal signaling during gastrulation. *Mech Dev*, 123(8):614–25, Aug 2006. doi: S0925-4773(06)00070-0[pii]10.1016/j.mod.2006.06.004. URL http://www.ncbi.nlm.nih.gov/entrez/query.fcgi?cmd=Retrieve&db=PubMed&dopt=Citation&list_uids=16860542.

Cao, Y., Oswald, F., Wacker, S., Bundschu, K., and Knochel, W. Reversal of xenopus oct25 function by disruption of the pou domain structure. *J Biol Chem*, 285(11):8408–21, Mar 2010. doi: M109.064386[pii]10.1074/jbc.M109.064386. URL http://www.ncbi.nlm.nih.gov/entrez/query.fcgi?cmd=Retrieve&db=PubMed&dopt=Citation&list_uids=20064932.

Carmell, M., Girard, A., van de Kant, H., Bourc'his, D., Bestor, T., de Rooij, D., and Hannon, G. Miwi2 is essential for spermatogenesis and repression of transposons in the mouse male germline. *Dev Cell*, 12(4):503–14, Apr 2007. doi: S1534-5807(07)00100-1[pii]10.1016/j.devcel.2007.03.001. URL http://www.ncbi.nlm.nih.gov/entrez/query.fcgi?cmd=Retrieve&db=PubMed&dopt=Citation&list_uids=17395546.

Catala, M., Teillet, M., and Douarin, N.L. Organization and development of the tail bud analyzed with the quail-chick chimaera system. *Mech Dev*, 51(1):51–65, May 1995. doi: 092547739500350A[pii]. URL http://www.ncbi.nlm.nih.gov/entrez/query.fcgi?cmd=Retrieve&db=PubMed&dopt=Citation&list_uids=7669693.

Chambers, I. The molecular basis of pluripotency in mouse embryonic stem cells. *Cloning Stem Cells*, 6(4): 386–91, 2004. doi: 10.1089/clo.2004.6.386. URL http://www.ncbi.nlm.nih.gov/entrez/query.fcgi?cmd=Retrieve&db=PubMed&dopt=Citation&list_uids=15671667.

Chambers, I., Colby, D., Robertson, M., Nichols, J., Lee, S., Tweedie, S., and Smith, A. Functional expression cloning of nanog, a pluripotency sustaining factor in embryonic stem cells. *Cell*, 113(5):643–55, May 2003. doi: S0092867403003921[pii]. URL http://www.ncbi.nlm.nih.gov/entrez/query.fcgi?cmd=Retrieve&db=PubMed&dopt=Citation&list_uids=12787505.

Chapman, S., Schubert, F., Schoenwolf, G., and Lumsden, A. Analysis of spatial and temporal gene expression patterns in blastula and gastrula stage chick embryos. *Dev Biol*, 245(1):187–99, May 2002. doi: 10.1006/dbio.2002.0641S001216060290641X[pii]. URL http://www.ncbi.nlm.nih.gov/entrez/query.fcgi?cmd=Retrieve&db=PubMed&dopt=Citation&list_uids=11969265.

Chernoff, E. Spinal cord regeneration: a phenomenon unique to urodeles? *Int J Dev Biol*, 40(4):823–31, Aug 1996. URL http://www.ncbi.nlm.nih.gov/entrez/query.fcgi?cmd=Retrieve&db=PubMed&dopt=Citation&list_uids=8877457.

Chernoff, E., Stocum, D., Nye, H., and Cameron, J. Urodele spinal cord regeneration and related processes. *Dev Dyn*, 226(2):295–307, Feb 2003. doi: 10.1002/dvdy.10240. URL http://www.ncbi.nlm.nih.gov/entrez/query.fcgi?cmd=Retrieve&db=PubMed&dopt=Citation&list_uids=12557207.

Chiozzi, P., Sanz, J., Ferrari, D., Falzoni, S., Aleotti, A., Buell, G., Collo, G., and Virgilio, F.D. Spontaneous cell fusion in macrophage cultures expressing high levels of the p2z/p2x7 receptor. *J Cell Biol*, 138 (3):697–706, Aug 1997. URL http://www.ncbi.nlm.nih.gov/entrez/query.fcgi?cmd=Retrieve&db=PubMed&dopt=Citation&list_uids=9245796.

Christen, B., Robles, V., Raya, M., Paramonov, I., and Belmonte, J.I. Regeneration and reprogramming compared. *BMC Biol*, 8:5, 2010. doi: 1741-7007-8-5[pii]10.1186/1741-7007-8-5. URL http://www.ncbi.nlm.nih.gov/entrez/query.fcgi?cmd=Retrieve&db=PubMed&dopt=Citation&list_uids=20089153.

Chuai, M. and Weijer, C. Who moves whom during primitive streak formation in the chick embryo. *HFSP J*, 3(2):71–6, 2009. doi: 10.2976/1.3103933. URL http://www.ncbi.nlm.nih.gov/entrez/query.fcgi?cmd=Retrieve&db=PubMed&dopt=Citation&list_uids=19794819.

Clarke, D., Johansson, C., Wilbertz, J., Veress, B., Nilsson, E., Karlstrom, H., Lendahl, U., and Frisen, J. Generalized potential of adult neural stem cells. *Science*, 288(5471):1660–3, Jun 2000. doi: 8573[pii]. URL http://www.ncbi.nlm.nih.gov/entrez/query.fcgi?cmd=Retrieve&db=PubMed&dopt=Citation&list_uids=10834848.

Curtis, W. and Hickman, J. Effects of x-rays and radium upon regeneration in planarians. *Anat. Rec.*, 34: 145–146, 1926.

Dailey, L., Yuan, H., and Basilico, C. Interaction between a novel f9-specific factor and octamer-binding proteins is required for cell-type-restricted activity of the fibroblast growth factor 4 enhancer. *Mol Cell Biol*, 14 (12):7758–69, Dec 1994. URL http://www.ncbi.nlm.nih.gov/entrez/query.fcgi?cmd=Retrieve&db=PubMed&dopt=Citation&list_uids=7969117.

Downs, K. Systematic localization of oct-3/4 to the gastrulating mouse conceptus suggests manifold roles in mammalian development. *Dev Dyn*, 237(2):464–75, Feb 2008. doi: 10.1002/dvdy.21438. URL http://www.ncbi.nlm.nih.gov/entrez/query.fcgi?cmd=Retrieve&db=PubMed&dopt=Citation&list_uids=18213575.

Egar, M. and Singer, M. The role of ependyma in spinal cord regeneration in the urodele, triturus. *Exp Neurol*, 37(2):422–30, Nov 1972. doi: 0014-4886(72)90085-4[pii]. URL http://www.ncbi.nlm.nih.gov/entrez/query.fcgi?cmd=Retrieve&db=PubMed&dopt=Citation&list_uids=4637959.

Enelow, R., Sullivan, G., Carper, H., and Mandell, G. Induction of multinucleated giant cell formation from in vitro culture of human monocytes with interleukin-3 and interferon-gamma: comparison with other stimulating factors. *Am J Respir Cell Mol Biol*, 6(1):57–62, Jan 1992. doi: 10.1165/ajrcmb/6.1.57. URL http://www.ncbi.nlm.nih.gov/entrez/query.fcgi?cmd=Retrieve&db=PubMed&dopt=Citation&list_uids=1728295.

Eriksson, P., Perfilieva, E., Bjork-Eriksson, T., Alborn, A., Nordborg, C., Peterson, D., and Gage, F. Neurogenesis in the adult human hippocampus. *Nat Med*, 4(11):1313–7, Nov 1998. doi: 10.1038/3305. URL http://www.ncbi.nlm.nih.gov/entrez/query.fcgi?cmd=Retrieve&db=PubMed&dopt=Citation&list_uids=9809557.

Falzoni, S., Munerati, M., Ferrari, D., Spisani, S., Moretti, S., and Virgilio, F.D. The purinergic p2z receptor of human macrophage cells. characterization and possible physiological role. *J Clin Invest*, 95(3):1207–16, Mar 1995. doi: 10.1172/JCI117770. URL http://www.ncbi.nlm.nih.gov/entrez/query.fcgi?cmd=Retrieve&db=PubMed&dopt=Citation&list_uids=7883969.

Ferrari, G., Angelis, G.C.D., Coletta, M., Paolucci, E., Stornaiuolo, A., Cossu, G., and Mavilio, F. Muscle regeneration by bone marrow-derived myogenic progenitors. *Science*, 279(5356):1528–30, Mar 1998. URL http://www.ncbi.nlm.nih.gov/entrez/query.fcgi?cmd=Retrieve&db=PubMed&dopt=Citation&list_uids=9488650.

Ferretti, P., Zhang, F., and O'Neill, P. Changes in spinal cord regenerative ability through phylogenesis and development: lessons to be learnt. *Dev Dyn*, 226(2):245–56, Feb 2003. doi: 10.1002/dvdy.

10226. URL http://www.ncbi.nlm.nih.gov/entrez/query.fcgi?cmd=Retrieve&db=PubMed&dopt=Citation&list_uids=12557203.

Frankenberg, S., Tisdall, D., and Selwood, L. Identification of a homologue of pou5f1 (oct3/4) in a marsupial, the brushtail possum. *Mol Reprod Dev*, 58(3):255–61, Mar 2001. doi: 10.1002/1098-2795(200103)58:3⟨255::AID-MRD2⟩3.0.CO;2-3[pii]10.1002/1098-2795(200103)58:3⟨255::AID-MRD2⟩3.0.CO;2-3. URL http://www.ncbi.nlm.nih.gov/entrez/query.fcgi?cmd=Retrieve&db=PubMed&dopt=Citation&list_uids=11170265.

Frankenberg, S., Pask, A., and Renfree, M. The evolution of class v pou domain transcription factors in vertebrates and their characterisation in a marsupial. *Dev Biol*, 337(1):162–70, Jan 2010. doi: S0012-1606(09)01276-7[pii]10.1016/j.ydbio.2009.10.017. URL http://www.ncbi.nlm.nih.gov/entrez/query.fcgi?cmd=Retrieve&db=PubMed&dopt=Citation&list_uids=19850032.

Gaete, M., Munoz, R., Sanchez, N., Tampe, R., Moreno, M., Contreras, E., Lee-Liu, D., and Larrain, J. Spinal cord regeneration in xenopus tadpoles proceeds through activation of sox2-positive cells. *Neural Dev*, 7:13, 2012. doi: 1749-8104-7-13[pii]10.1186/1749-8104-7-13. URL http://www.ncbi.nlm.nih.gov/entrez/query.fcgi?cmd=Retrieve&db=PubMed&dopt=Citation&list_uids=22537391.

Galli, R., Borello, U., Gritti, A., Minasi, M., Bjornson, C., Coletta, M., Mora, M., Angelis, M.D., Fiocco, R., Cossu, G., and Vescovi, A. Skeletal myogenic potential of human and mouse neural stem cells. *Nat Neurosci*, 3(10):986–91, Oct 2000. doi: 10.1038/79924. URL http://www.ncbi.nlm.nih.gov/entrez/query.fcgi?cmd=Retrieve&db=PubMed&dopt=Citation&list_uids=11017170.

Galliot, B. Signaling molecules in regenerating hydra. *Bioessays*, 19(1):37–46, Jan 1997. URL http://www.ncbi.nlm.nih.gov/entrez/query.fcgi?cmd=Retrieve&db=PubMed&dopt=Citation&list_uids=19492476.

Gofflot, F., Hall, M., and Morriss-Kay, G. Genetic patterning of the developing mouse tail at the time of posterior neuropore closure. *Dev Dyn*, 210(4):431–45, Dec 1997. doi: 10.1002/(SICI)1097-0177(199712)210:4⟨431::AID-AJA7⟩3.0.CO;2-H[pii]10.1002/(SICI)1097-0177(199712)210:4⟨431::AID-AJA7⟩3.0.CO;2-H. URL http://www.ncbi.nlm.nih.gov/entrez/query.fcgi?cmd=Retrieve&db=PubMed&dopt=Citation&list_uids=9415428.

Gont, L., Steinbeisser, H., Blumberg, B., and de Robertis, E. Tail formation as a continuation of gastrulation: the multiple cell populations of the xenopus tailbud derive from the late blastopore lip. *Development*, 119 (4):991–1004, Dec 1993. URL http://www.ncbi.nlm.nih.gov/entrez/query.fcgi?cmd=Retrieve&db=PubMed&dopt=Citation&list_uids=7916680.

Habermann, B., Bebin, A., Herklotz, S., Volkmer, M., Eckelt, K., Pehlke, K., Epperlein, H., Schackert, H., Wiebe, G., and Tanaka, E. An ambystoma mexicanum est sequencing project: analysis of 17,352 expressed sequence tags from embryonic and regenerating blastema cdna libraries. *Genome Biol*, 5(9):R67, 2004. doi: 10.1186/gb-2004-5-9-r67gb-2004-5-9-r67[pii]. URL http://www.ncbi.nlm.nih.gov/entrez/query.fcgi?cmd=Retrieve&db=PubMed&dopt=Citation&list_uids=15345051.

Han, M., Yang, X., Lee, J., Allan, C., and Muneoka, K. Development and regeneration of the neonatal digit tip in mice. *Dev Biol*, 315(1):125–35, Mar 2008. doi: S0012-1606(07)01608-9[pii]10.1016/j.ydbio.2007.12.025. URL http://www.ncbi.nlm.nih.gov/entrez/query.fcgi?cmd=Retrieve&db=PubMed&dopt=Citation&list_uids=18234177.

Handrigan, G. Concordia discors: duality in the origin of the vertebrate tail. *J Anat*, 202(Pt 3):255–67, Mar 2003. URL http://www.ncbi.nlm.nih.gov/entrez/query.fcgi?cmd=Retrieve&db=PubMed&dopt=Citation&list_uids=12713266.

Hata, S., Namae, M., and Nishina, H. Liver development and regeneration: from laboratory study to clinical therapy. *Dev Growth Differ*, 49(2):163–70, Feb 2007. doi: DGD910[pii]10.1111/j.1440-169X.2007.00910.x. URL http://www.ncbi.nlm.nih.gov/entrez/query.fcgi?cmd=Retrieve&db=PubMed&dopt=Citation&list_uids=17335437.

Hayashi, T., Mizuno, N., Ueda, Y., Okamoto, M., and Kondoh, H. Fgf2 triggers iris-derived lens regeneration in newt eye. *Mech Dev*, 121(6):519–26, Jun 2004. doi: 10.1016/j.mod.2004.04.010S0925477304000917[pii]. URL http://www.ncbi.nlm.nih.gov/entrez/query.fcgi?cmd=Retrieve&db=PubMed&dopt=Citation&list_uids=15172683.

Hinkley, C., Martin, J., Leibham, D., and Perry, M. Sequential expression of multiple pou proteins during amphibian early development. *Mol Cell Biol*, 12(2):638–49, Feb 1992. URL http://www.ncbi.nlm.nih.gov/entrez/query.fcgi?cmd=Retrieve&db=PubMed&dopt=Citation&list_uids=1732736.

Holder, N. and Clarke, J. Is there a correlation between continuous neurogenesis and directed axon regeneration in the vertebrate nervous system? *Trends Neurosci*, 11(3):94–9, Mar 1988. doi: 0166-2236(88)90151-8[pii]. URL http://www.ncbi.nlm.nih.gov/entrez/query.fcgi?cmd=Retrieve&db=PubMed&dopt=Citation&list_uids=2465614.

Holder, N., Clarke, J., Stephens, N., Wilson, S., Orsi, C., Bloomer, T., and Tonge, D. Continuous growth of the motor system in the axolotl. *J Comp Neurol*, 303(4):534–50, Jan 1991. doi: 10.1002/cne.903030403. URL http://www.ncbi.nlm.nih.gov/entrez/query.fcgi?cmd=Retrieve&db=PubMed&dopt=Citation&list_uids=2013645.

Holmdahl, D. Experimentelle untersuchungen ueber die lage der grenze zwischen primaerer und sekundaerer koerperentwicklung beim huhn. *Anat. Anz.*, 59:393–396, 1925.

Huangfu, D., Maehr, R., Guo, W., Eijkelenboom, A., Snitow, M., Chen, A., and Melton, D. Induction of pluripotent stem cells by defined factors is greatly improved by small-molecule compounds. *Nat Biotechnol*, 26(7):795–7, Jul 2008a. doi: nbt1418[pii]10.1038/nbt1418. URL `http://www.ncbi.nlm.nih.gov/entrez/query.fcgi?cmd=Retrieve&db=PubMed&dopt=Citation&list_uids=18568017`.

Huangfu, D., Osafune, K., Maehr, R., Guo, W., Eijkelenboom, A., Chen, S., Muhlestein, W., and Melton, D. Induction of pluripotent stem cells from primary human fibroblasts with only oct4 and sox2. *Nat Biotechnol*, 26(11):1269–75, Nov 2008b. doi: nbt.1502[pii]10.1038/nbt.1502. URL `http://www.ncbi.nlm.nih.gov/entrez/query.fcgi?cmd=Retrieve&db=PubMed&dopt=Citation&list_uids=18849973`.

Ito, M., Hayashi, T., Kuroiwa, A., and Okamoto, M. Lens formation by pigmented epithelial cell reaggregate from dorsal iris implanted into limb blastema in the adult newt. *Dev Growth Differ*, 41(4):429–40, Aug 1999. URL `http://www.ncbi.nlm.nih.gov/entrez/query.fcgi?cmd=Retrieve&db=PubMed&dopt=Citation&list_uids=10466930`.

Jhamb, D., Rao, N., Milner, D., Song, F., Cameron, J., Stocum, D., and Palakal, M. Network based transcription factor analysis of regenerating axolotl limbs. *BMC Bioinformatics*, 12:80, 2011. doi: 1471-2105-12-80[pii]10.1186/1471-2105-12-80. URL `http://www.ncbi.nlm.nih.gov/entrez/query.fcgi?cmd=Retrieve&db=PubMed&dopt=Citation&list_uids=21418574`.

Johansson, C., Momma, S., Clarke, D., Risling, M., Lendahl, U., and Frisen, J. Identification of a neural stem cell in the adult mammalian central nervous system. *Cell*, 96(1):25–34, Jan 1999. doi: S0092-8674(00)80956-3[pii]. URL `http://www.ncbi.nlm.nih.gov/entrez/query.fcgi?cmd=Retrieve&db=PubMed&dopt=Citation&list_uids=9989494`.

Johnson, A., Crother, B., White, M., Patient, R., Bachvarova, R., Drum, M., and Masi, T. Regulative germ cell specification in axolotl embryos: a primitive trait conserved in the mammalian lineage. *Philos Trans R Soc Lond B Biol Sci*, 358(1436):1371–9, Aug 2003a. doi: 10.1098/rstb.2003.1331. URL `http://www.ncbi.nlm.nih.gov/entrez/query.fcgi?cmd=Retrieve&db=PubMed&dopt=Citation&list_uids=14511484`.

Johnson, A., Drum, M., Bachvarova, R., Masi, T., White, M., and Crother, B. Evolution of predetermined germ cells in vertebrate embryos: implications for macroevolution. *Evol Dev*, 5(4):414–31, Jul 2003b. doi: 3048[pii]. URL `http://www.ncbi.nlm.nih.gov/entrez/query.fcgi?cmd=Retrieve&db=PubMed&dopt=Citation&list_uids=12823457`.

Jones, D., Taylor, W., and Thornton, J. The rapid generation of mutation data matrices from protein sequences. *Comput Appl Biosci*, 8(3):275–82, Jun 1992. URL http://www.ncbi.nlm.nih.gov/entrez/query.fcgi?cmd=Retrieve&db=PubMed&dopt=Citation&list_uids=1633570.

Kanki, J. and Ho, R. The development of the posterior body in zebrafish. *Development*, 124(4):881–93, Feb 1997. URL http://www.ncbi.nlm.nih.gov/entrez/query.fcgi?cmd=Retrieve&db=PubMed&dopt=Citation&list_uids=9043069.

Karsenty, G. Transcriptional control of skeletogenesis. *Annu Rev Genomics Hum Genet*, 9:183–96, 2008. doi: 10.1146/annurev.genom.9.081307.164437. URL http://www.ncbi.nlm.nih.gov/entrez/query.fcgi?cmd=Retrieve&db=PubMed&dopt=Citation&list_uids=18767962.

Kehler, J., Tolkunova, E., Koschorz, B., Pesce, M., Gentile, L., Boiani, M., Lomeli, H., Nagy, A., McLaughlin, K., Scholer, H., and Tomilin, A. Oct4 is required for primordial germ cell survival. *EMBO Rep*, 5(11):1078–83, Nov 2004. doi: 7400279[pii]10.1038/sj.embor.7400279. URL http://www.ncbi.nlm.nih.gov/entrez/query.fcgi?cmd=Retrieve&db=PubMed&dopt=Citation&list_uids=15486564.

Kim, J., Zaehres, H., Wu, G., Gentile, L., Ko, K., Sebastiano, V., Arauzo-Bravo, M., Ruau, D., Han, D., Zenke, M., and Scholer, H. Pluripotent stem cells induced from adult neural stem cells by reprogramming with two factors. *Nature*, 454(7204):646–50, Jul 2008. doi: nature07061[pii]10.1038/nature07061. URL http://www.ncbi.nlm.nih.gov/entrez/query.fcgi?cmd=Retrieve&db=PubMed&dopt=Citation&list_uids=18594515.

Kim, J., Greber, B., Arauzo-Bravo, M., Meyer, J., Park, K., Zaehres, H., and Scholer, H. Direct reprogramming of human neural stem cells by oct4. *Nature*, 461(7264):649–3, Oct 2009a. doi: nature08436[pii]10.1038/nature08436. URL http://www.ncbi.nlm.nih.gov/entrez/query.fcgi?cmd=Retrieve&db=PubMed&dopt=Citation&list_uids=19718018.

Kim, J., Sebastiano, V., Wu, G., Arauzo-Bravo, M., Sasse, P., Gentile, L., Ko, K., Ruau, D., Ehrich, M., van den Boom, D., Meyer, J., Hubner, K., Bernemann, C., Ortmeier, C., Zenke, M., Fleischmann, B., Zaehres, H., and Scholer, H. Oct4-induced pluripotency in adult neural stem cells. *Cell*, 136(3):411–9, Feb 2009b. doi: S0092-8674(09)00071-3[pii]10.1016/j.cell.2009.01.023. URL http://www.ncbi.nlm.nih.gov/entrez/query.fcgi?cmd=Retrieve&db=PubMed&dopt=Citation&list_uids=19203577.

Knopf, F., Hammond, C., Chekuru, A., Kurth, T., Hans, S., Weber, C., Mahatma, G., Fisher, S., Brand, M., Schulte-Merker, S., and Weidinger, G. Bone regenerates via dedifferentiation of osteoblasts in the zebrafish fin. *Dev Cell*, 20(5):713–24, May 2011. doi: S1534-5807(11)00165-1[pii]10.1016/j.devcel.2011.04.014. URL http://www.ncbi.nlm.nih.gov/entrez/query.fcgi?cmd=Retrieve&db=PubMed&dopt=Citation&list_uids=21571227.

Korol, A. Multipoint 2.2. *http://www.multiqtl.com*, 2003.

Kosambi, D. The estimation of map distances from recombination values. *Ann Eugen*, 12:172–175, 1944.

Kragl, M., Knapp, D., Nacu, E., Khattak, S., Maden, M., Epperlein, H., and Tanaka, E. Cells keep a memory of their tissue origin during axolotl limb regeneration. *Nature*, 460(7251):60–5, Jul 2009. doi: nature08152[pii]10.1038/nature08152. URL `http://www.ncbi.nlm.nih.gov/entrez/query.fcgi?cmd=Retrieve&db=PubMed&dopt=Citation&list_uids=19571878`.

Krause, D., Theise, N., Collector, M., Henegariu, O., Hwang, S., Gardner, R., Neutzel, S., and Sharkis, S. Multi-organ, multi-lineage engraftment by a single bone marrow-derived stem cell. *Cell*, 105(3):369–77, May 2001. doi: S0092-8674(01)00328-2[pii]. URL `http://www.ncbi.nlm.nih.gov/entrez/query.fcgi?cmd=Retrieve&db=PubMed&dopt=Citation&list_uids=11348593`.

Kuramochi-Miyagawa, S., Kimura, T., Ijiri, T., Isobe, T., Asada, N., Fujita, Y., Ikawa, M., Iwai, N., Okabe, M., Deng, W., Lin, H., Matsuda, Y., and Nakano, T. Mili, a mammalian member of piwi family gene, is essential for spermatogenesis. *Development*, 131(4):839–49, Feb 2004. doi: 10.1242/dev.00973dev.00973[pii]. URL `http://www.ncbi.nlm.nih.gov/entrez/query.fcgi?cmd=Retrieve&db=PubMed&dopt=Citation&list_uids=14736746`.

Kuroda, T., Tada, M., Kubota, H., Kimura, H., Hatano, S., Suemori, H., Nakatsuji, N., and Tada, T. Octamer and sox elements are required for transcriptional cis regulation of nanog gene expression. *Mol Cell Biol*, 25(6):2475–85, Mar 2005. doi: 25/6/2475[pii]10.1128/MCB.25.6.2475-2485.2005. URL `http://www.ncbi.nlm.nih.gov/entrez/query.fcgi?cmd=Retrieve&db=PubMed&dopt=Citation&list_uids=15743839`.

Lagasse, E., Connors, H., Al-Dhalimy, M., Reitsma, M., Dohse, M., Osborne, L., Wang, X., Finegold, M., Weissman, I., and Grompe, M. Purified hematopoietic stem cells can differentiate into hepatocytes in vivo. *Nat Med*, 6(11):1229–34, Nov 2000. doi: 10.1038/81326. URL `http://www.ncbi.nlm.nih.gov/entrez/query.fcgi?cmd=Retrieve&db=PubMed&dopt=Citation&list_uids=11062533`.

Lange, C. Studies on the cellular basis of radiation lethality. i. the pattern of mortality in the whole-body irradiated planarian (tricladida, paludicola). *Int J Radiat Biol Relat Stud Phys Chem Med*, 13(6):511–30, 1968. URL `http://www.ncbi.nlm.nih.gov/entrez/query.fcgi?cmd=Retrieve&db=PubMed&dopt=Citation&list_uids=5301980`.

Lavial, F., Acloque, H., Bertocchini, F., Macleod, D., Boast, S., Bachelard, E., Montillet, G., Thenot, S., Sang, H., Stern, C., Samarut, J., and Pain, B. The oct4 homologue pouv and nanog regulate pluripotency in chicken embryonic stem cells. *Development*, 134(19):3549–63, Oct 2007a. doi: 134/19/3549[pii]10.1242/dev.006569. URL `http://www.ncbi.nlm.nih.gov/entrez/query.fcgi?cmd=Retrieve&db=PubMed&dopt=Citation&list_uids=17827181`.

Lavial, F., Acloque, H., Bertocchini, F., Macleod, D., Boast, S., Bachelard, E., Montillet, G., Thenot, S., Sang, H., Stern, C., Samarut, J., and Pain, B. The oct4 homologue pouv and nanog regulate pluripotency in chicken embryonic stem cells. *Development*, 134(19):3549–63, Oct 2007b. doi: 134/19/3549[pii]10.1242/dev.006569. URL http://www.ncbi.nlm.nih.gov/entrez/query.fcgi?cmd=Retrieve&db=PubMed&dopt=Citation&list_uids=17827181.

Lendahl, U., Zimmerman, L., and McKay, R. Cns stem cells express a new class of intermediate filament protein. *Cell*, 60(4):585–95, Feb 1990. doi: 0092-8674(90)90662-X[pii]. URL http://www.ncbi.nlm.nih.gov/entrez/query.fcgi?cmd=Retrieve&db=PubMed&dopt=Citation&list_uids=1689217.

Lenhoff, S. and Lenhoff, H. Hydra and the birth of experimental biology, 1744: Abraham trembley's memoirs concerning the natural history of a type of freshwater polyp with arms shaped like horns. *Pacific Grove California: Boxwood Press*, 1986.

Loh, Y., Agarwal, S., Park, I., Urbach, A., Huo, H., Heffner, G., Kim, K., Miller, J., Ng, K., and Daley, G. Generation of induced pluripotent stem cells from human blood. *Blood*, 113(22):5476–9, May 2009. doi: blood-2009-02-204800[pii]10.1182/blood-2009-02-204800. URL http://www.ncbi.nlm.nih.gov/entrez/query.fcgi?cmd=Retrieve&db=PubMed&dopt=Citation&list_uids=19299331.

Lunde, K., Belting, H., and Driever, W. Zebrafish pou5f1/pou2, homolog of mammalian oct4, functions in the endoderm specification cascade. *Curr Biol*, 14(1):48–55, Jan 2004. doi: S0960982203008649[pii]. URL http://www.ncbi.nlm.nih.gov/entrez/query.fcgi?cmd=Retrieve&db=PubMed&dopt=Citation&list_uids=14711414.

Maki, N., Suetsugu-Maki, R., Tarui, H., Agata, K., Rio-Tsonis, K.D., and Tsonis, P. Expression of stem cell pluripotency factors during regeneration in newts. *Dev Dyn*, 238(6):1613–6, Jun 2009. doi: 10.1002/dvdy.21959. URL http://www.ncbi.nlm.nih.gov/entrez/query.fcgi?cmd=Retrieve&db=PubMed&dopt=Citation&list_uids=19384853.

Mann, D., Yates, P., and Barton, C. The dna content of purkinje cells in mammals. *J Comp Neurol*, 180 (2):345–7, Jul 1978. doi: 10.1002/cne.901800210. URL http://www.ncbi.nlm.nih.gov/entrez/query.fcgi?cmd=Retrieve&db=PubMed&dopt=Citation&list_uids=659665.

Manuelidis, L. and Manuelidis, E. On the dna content of cerebellar purkinje cells in vivo and in vitro. *Exp Neurol*, 43(1):192–206, Apr 1974. doi: 0014-4886(74)90140-X[pii]. URL http://www.ncbi.nlm.nih.gov/entrez/query.fcgi?cmd=Retrieve&db=PubMed&dopt=Citation&list_uids=4818787.

Mares, V., Lodin, Z., and Sacha, J. A cytochemical and autoradiographic study of nuclear dna in mouse purkinje cells. *Brain Res*, 53(2):273–89, Apr 1973. doi: 0006-8993(73)90214-X[pii]. URL http://www.ncbi.nlm.nih.gov/entrez/query.fcgi?cmd=Retrieve&db=PubMed&dopt=Citation&list_uids=4735887.

Marlow, F. and Mullins, M. Bucky ball functions in balbiani body assembly and animal-vegetal polarity in the oocyte and follicle cell layer in zebrafish. *Dev Biol*, 321(1):40–50, Sep 2008. doi: S0012-1606(08)00916-0[pii]10.1016/j.ydbio.2008.05.557. URL http://www.ncbi.nlm.nih.gov/entrez/query.fcgi?cmd=Retrieve&db=PubMed&dopt=Citation&list_uids=18582455.

Martinez, D. Mortality patterns suggest lack of senescence in hydra. *Exp Gerontol*, 33(3):217–25, May 1998. doi: S0531-5565(97)00113-7[pii]. URL http://www.ncbi.nlm.nih.gov/entrez/query.fcgi?cmd=Retrieve&db=PubMed&dopt=Citation&list_uids=9615920.

Mathis, L. and Nicolas, J. Different clonal dispersion in the rostral and caudal mouse central nervous system. *Development*, 127(6):1277–90, Mar 2000. URL http://www.ncbi.nlm.nih.gov/entrez/query.fcgi?cmd=Retrieve&db=PubMed&dopt=Citation&list_uids=10683180.

McGrew, M., Sherman, A., Lillico, S., Ellard, F., Radcliffe, P., Gilhooley, H., Mitrophanous, K., Cambray, N., Wilson, V., and Sang, H. Localised axial progenitor cell populations in the avian tail bud are not committed to a posterior hox identity. *Development*, 135(13):2289–99, Jul 2008. doi: dev.022020[pii]10.1242/dev.022020. URL http://www.ncbi.nlm.nih.gov/entrez/query.fcgi?cmd=Retrieve&db=PubMed&dopt=Citation&list_uids=18508860.

McHedlishvili, L., Epperlein, H., Telzerow, A., and Tanaka, E. A clonal analysis of neural progenitors during axolotl spinal cord regeneration reveals evidence for both spatially restricted and multipotent progenitors. *Development*, 134(11):2083–93, Jun 2007. doi: 134/11/2083[pii]10.1242/dev.02852. URL http://www.ncbi.nlm.nih.gov/entrez/query.fcgi?cmd=Retrieve&db=PubMed&dopt=Citation&list_uids=17507409.

Mezey, E., Chandross, K., Harta, G., Maki, R., and McKercher, S. Turning blood into brain: cells bearing neuronal antigens generated in vivo from bone marrow. *Science*, 290(5497):1779–82, Dec 2000. doi: 9025[pii]. URL http://www.ncbi.nlm.nih.gov/entrez/query.fcgi?cmd=Retrieve&db=PubMed&dopt=Citation&list_uids=11099419.

Millane, R., Kanska, J., Duffy, D., Seoighe, C., Cunningham, S., Plickert, G., and Frank, U. Induced stem cell neoplasia in a cnidarian by ectopic expression of a pou domain transcription factor. *Development*, 138 (12):2429–39, Jun 2011. doi: 138/12/2429[pii]10.1242/dev.064931. URL http://www.ncbi.nlm.nih.gov/entrez/query.fcgi?cmd=Retrieve&db=PubMed&dopt=Citation&list_uids=21610024.

Mitsui, K., Tokuzawa, Y., Itoh, H., Segawa, K., Murakami, M., Takahashi, K., Maruyama, M., Maeda, M., and Yamanaka, S. The homeoprotein nanog is required for maintenance of pluripotency in mouse epiblast and es cells. *Cell*, 113(5):631–42, May 2003. doi: S0092867403003933[pii]. URL http://www.ncbi.nlm.nih.gov/entrez/query.fcgi?cmd=Retrieve&db=PubMed&dopt=Citation&list_uids=12787504.

Monaghan, J., Epp, L., Putta, S., Page, R., Walker, J., Beachy, C., Zhu, W., Pao, G., Verma, I., Hunter, T., Bryant, S., Gardiner, D., Harkins, T., and Voss, S. Microarray and cdna sequence analysis of transcription during nerve-dependent limb regeneration. *BMC Biol*, 7:1, 2009. doi: 1741-7007-7-1[pii] 10.1186/1741-7007-7-1. URL http://www.ncbi.nlm.nih.gov/entrez/query.fcgi?cmd=Retrieve&db=PubMed&dopt=Citation&list_uids=19144100.

Morita, S., Kojima, T., and Kitamura, T. Plat-e: an efficient and stable system for transient packaging of retroviruses. *Gene Ther*, 7(12):1063–6, Jun 2000. doi: 10.1038/sj.gt.3301206. URL http://www.ncbi.nlm.nih.gov/entrez/query.fcgi?cmd=Retrieve&db=PubMed&dopt=Citation&list_uids=10871756.

Morrison, G. and Brickman, J. Conserved roles for oct4 homologues in maintaining multipotency during early vertebrate development. *Development*, 133(10):2011–22, May 2006. doi: 133/10/2011[pii]10.1242/dev.02362. URL http://www.ncbi.nlm.nih.gov/entrez/query.fcgi?cmd=Retrieve&db=PubMed&dopt=Citation&list_uids=16651543.

Morrison, S., Shah, N., and Anderson, D. Regulatory mechanisms in stem cell biology. *Cell*, 88(3):287–98, Feb 1997. doi: S0092-8674(00)81867-X[pii]. URL http://www.ncbi.nlm.nih.gov/entrez/query.fcgi?cmd=Retrieve&db=PubMed&dopt=Citation&list_uids=9039255.

Nichols, J., Zevnik, B., Anastassiadis, K., Niwa, H., Klewe-Nebenius, D., Chambers, I., Scholer, H., and Smith, A. Formation of pluripotent stem cells in the mammalian embryo depends on the pou transcription factor oct4. *Cell*, 95(3):379–91, Oct 1998. doi: S0092-8674(00)81769-9[pii]. URL http://www.ncbi.nlm.nih.gov/entrez/query.fcgi?cmd=Retrieve&db=PubMed&dopt=Citation&list_uids=9814708.

Nicolas, J., Mathis, L., Bonnerot, C., and Saurin, W. Evidence in the mouse for self-renewing stem cells in the formation of a segmented longitudinal structure, the myotome. *Development*, 122(9):2933–46, Sep 1996. URL http://www.ncbi.nlm.nih.gov/entrez/query.fcgi?cmd=Retrieve&db=PubMed&dopt=Citation&list_uids=8787766.

Niu, M. The differentiation of gastrula ectoderm in medium conditioned by axial mesoderm. *Proc. Nat. Acad. Sci.*, 39(298):985–989, 1953.

Niwa, H. Molecular mechanism to maintain stem cell renewal of es cells. *Cell Struct Funct*, 26(3):137–48, Jun 2001. URL http://www.ncbi.nlm.nih.gov/entrez/query.fcgi?cmd=Retrieve&db=PubMed&dopt=Citation&list_uids=11565806.

Niwa, H., Miyazaki, J., and Smith, A. Quantitative expression of oct-3/4 defines differentiation, dedifferentiation or self-renewal of es cells. *Nat Genet*, 24(4):372–6, Apr 2000. doi: 10.1038/74199. URL http://www.ncbi.nlm.nih.gov/entrez/query.fcgi?cmd=Retrieve&db=PubMed&dopt=Citation&list_uids=10742100.

Niwa, H., Sekita, Y., Tsend-Ayush, E., and Grutzner, F. Platypus pou5f1 reveals the first steps in the evolution of trophectoderm differentiation and pluripotency in mammals. *Evol Dev*, 10(6):671–82, Nov 2008. doi: EDE280[pii]10.1111/j.1525-142X.2008.00280.x. URL http://www.ncbi.nlm.nih.gov/entrez/query.fcgi?cmd=Retrieve&db=PubMed&dopt=Citation&list_uids=19021737.

O'Donnell, K. and Boeke, J. Mighty piwis defend the germline against genome intruders. *Cell*, 129(1):37–44, Apr 2007. doi: S0092-8674(07)00396-0[pii]10.1016/j.cell.2007.03.028. URL http://www.ncbi.nlm.nih.gov/entrez/query.fcgi?cmd=Retrieve&db=PubMed&dopt=Citation&list_uids=17418784.

O'Hara, C., Egar, M., and Chernoff, E. Reorganization of the ependyma during axolotl spinal cord regeneration: changes in intermediate filament and fibronectin expression. *Dev Dyn*, 193(2):103–15, Feb 1992. doi: 10.1002/aja.1001930202. URL http://www.ncbi.nlm.nih.gov/entrez/query.fcgi?cmd=Retrieve&db=PubMed&dopt=Citation&list_uids=1374657.

Okano, H., Ogawa, Y., Nakamura, M., Kaneko, S., Iwanami, A., and Toyama, Y. Transplantation of neural stem cells into the spinal cord after injury. *Semin Cell Dev Biol*, 14(3):191–8, Jun 2003. URL http://www.ncbi.nlm.nih.gov/entrez/query.fcgi?cmd=Retrieve&db=PubMed&dopt=Citation&list_uids=12948354.

Okita, K., Ichisaka, T., and Yamanaka, S. Generation of germline-competent induced pluripotent stem cells. *Nature*, 448(7151):313–7, Jul 2007. doi: nature05934[pii]10.1038/nature05934. URL http://www.ncbi.nlm.nih.gov/entrez/query.fcgi?cmd=Retrieve&db=PubMed&dopt=Citation&list_uids=17554338.

Okumura-Nakanishi, S., Saito, M., Niwa, H., and Ishikawa, F. Oct-3/4 and sox2 regulate oct-3/4 gene in embryonic stem cells. *J Biol Chem*, 280(7):5307–17, Feb 2005. doi: M410015200[pii]10.1074/jbc.M410015200. URL http://www.ncbi.nlm.nih.gov/entrez/query.fcgi?cmd=Retrieve&db=PubMed&dopt=Citation&list_uids=15557334.

Onal, P., Grun, D., Adamidi, C., Rybak, A., Solana, J., Mastrobuoni, G., Wang, Y., Rahn, H., Chen, W., Kempa, S., Ziebold, U., and Rajewsky, N. Gene expression of pluripotency determinants is conserved between mammalian and planarian stem cells. *EMBO J*, 31(12):2755–69, Jun 2012. doi: emboj2012110[pii]10.1038/emboj.2012.110. URL http://www.ncbi.nlm.nih.gov/entrez/query.fcgi?cmd=Retrieve&db=PubMed&dopt=Citation&list_uids=22543868.

Pan, G., Chang, Z., Scholer, H., and Pei, D. Stem cell pluripotency and transcription factor oct4. *Cell Res*, 12(5-6):321–9, Dec 2002. doi: 10.1038/sj.cr.7290134. URL http://www.ncbi.nlm.nih.gov/entrez/query.fcgi?cmd=Retrieve&db=PubMed&dopt=Citation&list_uids=12528890.

Parwaresch, M., Kreipe, H., and Radzun, H. Human macrophage hybrid forming spontaneous giant cells. *Virchows Arch B Cell Pathol Incl Mol Pathol*, 51(2):89–96, 1986. URL http://www.ncbi.nlm.nih.gov/entrez/query.fcgi?cmd=Retrieve&db=PubMed&dopt=Citation&list_uids=2873682.

Pesce, M. and Scholer, H. Oct-4: gatekeeper in the beginnings of mammalian development. *Stem Cells*, 19 (4):271–8, 2001. doi: 10.1634/stemcells.19-4-271. URL http://www.ncbi.nlm.nih.gov/entrez/query.fcgi?cmd=Retrieve&db=PubMed&dopt=Citation&list_uids=11463946.

Petersen, B., Bowen, W., Patrene, K., Mars, W., Sullivan, A., Murase, N., Boggs, S., Greenberger, J., and Goff, J. Bone marrow as a potential source of hepatic oval cells. *Science*, 284(5417):1168–70, May 1999. URL http://www.ncbi.nlm.nih.gov/entrez/query.fcgi?cmd=Retrieve&db=PubMed&dopt=Citation&list_uids=10325227.

Putta, S., Smith, J., Walker, J., Rondet, M., Weisrock, D., Monaghan, J., Samuels, A., Kump, K., King, D., Maness, N., Habermann, B., Tanaka, E., Bryant, S., Gardiner, D., Parichy, D., and Voss, S. From biomedicine to natural history research: Est resources for ambystomatid salamanders. *BMC Genomics*, 5(1):54, Aug 2004. doi: 10.1186/1471-2164-5-541471-2164-5-54[pii]. URL http://www.ncbi.nlm.nih.gov/entrez/query.fcgi?cmd=Retrieve&db=PubMed&dopt=Citation&list_uids=15310388.

Ralser, M., Querfurth, R., Warnatz, H., Lehrach, H., Yaspo, M., and Krobitsch, S. An efficient and economic enhancer mix for pcr. *Biochem Biophys Res Commun*, 347(3):747–51, Sep 2006. doi: S0006-291X(06)01470-7[pii]10.1016/j.bbrc.2006.06.151. URL http://www.ncbi.nlm.nih.gov/entrez/query.fcgi?cmd=Retrieve&db=PubMed&dopt=Citation&list_uids=16842759.

Ramachandran, R., Fausett, B., and Goldman, D. Ascl1a regulates muller glia dedifferentiation and retinal regeneration through a lin-28-dependent, let-7 microrna signalling pathway. *Nat Cell Biol*, 12(11):1101–7, Nov 2010. doi: ncb2115[pii]10.1038/ncb2115. URL http://www.ncbi.nlm.nih.gov/entrez/query.fcgi?cmd=Retrieve&db=PubMed&dopt=Citation&list_uids=20935637.

Remenyi, A., Lins, K., Nissen, L., Reinbold, R., Scholer, H., and Wilmanns, M. Crystal structure of a pou/hmg/dna ternary complex suggests differential assembly of oct4 and sox2 on two enhancers. *Genes Dev*, 17(16):2048–59, Aug 2003. doi: 10.1101/gad.26930317/16/2048[pii]. URL http://www.ncbi.nlm.nih.gov/entrez/query.fcgi?cmd=Retrieve&db=PubMed&dopt=Citation&list_uids=12923055.

Reynolds, B. and Weiss, S. Generation of neurons and astrocytes from isolated cells of the adult mammalian central nervous system. *Science*, 255(5052):1707–10, Mar 1992. URL http://www.ncbi.nlm.nih.gov/entrez/query.fcgi?cmd=Retrieve&db=PubMed&dopt=Citation&list_uids=1553558.

Reynolds, B. and Weiss, S. Clonal and population analyses demonstrate that an egf-responsive mammalian embryonic cns precursor is a stem cell. *Dev Biol*, 175(1):1–13, Apr 1996. doi: S0012-1606(96)90090-1[pii]

10.1006/dbio.1996.0090. URL http://www.ncbi.nlm.nih.gov/entrez/query.fcgi?cmd=Retrieve&db=PubMed&dopt=Citation&list_uids=8608856.

Richardson, P., McGuinness, U., and Aguayo, A. Axons from cns neurons regenerate into pns grafts. *Nature*, 284(5753):264–5, Mar 1980. URL http://www.ncbi.nlm.nih.gov/entrez/query.fcgi?cmd=Retrieve&db=PubMed&dopt=Citation&list_uids=7360259.

Rinkevich, Y., Rosner, A., Rabinowitz, C., Lapidot, Z., Moiseeva, E., and Rinkevich, B. Piwi positive cells that line the vasculature epithelium, underlie whole body regeneration in a basal chordate. *Dev Biol*, 345(1): 94–104, Sep 2010. doi: S0012-1606(10)00803-1[pii]10.1016/j.ydbio.2010.05.500. URL http://www.ncbi.nlm.nih.gov/entrez/query.fcgi?cmd=Retrieve&db=PubMed&dopt=Citation&list_uids=20553710.

Rodda, D., Chew, J., Lim, L., Loh, Y., Wang, B., Ng, H., and Robson, P. Transcriptional regulation of nanog by oct4 and sox2. *J Biol Chem*, 280(26):24731–7, Jul 2005. doi: M502573200[pii]10.1074/jbc.M502573200. URL http://www.ncbi.nlm.nih.gov/entrez/query.fcgi?cmd=Retrieve&db=PubMed&dopt=Citation&list_uids=15860457.

Ronquist, F., Teslenko, M., van der Mark, P., Ayres, D., Darling, A., Hohna, S., Larget, B., Liu, L., Suchard, M., and Huelsenbeck, J. Mrbayes 3.2: efficient bayesian phylogenetic inference and model choice across a large model space. *Syst Biol*, 61(3):539–42, May 2011. doi: sys029[pii]10.1093/sysbio/sys029. URL http://www.ncbi.nlm.nih.gov/entrez/query.fcgi?cmd=Retrieve&db=PubMed&dopt=Citation&list_uids=22357727.

Saigou, Y., Kamimura, Y., Inoue, M., Kondoh, H., and Uchikawa, M. Regulation of sox2 in the preplacodal cephalic ectoderm and central nervous system by enhancer n-4. *Dev Growth Differ*, 52(5):397–408, Jun 2010. doi: DGD1180[pii]10.1111/j.1440-169X.2010.01180.x. URL http://www.ncbi.nlm.nih.gov/entrez/query.fcgi?cmd=Retrieve&db=PubMed&dopt=Citation&list_uids=20507355.

Sakakibara, S. and Okano, H. Expression of neural rna-binding proteins in the postnatal cns: implications of their roles in neuronal and glial cell development. *J Neurosci*, 17(21):8300–12, Nov 1997. URL http://www.ncbi.nlm.nih.gov/entrez/query.fcgi?cmd=Retrieve&db=PubMed&dopt=Citation&list_uids=9334405.

Sanchez-Sanchez, A., Camp, E., Garcia-Espana, A., Leal-Tassias, A., and Mullor, J. Medaka oct4 is expressed during early embryo development, and in primordial germ cells and adult gonads. *Dev Dyn*, 239(2):672–9, Feb 2010. doi: 10.1002/dvdy.22198. URL http://www.ncbi.nlm.nih.gov/entrez/query.fcgi?cmd=Retrieve&db=PubMed&dopt=Citation&list_uids=20034054.

Sanchez-Sanchez, A., Camp, E., and Mullor, J. Fishing pluripotency mechanisms in vivo. *Int J Biol Sci*, 7(4):410–7, 2011. URL http://www.ncbi.nlm.nih.gov/entrez/query.fcgi?cmd=Retrieve&db=PubMed&dopt=Citation&list_uids=21547058.

Sato, N., Sanjuan, I., Heke, M., Uchida, M., Naef, F., and Brivanlou, A. Molecular signature of human embryonic stem cells and its comparison with the mouse. *Dev Biol*, 260(2):404–13, Aug 2003. doi: S0012160603002562[pii]. URL http://www.ncbi.nlm.nih.gov/entrez/query.fcgi?cmd=Retrieve&db=PubMed&dopt=Citation&list_uids=12921741.

Sauer, B. Inducible gene targeting in mice using the cre/lox system. *Methods*, 14(4):381–92, Apr 1998. doi: S1046-2023(98)90593-X[pii]10.1006/meth.1998.0593. URL http://www.ncbi.nlm.nih.gov/entrez/query.fcgi?cmd=Retrieve&db=PubMed&dopt=Citation&list_uids=9608509.

Schmid, V. and Alder, H. Isolated, mononucleated, striated muscle can undergo pluripotent transdifferentiation and form a complex regenerate. *Cell*, 38(3):801–9, Oct 1984. doi: 0092-8674(84)90275-7[pii]. URL http://www.ncbi.nlm.nih.gov/entrez/query.fcgi?cmd=Retrieve&db=PubMed&dopt=Citation&list_uids=6149022.

Scholer, H. Octamania: the pou factors in murine development. *Trends Genet*, 7(10):323–9, Oct 1991. doi: 0168-9525(91)90422-M[pii]. URL http://www.ncbi.nlm.nih.gov/entrez/query.fcgi?cmd=Retrieve&db=PubMed&dopt=Citation&list_uids=1781030.

Scholer, H., Ruppert, S., Suzuki, N., Chowdhury, K., and Gruss, P. New type of pou domain in germ line-specific protein oct-4. *Nature*, 344(6265):435–9, Mar 1990. doi: 10.1038/344435a0. URL http://www.ncbi.nlm.nih.gov/entrez/query.fcgi?cmd=Retrieve&db=PubMed&dopt=Citation&list_uids=1690859.

Selleck, M. and Stern, C. Fate mapping and cell lineage analysis of hensen's node in the chick embryo. *Development*, 112(2):615–26, Jun 1991. URL http://www.ncbi.nlm.nih.gov/entrez/query.fcgi?cmd=Retrieve&db=PubMed&dopt=Citation&list_uids=1794328.

Singh, S., Holdway, J., and Poss, K. Regeneration of amputated zebrafish fin rays from de novo osteoblasts. *Dev Cell*, 22(4):879–86, Apr 2012. doi: S1534-5807(12)00129-3[pii]10.1016/j.devcel.2012.03.006. URL http://www.ncbi.nlm.nih.gov/entrez/query.fcgi?cmd=Retrieve&db=PubMed&dopt=Citation&list_uids=22516203.

Sive, H., Grainger, R., and Harland, R. Animal cap isolation from xenopus laevis. *CSH Protoc*, 2007:pdb prot4744, 2007. URL http://www.ncbi.nlm.nih.gov/entrez/query.fcgi?cmd=Retrieve&db=PubMed&dopt=Citation&list_uids=21357092.

Smith, A., Avaron, F., Guay, D., Padhi, B., and Akimenko, M. Inhibition of bmp signaling during zebrafish fin regeneration disrupts fin growth and scleroblasts differentiation and function. *Dev Biol*, 299(2):438–54, Nov 2006. doi: S0012-1606(06)01086-4[pii]10.1016/j.ydbio.2006.08.016. URL `http://www.ncbi.nlm.nih.gov/entrez/query.fcgi?cmd=Retrieve&db=PubMed&dopt=Citation&list_uids=16959242`.

Smith, J., Kump, D., Walker, J., Parichy, D., and Voss, S. A comprehensive expressed sequence tag linkage map for tiger salamander and mexican axolotl: enabling gene mapping and comparative genomics in ambystoma. *Genetics*, 171(3):1161–71, Nov 2005. doi: genetics.105.046433[pii]10.1534/genetics.105.046433. URL `http://www.ncbi.nlm.nih.gov/entrez/query.fcgi?cmd=Retrieve&db=PubMed&dopt=Citation&list_uids=16079226`.

Snir, M., Ofir, R., Elias, S., and Frank, D. Xenopus laevis pou91 protein, an oct3/4 homologue, regulates competence transitions from mesoderm to neural cell fates. *EMBO J*, 25(15):3664–74, Aug 2006. doi: 7601238[pii]10.1038/sj.emboj.7601238. URL `http://www.ncbi.nlm.nih.gov/entrez/query.fcgi?cmd=Retrieve&db=PubMed&dopt=Citation&list_uids=16858397`.

Sobkow, L., Epperlein, H., Herklotz, S., Straube, W., and Tanaka, E. A germline gfp transgenic axolotl and its use to track cell fate: dual origin of the fin mesenchyme during development and the fate of blood cells during regeneration. *Dev Biol*, 290(2):386–97, Feb 2006. doi: S0012-1606(05)00863-8[pii]10.1016/j.ydbio.2005.11.037. URL `http://www.ncbi.nlm.nih.gov/entrez/query.fcgi?cmd=Retrieve&db=PubMed&dopt=Citation&list_uids=16387293`.

Stevenson, T. Fingertip and nailbed injuries. *Orthop Clin North Am*, 23(1):149–59, Jan 1992. URL `http://www.ncbi.nlm.nih.gov/entrez/query.fcgi?cmd=Retrieve&db=PubMed&dopt=Citation&list_uids=1729663`.

Takahashi, K. and Yamanaka, S. Induction of pluripotent stem cells from mouse embryonic and adult fibroblast cultures by defined factors. *Cell*, 126(4):663–76, Aug 2006. doi: S0092-8674(06)00976-7[pii]10.1016/j.cell.2006.07.024. URL `http://www.ncbi.nlm.nih.gov/entrez/query.fcgi?cmd=Retrieve&db=PubMed&dopt=Citation&list_uids=16904174`.

Takahashi, K., Tanabe, K., Ohnuki, M., Narita, M., Ichisaka, T., Tomoda, K., and Yamanaka, S. Induction of pluripotent stem cells from adult human fibroblasts by defined factors. *Cell*, 131(5):861–72, Nov 2007. doi: S0092-8674(07)01471-7[pii]10.1016/j.cell.2007.11.019. URL `http://www.ncbi.nlm.nih.gov/entrez/query.fcgi?cmd=Retrieve&db=PubMed&dopt=Citation&list_uids=18035408`.

Takeda, H., Matsuzaki, T., Oki, T., Miyagawa, T., and Amanuma, H. A novel pou domain gene, zebrafish pou2: expression and roles of two alternatively spliced twin products in early development. *Genes Dev*,

8(1):45–59, Jan 1994. URL http://www.ncbi.nlm.nih.gov/entrez/query.fcgi?cmd=Retrieve&db=PubMed&dopt=Citation&list_uids=8288127.

Tam, P., Khoo, P., Wong, N., Tsang, T., and Behringer, R. Regionalization of cell fates and cell movement in the endoderm of the mouse gastrula and the impact of loss of lhx1(lim1) function. *Dev Biol*, 274(1): 171–87, Oct 2004. doi: 10.1016/j.ydbio.2004.07.005S0012-1606(04)00465-8[pii]. URL http://www.ncbi.nlm.nih.gov/entrez/query.fcgi?cmd=Retrieve&db=PubMed&dopt=Citation&list_uids=15355796.

Tanaka, E. and Ferretti, P. Considering the evolution of regeneration in the central nervous system. *Nat Rev Neurosci*, 10(10):713–23, Oct 2009. doi: nrn2707[pii]10.1038/nrn2707. URL http://www.ncbi.nlm.nih.gov/entrez/query.fcgi?cmd=Retrieve&db=PubMed&dopt=Citation&list_uids=19763104.

Terada, N., Hamazaki, T., Oka, M., Hoki, M., Mastalerz, D., Nakano, Y., Meyer, E., Morel, L., Petersen, B., and Scott, E. Bone marrow cells adopt the phenotype of other cells by spontaneous cell fusion. *Nature*, 416(6880):542–5, Apr 2002. doi: 10.1038/nature730nature730[pii]. URL http://www.ncbi.nlm.nih.gov/entrez/query.fcgi?cmd=Retrieve&db=PubMed&dopt=Citation&list_uids=11932747.

Theise, N., Nimmakayalu, M., Gardner, R., Illei, P., Morgan, G., Teperman, L., Henegariu, O., and Krause, D. Liver from bone marrow in humans. *Hepatology*, 32(1):11–6, Jul 2000. doi: S0270913900830116[pii] 10.1053/jhep.2000.9124. URL http://www.ncbi.nlm.nih.gov/entrez/query.fcgi?cmd=Retrieve&db=PubMed&dopt=Citation&list_uids=10869283.

Thornton, C. The histogenesis of the regenerating fore limb of larval amblystoma after exarticulation of the humerus. *J. Morphol.*, 62:219–241, 1938.

Tokuzawa, Y., Kaiho, E., Maruyama, M., Takahashi, K., Mitsui, K., Maeda, M., Niwa, H., and Yamanaka, S. Fbx15 is a novel target of oct3/4 but is dispensable for embryonic stem cell self-renewal and mouse development. *Mol Cell Biol*, 23(8):2699–708, Apr 2003. URL http://www.ncbi.nlm.nih.gov/entrez/query.fcgi?cmd=Retrieve&db=PubMed&dopt=Citation&list_uids=12665572.

Tsonis, P. Regeneration in vertebrates. *Dev Biol*, 221(2):273–84, May 2000. doi: 10.1006/dbio.2000.9667S0012-1606(00)99667-2[pii]. URL http://www.ncbi.nlm.nih.gov/entrez/query.fcgi?cmd=Retrieve&db=PubMed&dopt=Citation&list_uids=10790325.

Tucker, A. and Slack, J. Tail bud determination in the vertebrate embryo. *Curr Biol*, 5(7):807–13, Jul 1995a. doi: S0960-9822(95)00158-8[pii]. URL http://www.ncbi.nlm.nih.gov/entrez/query.fcgi?cmd=Retrieve&db=PubMed&dopt=Citation&list_uids=7583128.

Tucker, A. and Slack, J. The xenopus laevis tail-forming region. *Development*, 121:249–262, 1995b.

Tzouanacou, E., Wegener, A., Wymeersch, F., Wilson, V., and Nicolas, J. Redefining the progression of lineage segregations during mammalian embryogenesis by clonal analysis. *Dev Cell*, 17(3):365–76, Sep 2009. doi: S1534-5807(09)00339-6[pii]10.1016/j.devcel.2009.08.002. URL `http://www.ncbi.nlm.nih.gov/entrez/query.fcgi?cmd=Retrieve&db=PubMed&dopt=Citation&list_uids=19758561`.

Uchikawa, M., Ishida, Y., Takemoto, T., Kamachi, Y., and Kondoh, H. Functional analysis of chicken sox2 enhancers highlights an array of diverse regulatory elements that are conserved in mammals. *Dev Cell*, 4(4): 509–19, Apr 2003. doi: S1534580703000881[pii]. URL `http://www.ncbi.nlm.nih.gov/entrez/query.fcgi?cmd=Retrieve&db=PubMed&dopt=Citation&list_uids=12689590`.

Vassilopoulos, G., Wang, P., and Russell, D. Transplanted bone marrow regenerates liver by cell fusion. *Nature*, 422(6934):901–904, 2003.

Voss, S., Kump, D., Putta, S., Pauly, N., Reynolds, A., Henry, R., Basa, S., Walker, J., and Smith, J. Origin of amphibian and avian chromosomes by fission, fusion, and retention of ancestral chromosomes. *Genome Res*, 21(8):1306–12, Aug 2011. doi: gr.116491.110[pii]10.1101/gr.116491.110. URL `http://www.ncbi.nlm.nih.gov/entrez/query.fcgi?cmd=Retrieve&db=PubMed&dopt=Citation&list_uids=21482624`.

Wagner, D., Wang, I., and Reddien, P. Clonogenic neoblasts are pluripotent adult stem cells that underlie planarian regeneration. *Science*, 332(6031):811–6, May 2011. doi: 332/6031/811[pii]10.1126/science.1203983. URL `http://www.ncbi.nlm.nih.gov/entrez/query.fcgi?cmd=Retrieve&db=PubMed&dopt=Citation&list_uids=21566185`.

Walder, S., Zhang, F., and Ferretti, P. Up-regulation of neural stem cell markers suggests the occurrence of dedifferentiation in regenerating spinal cord. *Dev Genes Evol*, 213(12):625–30, Dec 2003. doi: 10.1007/s00427-003-0364-2. URL `http://www.ncbi.nlm.nih.gov/entrez/query.fcgi?cmd=Retrieve&db=PubMed&dopt=Citation&list_uids=14608505`.

Wang, X., Willenbring, H., Akkari, Y., Torimaru, Y., Foster, M., Al-Dhalimy, M., Lagasse, E., Finegold, M., Olson, S., and Grompe, M. Cell fusion is the principal source of bone-marrow-derived hepatocytes. *Nature*, 422(6934):897–901, 2003.

Watanabe, K. Individual variation in the distribution of lens potency in wolffian lens regeneration. *Develop., Growth and Differ.,*, 20(2):169–177, 1978.

Wei, C., Miura, T., Robson, P., Lim, S., Xu, X., Lee, M., Gupta, S., Stanton, L., Luo, Y., Schmitt, J., Thies, S., Wang, W., Khrebtukova, I., Zhou, D., Liu, E., Ruan, Y., Rao, M., and Lim, B. Transcriptome profiling of human and murine escs identifies divergent paths required to maintain the stem cell state. *Stem Cells*, 23(2):166–85, Feb 2005. doi: 23/2/166[pii]10.1634/stemcells.2004-0162. URL `http://www.ncbi.nlm.nih.gov/entrez/query.fcgi?cmd=Retrieve&db=PubMed&dopt=Citation&list_uids=15671141`.

Weimann, J., Charlton, C., Brazelton, T., Hackman, R., and Blau, H. Contribution of transplanted bone marrow cells to purkinje neurons in human adult brains. *Proc Natl Acad Sci U S A*, 100(4):2088–93, Feb 2003. doi: 10.1073/pnas.0337659100337659100[pii]. URL http://www.ncbi.nlm.nih.gov/entrez/query.fcgi?cmd=Retrieve&db=PubMed&dopt=Citation&list_uids=12576546.

Weinmaster, G., Roberts, V., and Lemke, G. Notch2: a second mammalian notch gene. *Development*, 116(4):931–41, Dec 1992. URL http://www.ncbi.nlm.nih.gov/entrez/query.fcgi?cmd=Retrieve&db=PubMed&dopt=Citation&list_uids=1295745.

Wernig, M., Meissner, A., Foreman, R., Brambrink, T., Ku, M., Hochedlinger, K., Bernstein, B., and Jaenisch, R. In vitro reprogramming of fibroblasts into a pluripotent es-cell-like state. *Nature*, 448(7151):318–24, Jul 2007. doi: nature05944[pii]10.1038/nature05944. URL http://www.ncbi.nlm.nih.gov/entrez/query.fcgi?cmd=Retrieve&db=PubMed&dopt=Citation&list_uids=17554336.

Whitfield, T., Heasman, J., and Wylie, C. Early embryonic expression of xlpou-60, a xenopus pou-domain protein. *Dev Biol*, 169(2):759–69, Jun 1995. doi: 10.1006/dbio.1995.1185S0012-1606(85)71185-2[pii]. URL http://www.ncbi.nlm.nih.gov/entrez/query.fcgi?cmd=Retrieve&db=PubMed&dopt=Citation&list_uids=7781914.

Widenfalk, J., Lundstromer, K., Jubran, M., Brene, S., and Olson, L. Neurotrophic factors and receptors in the immature and adult spinal cord after mechanical injury or kainic acid. *J Neurosci*, 21(10):3457–75, May 2001. doi: 21/10/3457[pii]. URL http://www.ncbi.nlm.nih.gov/entrez/query.fcgi?cmd=Retrieve&db=PubMed&dopt=Citation&list_uids=11331375.

Wilson, V., Olivera-Martinez, I., and Storey, K. Stem cells, signals and vertebrate body axis extension. *Development*, 136(10):1591–604, May 2009. doi: 136/10/1591[pii]10.1242/dev.021246. URL http://www.ncbi.nlm.nih.gov/entrez/query.fcgi?cmd=Retrieve&db=PubMed&dopt=Citation&list_uids=19395637.

Wood, H. and Episkopou, V. Comparative expression of the mouse sox1, sox2 and sox3 genes from pre-gastrulation to early somite stages. *Mech Dev*, 86(1-2):197–201, Aug 1999. doi: S0925477399001161[pii]. URL http://www.ncbi.nlm.nih.gov/entrez/query.fcgi?cmd=Retrieve&db=PubMed&dopt=Citation&list_uids=10446282.

Wu, Z., Chen, J., Ren, J., Bao, L., Liao, J., Cui, C., Rao, L., Li, H., Gu, Y., Dai, H., Zhu, H., Teng, X., Cheng, L., and Xiao, L. Generation of pig induced pluripotent stem cells with a drug-inducible system. *J Mol Cell Biol*, 1(1):46–54, Oct 2009. doi: mjp003[pii]10.1093/jmcb/mjp003. URL http://www.ncbi.nlm.nih.gov/entrez/query.fcgi?cmd=Retrieve&db=PubMed&dopt=Citation&list_uids=19502222.

y Cajal, S.R. Degeneration and regeneration of the nervous system. *New York: Ox ford UP*, 1928.

Yamanaka, S. Strategies and new developments in the generation of patient-specific pluripotent stem cells. *Cell Stem Cell*, 1(1):39–49, Jun 2007. doi: S1934-5909(07)00018-5[pii]10.1016/j.stem.2007.05.012. URL http://www.ncbi.nlm.nih.gov/entrez/query.fcgi?cmd=Retrieve&db=PubMed&dopt=Citation&list_uids=18371333.

Yeom, Y., Fuhrmann, G., Ovitt, C., Brehm, A., Ohbo, K., Gross, M., Hubner, K., and Scholer, H. Germline regulatory element of oct-4 specific for the totipotent cycle of embryonal cells. *Development*, 122(3):881–94, Mar 1996. URL http://www.ncbi.nlm.nih.gov/entrez/query.fcgi?cmd=Retrieve&db=PubMed&dopt=Citation&list_uids=8631266.

Ying, Q., Nichols, J., Evans, E., and Smith, A. Changing potency by spontaneous fusion. *Nature*, 416(6880):545–8, Apr 2002. doi: 10.1038/nature729nature729[pii]. URL http://www.ncbi.nlm.nih.gov/entrez/query.fcgi?cmd=Retrieve&db=PubMed&dopt=Citation&list_uids=11932748.

Yoshizato, K. Growth potential of adult hepatocytes in mammals: highly replicative small hepatocytes with liver progenitor-like traits. *Dev Growth Differ*, 49(2):171–84, Feb 2007. doi: DGD918[pii]10.1111/j.1440-169X.2007.00918.x. URL http://www.ncbi.nlm.nih.gov/entrez/query.fcgi?cmd=Retrieve&db=PubMed&dopt=Citation&list_uids=17335438.

Yu, J., Vodyanik, M., Smuga-Otto, K., Antosiewicz-Bourget, J., Frane, J., Tian, S., Nie, J., Jonsdottir, G., Ruotti, V., Stewart, R., Slukvin, I., and Thomson, J. Induced pluripotent stem cell lines derived from human somatic cells. *Science*, 318(5858):1917–20, Dec 2007. doi: 1151526[pii]10.1126/science.1151526. URL http://www.ncbi.nlm.nih.gov/entrez/query.fcgi?cmd=Retrieve&db=PubMed&dopt=Citation&list_uids=18029452.

Yuan, H., Corbi, N., Basilico, C., and Dailey, L. Developmental-specific activity of the fgf-4 enhancer requires the synergistic action of sox2 and oct-3. *Genes Dev*, 9(21):2635–45, Nov 1995. URL http://www.ncbi.nlm.nih.gov/entrez/query.fcgi?cmd=Retrieve&db=PubMed&dopt=Citation&list_uids=7590241.